Response to Reviewer #1:

Review

First of all, we thank the referee for his positive general comments about the paper. We acknowledge him for his useful corrections and suggestions, which have helped us clarifying several points and improving the manuscript.

Below we provide our point-by-point responses to his individual comments. Before each response, the reviewer comments have been quoted between []. Corresponding information and corrections have been added to the revised version of the manuscript. Technical comments are also included in the revised version.

General Comments:

[1) The paper also discusses the use of daily vs. monthly ozone median averages in the trend analysis. This is a less frequently used approach. It has its positive and negative sides for understanding short and long-term variability in time series. The advantage of using daily median ozone values in the upper stratosphere makes sense as there is a physical process that relate Solar flux (SF) and ozone variability on the daily bases, but it cannot be clearly separated in layers below upper stratosphere. It will be good to have discussion on significance of the daily vs monthly SF contribution to the trend analyses for all layers (section 4.3.1 discusses only upper stratosphere layer trends).]

We thank the referee for pointing out this missing aspect of our analysis. It is true that most of the solar cycle variation of ozone occurs in the stratosphere, even in the lowermost stratosphere (e.g. Soukharev and Hood, 2006). However, the use of daily median ozone values in the layers below (UTLS and MLT) is justified in our analysis by the coarse vertical resolution of IASI (full-width at half-maximum of the averaging kernels) which is such that upper and lower atmospheric levels contribute to each other.

As expected, the use of daily medians mainly helps in reducing the uncertainty associated with the trends (i.e. in discriminating between a linear trend and the solar flux effect) in the UST column where the ozone hole recovery is clearly identified, but it also reduces the uncertainty in the lower layers (cfr Table 2 of the manuscript), principally in the MLST and the UTLS where the solar cycle is an important driver (cfr Figure 8 of the manuscript). This is now specifically mentioned in Sections 4.3.2 of the revised version:

"We show that the daily and monthly trends in all layers and all latitude bands fall within each other uncertainties, but that the use of daily median strongly helps in reducing everywhere the uncertainty associated with the trends for the reasons discussed above (Section 4.3.1). This is particularly observed in the UST where the ozone hole recovery would occur, but also in the MLST and the UTLS where the solar cycle variation of ozone is the largest (see Figure 8). As a consequence, …"

This result is important as it tends to indicate that daily data should be preferred to monthly data for deriving significant trends. This gives in our opinion convincing evidence of the benefit of IASI in terms of frequency sampling for the assessment of O_3 trends.

[2) The paper proposed the use of daily data for separation of the Solar signal from the trend contained in the 6-years long time series, but it is not clear from the text that it improves the model fit in all layers and latitude bands (i.e. residuals). This should be discussed in more details in the paper, including showing results in other than US layers.]

In the example provided in Figure 9 of the manuscript (UST in 30°S-50°S), we show that the daily data considerably improves the regression model in terms of residuals (44% in daily *vs* 60% in monthly data) and of trend uncertainty (1.74±0.77 in daily vs1.21±1.30 in monthly data). This translates to larger relative differences between the regression with and without the linear term in daily data (17%) than in monthly data (10%), which indicates a larger compensation effect in the latter. The averaged relative residuals are now indicated in the middle panels in the revised Figure 9, which also illustrates the differences between the two regression models (with and without the linear trend term), as suggested by the referee in one of the technical comments. The offset between the two models is observed for most of layers and latitudinal bands particularly where either O_3 recovery or solar effect signal is important, which is consistent with the decrease in trend uncertainty.

We present in Figure 1 below (same as Figure 9 of the manuscript) one additional example (MLST in 30°S-50°S) characterized by a large significant negative trend in both daily and monthly data (see Table 2 of the manuscript) with a large offset between the two regression models. With this example, we show that even if both residuals and trends are similar in daily and monthly data (-2.17±0.58DU/Yr in daily data vs -2.36±1.80 DU/Yr in monthly data, see Table 2 of the manuscript), the higher co-linearity of the linear and the solar flux terms in monthly data in comparisons with daily data translates to a much larger trend uncertainty (a factor of ~3 in this example).

This is now better explained in Sections 4.3.1 of the revised version:
- "This effective co-linearity of the linear and the monthly solar flux terms translates to larger model fit residuals (44% in daily averages *vs* 60% in monthly averages), to larger relative differences between the two regression models (with and without the linear term) (17% in daily vs 10% in monthly data), and to larger uncertainty on the trend coefficients when using the monthly data in comparison with the daily data."
- "The same conclusions can be drawn from the fits in other layers and latitude bands, especially those where the solar cycle variation of ozone is largest (MLST and UTLS) or where the ozone recovery occurs (UST). A larger trend uncertainty associated with monthly data *vs* daily data is found in all situations (see Table 2, Section 4.3.2)."

[3) One note, the "US" abbreviation for upper stratosphere in the text was confusing to me, as it is typically used for geographical domain of the United States. I would have preferred to have the "UST" abbreviation. "MLS" is also an acronym commonly used for the satellite (Microwave Limb Sounder) ozone data, it therefore it would be better to change it to "MLST".]
We thank the referee for pointing that out. These acronyms have been changed to UST and MLST throughout the revised version of the manuscript.

Specific comments:

[1) P. 12, lines 260-261. Can you please provide more details on how the correction for the autocorrelation is applied to uncertainties of the fit?]

We calculated the uncertainty of the fitted parameters by computing the standard error with an effective sample size (n*) of independent information based on the lag-1 autocorrelation coefficient correlation of the noise residual ($n^* = n \cdot \frac{1-\Phi}{1+\Phi}$) as in Santer al. (2000).This is now better explained in Section 3.1 of the revised version:

"The constant term (Cst) and the coefficients a_n, b_n, x_j are estimated by least-squares method and their standard errors (σ_e) are calculated from the covariance matrix of the coefficients and corrected to take into account the uncertainty due to the autocorrelation of the noise residuals as discussed in Santer et al. (2000) and references therein:

$$\sigma_e^2 = (Y^T Y)^{-1} \cdot \frac{\sum_t [O_3(t) - yY(t)]^2}{n-m} \cdot \frac{1+\Phi}{1-\Phi} \quad (3)$$

Where Y is the matrix with the covariates ($trend, \cos(n\omega t), \sin(n\omega t), X_{norm,j}$) sorted column wise, y is the vector of the regression coefficients corresponding to the columns of Y , n is the number of daily (or monthly) data points in the time series, m is the number of fitted parameters, and Φ , the lag-1 autocorrelation of the residuals."

[2) P.14, lines 301-303. It is clear from the paper that the IASI has information in the MLT layer, which is between surface and _ 8 km. On the other hand, IASI sensitivity to ozone variability below 4 km is not clearly discussed. Figure 4 suggests 20-40 % total error of the retrieval at the bottom of each of 3 plots for different atitude bands. Figure 5 shows that about 20-40 % ozone variability is observed in the lowest 4 km, with the exception of tropical region. AKs for 0-4 km altitude likely have large contribution from layers above. Is it possible to discern actual day-to-day ozone variability below 4 km and trend that is above the retrieval noise? The information on the AP contribution in MLT (similar to the Figure 2 discussion) can be discussed in this section to help with the sensitivity assessment. This section needs to expand the discussion on information in the MLT.]

The referee is right; AKs below 4 km altitude suggest a large contribution from the upper layers. Based on AKs profile shapes, one should generally better not consider analyzing the ground-300hPa tropospheric column separately in sub-layers since each of them contributes to each other, nor analyzing the lowermost troposphere because of the sharp decrease of sensitivity down to the surface which is inherent to nadir thermal IR sounding in cases of low surface temperature or low thermal contrast (see Figure 4 of the manuscript). As a result, the variability can hardly be discussed independently below 4 km and this is why no trends were given for the lowermost troposphere.

However, one exception is found in spring-summer 30°N-50°N latitude band where the detected variability below 4 km (between ~30% and ~45%, see Figure 5 of the manuscript) is larger than the retrieval error (lower than 25%, see Figure 4 (b) of the manuscript). As mentioned in the paper, this variability could potentially be linked to photochemical production of O_3 associated

with anthropogenic precursor emissions. The a priori contribution in the ground-700hPa column, as suggested from Figure 2 of the manuscript for the ground-300hPa column, is the lowest in this region and during that period. It has been estimated to 10-20% over the continental regions.

This is now better explained in both the revised Section 2 and Section 4.1, and some words of caution about the detectable ozone variability in the lower troposphere have been added as well.

[3) P.14 lines 314-315. Please clarify the statement "The fact that the patterns are similar in _10 km mainly reflects the low sensitivity of IASI to that level compared to the others." This is in regards to Figure 6. It would be good to explain a bit more about the patterns. Otherwise reader is left to guess if it is about seemingly no variability in the tropics (blue color indicates low concentrations), or similarity to results at 20 km, or something else. Figure 5 shows high relative ozone variability at 10 km level, but the range in absolute ozone concentrations might be small.]
This sentence has been changed to "The fact that the patterns in ~10km are similar to those in ~20 km mainly reflects the low sensitivity of IASI to that level compared to the others"

[4) P. 21,
a) lines 452-456, statement that ". . .linear term is not compensated by solar flax in daily averages" is not completely true, because the SF fitted signal from the model with and without the liner term (blue and orange lines shown in the bottom left panel of Figure 9) are not exactly the same (positive and negative coefficients).
b) Also, the difference between the orange and blue SF signal can be fitted with the linear slope.
c) Besides Figure 8, it will be useful to have a tabulated summary of the variables in the statistical model that were kept after iterative backward selection, and fitting uncertainties for all layers and latitude bands. Otherwise it is hard to get these numbers from the figure. It can be added in the Supplemental materials.]
a) The sentence has been corrected.
b) Exactly. This results from the exclusion of the linear term trend in the regression model. This is precisely what we expect from using daily data and daily solar signature instead of monthly ones: the offset when using daily data corresponds well to a trend over the IASI period. It results from the fact that, in daily data, the solar flux cannot completely compensate the linear trend (LT) term in the regression model because of its strong daily signature, while it largely compensates the LT in monthly data. See responses to comment 5a) and b) below. We now better explain Figure 9 in the revised Section 4.3.1.
c) We now provide in the revised version of the Supplementary Materials and here below, the Table S1 which summarizes the proxies retained in the stepwise backward elimination approach that are significant at the 95% level for each latitude band and for each partial column. Summarizing in one Table the fitted uncertainties for each retained fitted parameters, each latitude band and each layer is difficult and we have preferred to keep Figure 8 as it is. Nevertheless, to help the readers, the proxies which become statistically non-significant when accounting for the autocorrelation in the noise residuals at the end of the elimination process (with an uncertainty larger than its associated estimate; i.e. larger than 100% corresponding to an error bar overlapping the zero line) are indicated between parentheses in Table S1. This has been now mentioned in the revised version in Section 4.2.

[5) Additional Figure 9 comments:

a) The information in the middle panel is not very clear. It is stated that the deseasonalized IASI ozone data are plotted. Can you please explain the process of deseasonalization for data, such as how the seasonal cycle was derived – from data averages or from the model fit?
b) Whereas the model fit with the linear term included (light blue line) seems to follow the de-seasonalized IASI ozone data (dark blue), the model fit without the linear term (orange) is clearly low-biased from the data (dark blue line). It is not clear how the model fit can be done with the resulting mean offset from the data. Is it possible that the wrong constant term is used to calculate the model time series (orange) for this plot. My understanding of the discussion is that two separate models were used to obtain the data fit: one is with (blue) and another one is without (orange) the linear term. Please make corrections to the text if the single model is used, but the model result is plotted with and without the linear term.
c) On the other hand, in the case of the model fit without the linear term the SF signal contribution to the model fit for monthly mean data is much larger as compared to SF term in the daily data fit model. Is it due to the fact that solar flux seems to increase from 2008 to 2013, and for the analyzed time period seems to be comprise of a liner trend and the day-to-day variability that has significantly increased by 2011?]
a) Deseasonalized IASI data were obtained by substracting from the IASI ozone time series the seasonal cycle derived from the model fit. This has been now mentioned in the revised version.
b) and c) See responses to general comment 2).
As discussed in Section 4.3.1, two separate models have indeed been used, one with and one without the linear term. The offset (which is actually not constant but increasing over the time period, i.e. representative of a trend) between the both models precisely results from the fact that, in daily data, the solar flux cannot completely compensate the linear term trend because of its strong daily signature. In monthly data, the solar flux and linear trend terms are less distinguishable and we observe a much larger compensation effect: the SF signal is indeed much larger and the offset is consequently not as high as in daily data. This is now better explained in Section 4.3.1 of the revised version.

[6) p.22, lines 486-488. When comparing to the previous publications of the trend analysis, please mention the difference in the time period analyzed. I would replace “in agreement with previous studies” with “comparable to the results published in the previous studies”]
Thanks for pointing that out. It has been changed.

[7) p. 22,line 497 “change ‘was’ to ‘were’] It has been changed.

[8) p.23, line 506, change ‘conducting’ to “leading”] It has been changed.

[9) p.23, line 507-508, add at the end of the sentence “in winter (Table 3)”. Remove the next sentence.] It has been changed.

[10) P. 23, lines 508-510 add “NH” after “in summer”, and “SH” after “in winter”.] It has been changed.

[11) P. 23 lines 511-512. The discussion of the effects of the upper stratosphere temperature trends is important for the trend analysis. Can you please comment on the correlations between daily ozone and Solar flux, ozone and temperature, and possibility to discern temperature contribution to ozone variability from Solar flux in upper layers.]

Previous studies have shown that the various chemical production and loss mechanisms respond to the annual cycles of temperature and of different trace gases (i.e. stratospheric temperature is the main driver of ozone loss within the polar vortex, and this chemical destruction further favours low total ozone and thus less ozone radiative heating and lower stratospheric temperatures) and that all these effects are correlated: Temperature changes are linked to changes in the frequency of stratospheric warmings (e.g. due to QBO-induced secondary circulation, decreasing CO_2 cooling,…); Solar cycle plays a very clear influence on both ozone and stratospheric temperatures variations that are also correlated with the QBO. Please refer for example to Steinbrecht et al. (ACP, 2006) which reported results from a multiple linear regression analysis of both long-term total ozone TOMS observations and long-term temperature reanalyses, accounting for the 11-year solar cycle and QBO effects amongst others.

As mentioned throughout the manuscript, the complexity of the dynamical and chemical processes makes it difficult to unambiguously define simple and independant predictors in a statistical model (e.g. Mäder et al., 2007; Harris et al., 2008). We now mention in the conclusions that effects of changing stratospheric temperatures as well as changes in the Brewer-Dobson circulation should be investigated in a further study.

[12) P.25, lines 553-556.
a) This section discusses the MLT layer (ground-300 hPa). Please clarify what is meant by "As for the upper layers, ...". It is possible that the subject of the discussion has changed, and then it would be better to have a new paragraph.
b) Also, Tables 2 and 3 show negative trend in the IASI MLT layer , but it is stated here that it is in agreement with increases in ozone found in Arctic (Kivi et al, 2007) following changes in Arctic Oscillation. This statement needs further explanation how the negative ozone trend is related to the Arctic Oscillation during 2008-2013 time period.
c) Table 3 title has missing information about the second row of trend results. Please add after daily " (top) and monthly (bottom)", similar to the title in Table 2.]
a) and b) We thank the referee for pointing that mistake. This sentence has been deleted in the revised version.
c) "Same as Table 2" has been indicated in the title instead of repeating the description of Table 2 to shorten the Table 3 title.

[13) Supplemental material: The discussion on the tropospheric ozone variability (MLT) is largely concerned with the stratospheric origin of the tropospheric ozone which is tracked by means of the difference between total and ozone tagged by modeled NOx tracer (Figures S2 and S3). And this is a wonderful addition to the data analysis. However, the reader would also like to understand the contribution of the stratospheric ozone due to the shape of the AK, which is not discussed at all. It should be possible to assess this retrieval error by using truncated AK (zero weights for stratospheric ozone) for smoothing MOZART -4 profiles and then comparing it to the full IASI AK smoothed profiles.]
As suggested by referee #3, we now illustrate in the revised Supplement (Figure S4(a)) the fit of MOZART-4 O_3 and of $O_3^{tagged\_NOx}$ time series, in addition to the stratospheric contribution (Figure S4(b)), without accounting for the IASI sensitivity, to evaluate the effect of the smoothing error from the observational system. We prefer to adopt this approach instead of truncating the AK in the stratosphere, since residual stratospheric contributions will still be

reflected in AK from lower layers. Note also that the smoothing error [(A-I)Sa(A-I)^T] can be evaluated from the a priori contribution [Xa- (AXa)] provided in Figure S5(b) since they are both correlated; i.e., if the IASI sensitivity is low in the MLT, the smoothing error will be large as well as the contributions from the a priori and from the upper layers. When comparing Fig. S4(b) and Fig.S5(b), the differences suggest that the limited vertical sensitivity of IASI contributes a smaller part (~10%-20%) to the IASI stratospheric contribution than the natural stratospheric influence (~20% to 45%). In addition, the contribution of the real natural variability (originating from both the troposphere and the stratosphere through STE processes) into the MLT O_3 columns is also now illustrated in an additional figure (Fig. S6(a) and Fig.2 here below) and is estimated to be larger than 50% everywhere. For example, we interestingly show that in the 30N-50N band where the DOFS is the largest (See Fig.2(b)), this contribution reaches ~85% from which only ~30% originate from the stratosphere (Fig. S4(b)) and ~55% from the troposphere (Fig. S6(b)). This is now specifically mentioned in the last paragraph of Section 2 of the revised manuscript and in the Supplementary materials.

This further supports the findings that IASI is able to detect a large part of the real variability of O_3 in the N.H. troposphere, and that the increase in the observed concentrations and variability in the mid-latitudes N.H. during spring-summer likely indicate a photochemical production of O_3 associated with anthropogenic precursor emissions (Cfr. Section 4.1 of the manuscript).

Technical comments:

[Figure 1 – add a few minor ticks to the altitude axes]
It has been added.

[Figure 5 – "1*sigma" – is it correct expression, or it should be defined as sigma/ (median ozone value)*100?]
It should indeed be defined as [1σ(daily median O_3)/(daily median O_3)*100]. This has been corrected.

[Figure 9. It would be better to separate middle panel into two – for the model fit with and without the linear term. It would then allow for space in the plot to show the residual for both fits separately.]
We prefer to keep the middle panel as it is to more easily compare the regression models with the linear term trend included or not in the regression model and to highlight the increasing offset between the both models. But as suggested by the referee, we have added in the revised Figure 9 a panel illustrating the difference between the two regression models and the averaged relative residuals (%) have been indicated as well.

Table 1 List of the proxies retained in the stepwise backward elimination approach which are significant at the 95% level (see text for details) for each 20-degree latitude bands and for each partial column. Proxies are indicated for Solar flux (blue), QBO10 (green), QBO30 (orange), ENSO (red) and NAO (pink)/AAO (purple). Symbols indicated between parentheses refer to proxies which are not significant statistically when accounting for the autocorrelation in the noise residuals.

Proxies	**Ground-300hPa (Troposphere)**	**300-150hPa (UTLS)**	**150-25hPa (MLST)**	**25-3hPa (UST)**	**Total columns**
70°N-90°N	(O) (O) O O	O(O) O (O)	O (O) (O)O O	(O)O (O) O	O (O) O O O
50°N-70°N	O (O) (O) O (O)	O O (O) O	O (O) (O)O O	(O)(O)	O (O) (O)O O
30°N-50°N	(O) (O) (O)O	O(O)(O)O	O (O) O O(O)	O (O) (O)(O)	O (O) (O)O O
10°N-30°N	(O) (O) (O)	(O)O(O) O (O)	(O)(O)(O)O O	O (O) (O)	O (O) O O
10°S-10°N	(O) O (O) (O)(O)	O O O O O	(O) OO(O)(O)	O O O	(O) O O O(O)(O)
30°S-10°S	(O) (O)(O) (O)	(O)O(O) O (O)	O (O) O O (O)	(O)O O O (O)	(O) (O) O O O
50°S-30°S	(O) (O)(O) O (O)	(O)O(O) O O	O O O (O)	(O)O O O (O)	(O) (O) O O (O)
70°S-50°S	O (O) (O)	(O)O (O) O	(O)(O) O (O) O	(O)O O (O)	(O) (O) O O O
90°S-70°S	(O) O O	(O) O(O) O	(O)(O)(O)(O)(O)	O(O) O	(O)(O)(O)(O)(O)

Figure Caption

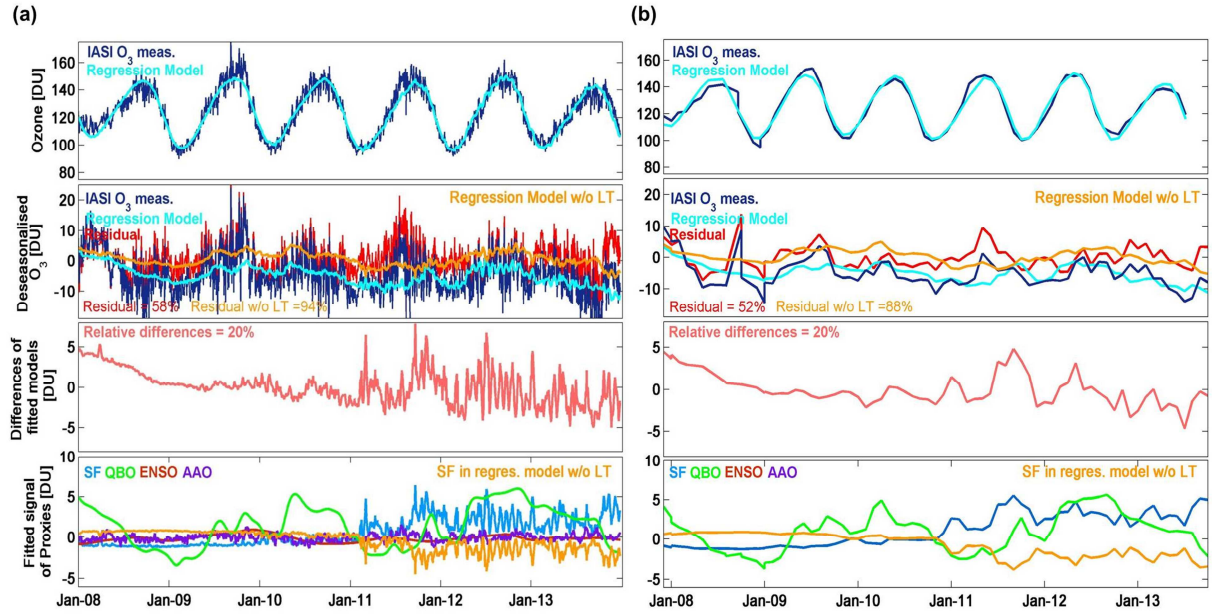

Figure 1. Daily (a) and monthly (b) time series of O_3 measurements and of the fitted regression model in the UST in the 30°S-50°S latitude band (top row), of the deseasonalised O_3 (2^d row), of the difference of the fitted models with and without the linear term (3^d row), and of the fitted signal of proxies ([regression coefficients*Proxy]): SF (blue), QBO (QBO^{10} + QBO^{30}; green), ENSO (red) and AAO (purple) (bottom) (given in DU). The averaged relative residuals are also indicated (%).

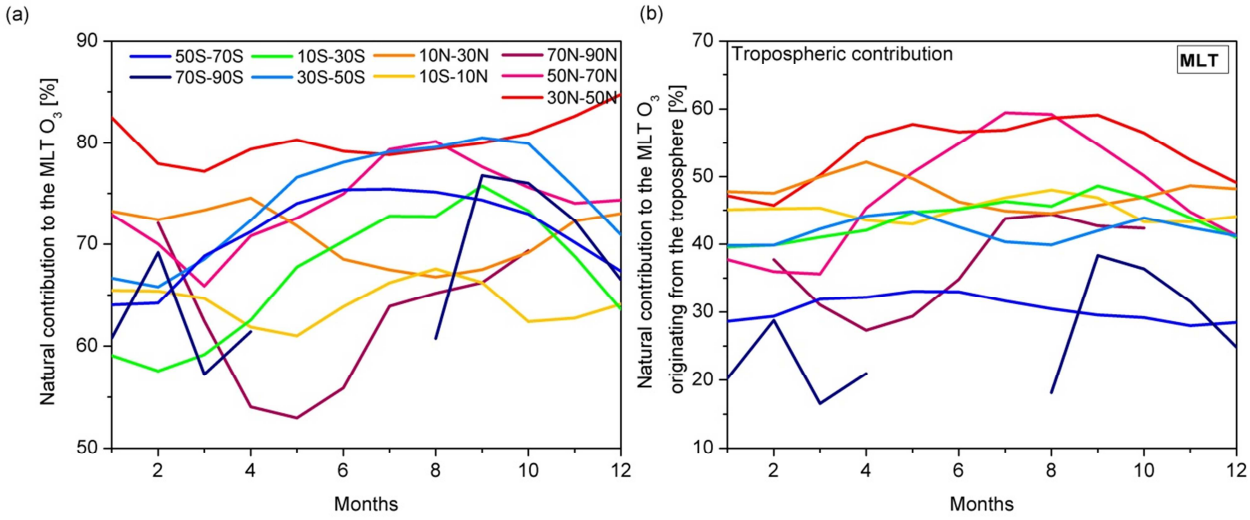

Figure 2: Contribution to the IASI MLT O_3 columns (%) (a) of the natural variability (troposphere and stratosphere) and (b) from the troposphere.

Response to Reviewer #2:

Review

First of all, we thank the referee for his positive general comments about the paper. We acknowledge him for his useful corrections and suggestions, which have helped us clarifying several points and improving the manuscript.

Below are developed our point-by-point responses to his individual comments. Before each response, the reviewer comments have been quoted between []. Corresponding information and corrections have been added to the revised version of the manuscript. Technical comments are also included in the revised version.

General Comments:

[1) This investigation is well done in general but fails to account for lags between the geophysical quantities such as QBO and ENSO and ozone variability in non-local regions.]
A typical time-lag relation between ozone and ENSO from 0 to 4 months was examined before the submission of the paper, but it did not show any improvement in terms of residuals and uncertainty of the fitted parameters. We interpret this by a weak apparent contribution of ENSO to the IASI ozone time series in zonal bands outside the Niño region 3.4. This is now specifically mentioned in Section 3.2.

Optimizing the regression model by including time-lags in different geophysical variables could be investigated in the future but this is beyond the scope of this study.

We acknowledge, however, in the revised Section 4.2 that the missing representation of time lags in the proxy times series may lead to underestimating the influence of some geophysical parameters on the O_3 variations, in particular that of ENSO and QBO in zonal bands outside the regions where these geophysical quantities are measured (i.e. Niño region 3.4 for ENSO and Singapore for QBO). The fact that the regression model could be improved this way is now also mentioned in the Conclusion.

[2) Following this analysis, the authors make a fairly convincing argument that the density of the IASI measurements allows for trend analysis even over short timescales, though the comparison between FTIR instruments and IASI should be more carefully done.]
We thank the referee for his suggestion. As one can expect from the FTIR measurements illustrated on Figure 10 of the manuscript, IASI time series with the same sampling as the ones of the FTIR leads to non-significant trends. This has been tested by applying the regression models on a subsampled IASI dataset with the same temporal resolution as that of the FTIR datasets. In all cases, we observe that the fitted trends inferred from IASI and FTIR are within the uncertainties of each other and that the uncertainties associated with the subsampled IASI datasets are significantly larger than the ones with the full daily dataset. These trend values have been added in Table 4 of the manuscript and this is mentioned in the revised Section 4.3.3.

We now conclude this section 4.3.3 with:

"Even if validating the IASI fitted trends with independent datasets is challenging due to the short-time period of available IASI measurements and the insufficient number of usable correlative measurements over such a short period, the results obtained for trends inferred from IASI *vs* FTIR tend to confirm the conclusion drawn in subsections 4.3.1 and 4.3.2, that the high temporal sampling of IASI provides good confidence in the determination of the trends even on periods shorter than those usually required from other observational means."

[3) The paper includes supplementary information with a model analysis aimed at quantifying how much the tropospheric ozone signal seen by IASI is "contaminated" by stratospheric ozone. It is unclear to me, however, that their approach quantifies how much of the tropospheric ozone that IASI sees is stratospheric due to the "smearing" of the averaging kernels (what they are trying to quantify) versus stratospheric air that has actually been transported into the troposphere.]

There are indeed two combined effects in the stratospheric contribution as seen by IASI in the troposphere: 1) the stratospheric influence simply calculated as the difference between the total simulated O_3 and the $O_3^{tagged\_NOx}$ and 2) an additional part due to the limited vertical sensitivity of IASI in the troposphere; the latter is accounted for by applying the IASI averaging kernels on the MOZART4 stratospheric contribution. This simulates the stratospheric part as observed by IASI in the troposphere. This is now better explained in the Supplement.

In addition, as suggested by both referees #1 and #3, we now illustrate in the revised Supplement (Figure S4a), the fit of MOZART-4 O_3 and of $O_3^{tagged\_NOx}$ time series, in addition to the stratospheric contribution (Figure S4b), without accounting for the IASI sensitivity to evaluate the effect of the smoothing error from the observational system (effect 2)). Note also that the smoothing error $[(A-I)Sa(A-I)^T]$ can be evaluated from the a priori contribution [Xa- (AXa)] provided in Figure S5(b) since they are both correlated; i.e., if the IASI sensitivity is low in the MLT, the smoothing error will be large as well as the contributions from the a priori and from the upper layers. When comparing Fig. S4(b) and Fig.S5(b), the differences suggest that the limited vertical sensitivity of IASI contributes a smaller part (~10%-20%) to the IASI stratospheric contribution than the natural stratospheric influence (~20% to 45%). In addition, the contribution of the real natural variability (originating from both the troposphere and the stratosphere through STE processes) into the MLT O_3 columns is also now illustrated in an additional figure (Fig. S6a) and is estimated to be larger than 50% everywhere. For example, we interestingly show that in the 30N-50N band where the DOFS is the largest (See Fig.3b), this contribution reaches ~85% from which only ~30% originate from the stratosphere (Fig. S4b) and ~55% from the troposphere (see Fig. S6(b) or Fig. 1 here below). This is now specifically mentioned in the last paragraph of Section 2 of the revised manuscript and in the Supplementary materials.

This further supports the findings that IASI is able to detect a large part of the real variability of O_3 in the N.H. troposphere, and that the increase in the observed concentrations and in the variability in the mid-latitudes N.H. during spring-summer likely indicate a photochemical production of O_3 associated with anthropogenic precursor emissions (Cfr. Section 4.1 of the manuscript).

Specific comments:

[1) Abstract
a) Page 27576, Line 3: Should there be a “the” before MetOp-A?
b)Page 27576, Line 5: “time development” is a little awkward – “temporal evolution” would be better.
c) Page 27576, Lines 15-19: The attribution of the trends is somewhat overstated in the abstract as compared to the paper. Perhaps “which is consistent with other studies suggesting a turnaround for stratospheric O3 recovery” and “possibly linked to the impact of decreasing ozone precursor emissions” would be more appropriate.]
a), b) and c) All corrections have been made.

[2) Introduction
a) Page 27577, Line 7: Suggest replacing “present” with “undergoes”.
b) Page 27578, Lines 17-18: The wording is difficult to follow. I suggest “by the possibility of using IASI measurements to discriminate O3 distributions.”]
a) and b) All corrections have been made.

[3) Section 2
a) Page 27579, Line 16: Given IASI’s 9:30 / 21:30 overpass time, I would not expect it to be as sensitive to changes in precursor emissions as instruments with afternoon overpass times. Have you used a model to assess this and what implications the overpass time might have in terms of quantifying the true trend associated with decreases in precursor emissions?
b) Page 27581, Lines 8-17: Please see comments on the supplementary material. It is unclear to me whether the model analysis the authors performed actually quantifies how much of the tropospheric ozone that IASI sees is stratospheric due to the “smearing” of the averaging kernels (what they are trying to quantify) versus stratospheric air that has actually been transported into the troposphere.]
a) The overpass time should not have such an impact due to the long lifetime of O_3 in the mid- and upper troposphere where the IASI sensitivity is the largest.
b) See general comment 3). This is now better explained in the Supplement.

[3) Section 3
a) Page 27581, Lines 20-21: Why just ODS-driven trends here? The authors are not specifically talking about stratospheric ozone, and in fact address tropospheric ozone trends driven by precursor emissions. Also, in both instances in this sentence, “trend” should be preceded by “the” or should be plural.
b) Page 27582, Lines 9-14: It would be very helpful if the authors could provide more detail here. Why was the time lag for the autocorrelation of the residuals assumed to be 1 day or 1 month? Given the lifetime of ozone, might it not be longer? What method was used to correct the coefficient estimates by accounting for this autocorrelation?
c) Page 27582, Lines 14-15: “robust” would be more accurate than “adequate”
d) Page 27583: In the analysis using geophysical variables, the zonal wind at 10 and 30hPa are used to represent the QBO. However, it is the QBO shear rather than the zonal wind itself that strongly affects the zonal distribution of ozone, which responds primarily to the anomalous QBO thermal wind circulation cell driven by the zonal wind gradient. While the temporal evolution of the shear is generally consistent with the temporal evolution of the zonal wind itself, there can be

important differences when the descent of a particular QBO phase is delayed or occurs faster than usual. The authors may want to compare the time series of the shear to that of the individual wind components to determine whether using the shear time series might make an important difference in their results.
e) Page 27583, Line 17: What is meant by “both components” here?
f) Page 27583, Line 27: “there is a” is needed before “predominance of easterlies”
g) General comment on Section 3: For many of the geophysical variables considered here, there may be important lags between the geophysical quantity and the ozone response in particular parts of the atmosphere. Lower stratospheric ozone in midlatitudes, for example, does show a QBO signal, but it lags the QBO winds in the tropics by a few months. Likewise, midlatitude ozone does not respond within a month to ENSO changes in the tropics. Optimizing the regressions including the possibility of time lags may be too involved for this paper, but the authors should at least acknowledge that they may be underestimating the role of geophysical variables in regions outside the location of the geophysical quantity for QBO, ENSO, NAO, and AAO.]

a) This sentence has been rewritten:
” In order to characterize the changes in ozone measured by IASI and to allow a proper separation of trend, …”

b) We calculated the uncertainty of the fitted parameters by computing the standard error with an effective sample size (n*) of independent information based on the lag-1 autocorrelation coefficient correlation of the noise residual ($n^* = n \cdot \frac{1-\Phi}{1+\Phi}$) as in Santer al. (2000).This is now better explained in Section 3.1 of the revised version with the Eq. (3).

The autocorrelation coefficients at various lags were examined for each layer in each latitude bands (cfr example for the 30N-50N band provided in Table below) and lag 1 appeared to be the most important in all cases. As a consequence, a time lag of one day (or one month) has been preferred to account for the correlation of the noise residuals.

30N-50N	*lag1*	*lag2*	*lag3*	*lag4*	*lag5*
MLT	**0.65**	0.54	0.49	0.47	0.44
UTLS	**0.62**	0.48	0.40	0.36	0.29
MLST	**0.75**	0.64	0.56	0.50	0.44
UST	**0.80**	0.68	0.62	0.56	0.49
TOTAL	**0.78**	0.69	0.62	0.58	0.54

c) This has been changed.
d) We thank the referee for his suggestion.
However, to the best of our knowledge, the time series of monthly averaged wind speed measurements done by the ground-station in Singapore is the most widely used proxy for the quasi-biennial oscillation (QBO). Previous studies on QBO have shown that the longitudinal differences in the phase of the QBO are small (e.g. Baldwin et al., 2001 and references therein), and, as a consequence, the dataset used in this study is supposed to represent well the equatorial belt.

We agree with the referee that analyzing the structure of the QBO by comparing the QBO shear with the zonal wind would be interesting. We feel however that this is beyond the scope of this study.

[Baldwin, M.P., L.J. Gray, T.J. Dunkerton, K. Hamilton, P.H. Haynes, W.J. Randel, J.R. Holton, M.J. Alexander, I. Hirota, T. Horinouchi, D.B.A. Jones, J.S. Kinnersley, C. Marquardt, K. Sato, and M. Takahashi, 2001: The Quasi-Biennial Oscillation. Reviews of Geophys., 39, 179-229.]

e) This is now specified: "The difficulty in discriminating solar flux and linear trend terms…".
f) It has been added.
g) See responses to General comment 1).

[4) Section 4
a) Page 27587, Line 16-18: Why don't we see ozone depletion in the Southern hemisphere stratosphere?
b) Page 27587, Lines18-19: There appears to be a difference between the Northern and Southern hemispheres in terms of how similar the 10 km panel is to the 19 km panel. Is this the case? What is the reason for the asymmetry?
c) Page 27587, Lines 10-26: What is the source of the noise at high latitudes?
d) Page 27588, line 3: It would be much clearer to say "color contours" rather than "colorscale"
e) Page 27588, lines 8-14: High midlatitude lower stratospheric ozone values in 2010 have been linked to the combined Easterly shear QBO and El Nino (Neu et al., Nature Geosci., 2014), and the failure to reproduce them with the regression may also be due to 1) the use of the zonal wind as a QBO proxy rather than the shear in the zonal wind and / or 2) the failure to account for lags between the QBO and ENSO and the response of midlatitude tratospheric ozone.
f) Page 27589, Lines 20-21: Is it clear that the spring maxima solely reflect STE, or is there also a seasonal dependence of the averaging kernels that makes the lower atmosphere more sensitive to the layers above during spring?
g) Page 27591, Lines 5-14: The QBO results for the midlatitudes may differ substantially if a lag were considered. The authors should at least acknowledge that by using zonal winds rather than shear and not considering a lag, they likely underestimate the QBO's importance in regions not directly impacted by the QBO winds.
h) Page 27591, Lines 15-22: The negative ENSO coefficient in the tropical UTLS is consistent with results from Neu et al., Nature Geosci., 2015.
i) Page 27592-27593, Lines 24-1: I don't understand what the percentages refer to here.
j) Page 27594, Line 14: need an "increase" in "reports a factor of two in"
k) Section 4.3.3: I am not sure I agree with the conclusions presented here. The authors show that total column trends from FTIR data and from IASI over different time periods do not agree and use this to argue that the sampling of IASI provides confidence in the determination of trends. However, to actually reach this conclusion, they would need to show that trends between IASI sub-sampled at the same times and locations as the FTIR measurements are consistent with those from the FTIRs (i.e. non-significant) for the overlapping period of the data (2008-2012). Only by doing so can they demonstrate the advantage of IASI sampling and show that it explains the difference between IASI and the FTIR measurements.]
a) As mentioned in Section 2, only daytime observations which are characterized by a good vertical sensitivity to the troposphere are used in this study. As a result, we do not include in this

study the variations due to the ozone hole formation (also mentioned in Section 4.2), which is otherwise well monitored by IASI using night-time measurements.
b) We observe indeed an asymmetry between the contribution of the MLST into the UTLS in the N.H. and the S.H. A deeper analysis of the correlation between the MLST and the UTLS layers as a function of IASI sensitivity and dynamics should be investigated to explain this observation. The stratosphere-troposphere exchanges could be part of the answer since they are expected to be larger in the N.H. than in the S.H. There are also significant hemispheric differences in the strength and behavior of the Brewer-Dobson circulation, which is usually the largest in the N.H., because of hemispheric differences in wave forcings. The use of a stratospheric chemical and transport model could help in quantifying this effect, but this is beyond the scope of the study.
c) This is because of the low temporal sampling of daytime IASI measurements in high latitudes.
d) It has been changed.
e) We thank the referee for pointing that out. These possible explanations have been added in the revised paper.
f) It is more probably related to the STE processes. There is indeed a seasonal dependence of the averaging kernels but the sensitivity is the lowest in the winter (implying more information coming from the stratosphere), not in spring.
g) See responses to General comment 1). This is now specified in this Section 4.2.
h) We thank the referee for pointing this reference which has been added.
i) The percentages represent the averaged fitted model residual relative to the IASI O_3 time series. This is now better explained.
j) It has been changed.
k) The influence of the FTIR temporal sampling on IASI is now tested in the revised paper. See general comment 2).

[5] Tables and Figures
Table 2: Caption is very unclear – it should say “based on daily (top values) and monthly (bottom values)”]
It has been changed.

[6] Supplementary Material
a) Lines 19-21: Why use constant emissions, particularly when the goal is investigate variations in ozone with time? Also, it is not clear whether the emissions are truly constant or simply have no interannual variability.
b) Lines 30-32: Are representative averaging kernels used, or scene-dependent averaging kernels?
c) Lines 37-40: This goes back to the previous question – if the averaging kernels underestimate the stratospheric influence on the partial column this could produce a bias.
d) Lines 47-48: One might expect the model to perform better in the southern hemisphere since the fire emissions do vary with time, but it isn’t clear that this is the case. Why not?
e) Section S.3: Given the large difference between the model and IASI, are the IASI averaging kernels (which must depend on ozone amount) still applicable to the model profiles? Also, the authors are using the difference between total ozone and the tagged ozone in MOZART (with the IASI averaging kernels) as a measure of the stratospheric influence on tropospheric ozone as seen by IASI. However, this term includes both stratospheric air that has been transported to the troposphere and the “smearing” of the stratospheric signal into the troposphere by the averaging

kernels. I understood the point of this analysis to be to understand how much the IASI tropospheric column is "contaminated" by stratospheric ozone due to the averaging kernels rather than to understand how much stratospheric ozone matters for tropospheric ozone variability. In this case, wouldn't a better measure be the difference in the difference between total ozone and tagged ozone with and without the IASI averaging kernels?
f) Line 76: The sentence beginning "This method allows" should be reworded.
g) Line 110: Again, I am confused as to whether the emissions have no variability at all or simply no interannual variability.
h) Lines 120-122: I don't think it's clear from this analysis that the decrease in tropospheric ozone is "much more important than what we estimate from IASI". The emissions-driven portion of it may be, but tropospheric ozone is a mixture of the emissions-driven ozone and ozone that enters through STE, and the authors have not convincingly shown that the "true" trend in this mixture of air is significantly larger than that observed by IASI (because they have not fully separated the influence of STE and the averaging kernels)]

a) As mentioned in the Supplement, the anthropogenic emissions have no variability at all, they are constant over years. On the contrary, biomass burning and biogenic emissions vary seasonally. This is now clearly mentioned in the revised supplement and a reference for the biogenic emissions has been added.

We have preferred the POLMIP emission dataset in this study because it has been built to represent as well as possible the anthropogenic emissions, particularly in the N.H.. The use of the POLMIP dataset in POLMIP models, amongst with MOZART-4, has also been extensively evaluated recently (Monks et al., ACP, 2014; Arnold et al., ACP, 2014; Emmons et al., ACP, 2015). The description of the dataset has been extended in the Section S1 of the revised Supplement.

b) We used the scene-dependent averaging kernels. Similarly to Wespes et al. (2012), the AvK of the different IASI observations contained in each MOZART grid have been considered to smooth the gridded MOZART profile interpolated on the IASI profile. This is now indicated in the Supplement.
c) See general comment 3). Because the IASI sensitivity is excellent in the stratosphere and smaller in the troposphere, the averaging kernels rather overestimate the stratospheric influence on the MLT column. This is now better explained in the Supplement and illustrated with Figures S4 and S5.
d) Large fire emissions are also observed in the N.H. (e.g; the fire NO emissions in the N.H. represent more than 60% of the global NO fire emissions in the POLMIP dataset; Siberia, South-East Asia and China regions account for ~30% of the total NO fire emissions). We relate the large positive bias of MOZART-4 in the MLT in equatorial belt (~25%) and extra-tropical regions in the Supplement to possible issues with horizontal transport in the model or overestimated ozone production efficiency at these latitudes.
e) See general comment 3). The stratospheric influence without accounting for the IASI averaging kernels is now shown in Fig. S4 of the Supplement and the MLT variability originating from the troposphere as seen by IASI is now quantified and illustrated in Fig. S6 and in Fig.1 here below.
f) This has been changed.
g) See comment 6a) above.

h) See general comment 3) and specific comment 6e) above. The conclusions in the Supplement have been rewritten accordingly.

Figure caption

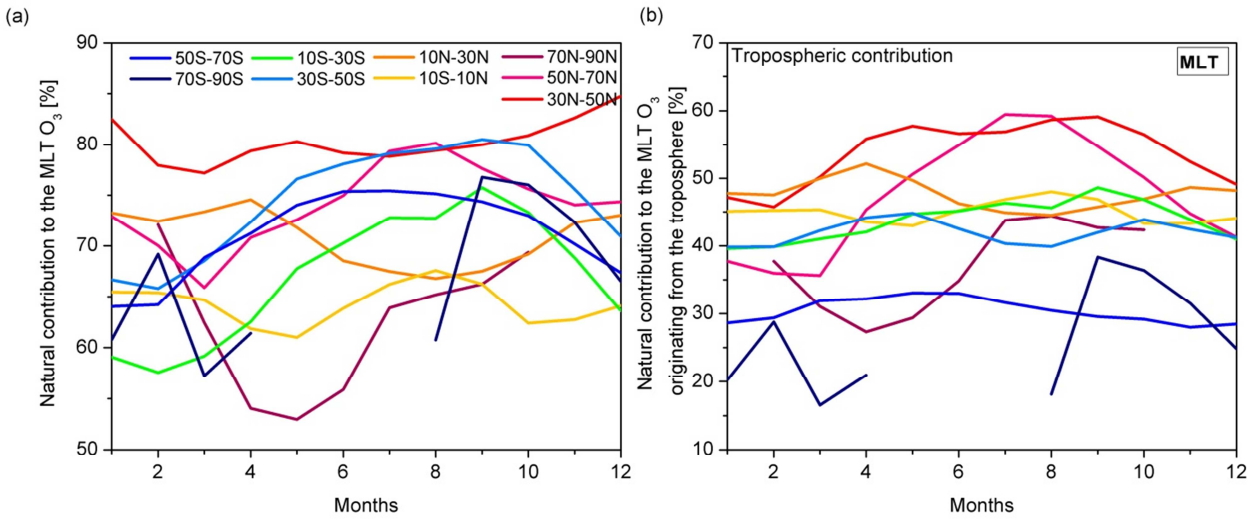

Figure 1: Contribution to the IASI MLT O_3 columns (%) (a) of the natural variability (troposphere and stratosphere) and (b) from the troposphere.

Response to Reviewer #3:

Review

We thank the referee for his useful comments, which have helped us clarifying several points and improving the manuscript. Below are our point-by-point responses to his comments and suggestions. Before each response, the reviewer comments have been quoted between []. Corresponding information and corrections have been added to the revised version of the manuscript.

General Comments:

[1) The motivation for the choice of conducting a multivariate regression to understand the variability observed is not very clearly explained. I guess its main purpose is to be able to eventually extract trends from the full signal, is that right? Section 4.2, providing the detail of each fitting parameter, is missing conclusion comments to guide the reader through the interest of all this work on large datasets. For example: what amount of variability is explained by each process included/fitted. Can it be a way to efficiently analyze controlling processes without using model simulations?]

The use of a multivariate regression model is a commonly and widely used method for analyzing variations in ozone columns records. The goal of the method is to attribute inter-annual, seasonal and non-seasonal variations in ozone measurements to physical processes that are known to affect the ozone records, and, as a consequence, to allow a proper separation of a trend. This is mentioned in the first paragraph of Section 3.1.

Section 4.2 relies on the fact that the multivariate regressors patterns, uncertainties and residuals errors have first to be examined to evaluate the performance of the model before drawing any conclusions on processes controlling the variations in IASI ozone record, including a trend analysis. This is now clearly mentioned in the first paragraph of Section 4.:

"The performance of the multiple linear model is evaluated in subsection 4.2 in terms of residuals errors, regression coefficients and associated uncertainties determined from the regression procedure (Section 3) to properly characterize the physical processes that are expected to affect the IASI ozone records"

Numbers quantifying the contribution of the various physical processes on the measured IASI O_3 records have been added in the description of Fig. 8 (b) in Section 4.2. A conclusion on the model performance is also given at the end of this Section:

"Our results demonstrate the representativeness of the fitted models in each layers and latitude bands. These good performances of the model allow examining the adjusted linear term trends in Section 4.3 below."

[2) The authors have chosen to provide an analysis of several altitude levels, chosen according to the IASI sensitivity profiles (provided by the averaging kernels). In Section 2 the IASI retrieval, the AK and associated DOFs are discussed, as well as the correlations between the observed concentrations and the a priori information used as an initial constrain. Although this

contribution is around 20-30Also, in Figure 1 the averaging kernels for the selected layers show significant overlap, so that all levels are not independent. This is mentioned throughout the paper but it would really be helpful to provide information on the vertical correlations between vertical levels in IASI. The authors discuss this problem in the supplemental material but I think that there are 2 effects combined in their discussion: the natural influence of the stratosphere on the tropospheric levels through STE, which has to be accounted for to understand observed variability of tropospheric O3 from any type of measurement; and the smoothing from the observational system used here. It is the later that is particularly critical because it may cause artefacts in the trends compared to what would be obtained using in situ observations for example. I guess it would be quite easy to evaluate this effect using the MOZART simulations and the stratospheric O3 tracer with and without applying the IASI AK. Another related question: could correlations in the observations be mistaken for dynamical processes (strat-trop exchanges) in the trend analysis? Because this part is confusing, the fact that tropospheric ozone from IASI can be used for trend analysis is still somewhat questionable after reading this paper... I think this could be easily improved.]

As mentioned by the referee, there are indeed two combined effects in the stratospheric contribution as seen by IASI in the troposphere: 1) the stratospheric influence calculated as the difference between the total simulated O_3 and the $O_3^{tagged\_NOx}$ and 2) an additional part due to the limited vertical sensitivity of IASI in the troposphere; the latter is accounted for by applying the IASI averaging kernels on the MOZART4 stratospheric contribution. This simulates the stratospheric part as observed by IASI in the troposphere. This is now better explained in the Supplement.

In addition, as suggested by referees #1 and #3, we now show in the revised Supplement (Figure S4a), the fit of MOZART-4 O_3 and of $O_3^{tagged\_NOx}$ time series, in addition to the stratospheric contribution (Figure S4 b), without accounting for the IASI sensitivity. This is done to evaluate the effect of the smoothing error from the observational system. Note also that the smoothing error $[(A-I)Sa(A-I)^T]$ can be evaluated from the a priori contribution [Xa- (AXa)] provided in Figure S5(b) since they are both correlated; i.e., if the IASI sensitivity is low in the MLT, the smoothing error will be large as well as the contributions from the a priori and from the upper layers. When comparing Fig. S4(b) and Fig.S5(b), the differences suggest that the limited vertical sensitivity of IASI contributes a smaller part (~10%-20%) to the IASI stratospheric contribution than the natural stratospheric influence (~20% to 45%). In addition, the contribution of the real natural variability (originating from both the troposphere and the stratosphere through STE processes) into the MLT O_3 columns is also now illustrated in an additional figure (Fig. S6(a) and Fig.2 here below) and is estimated to be larger than 50% everywhere. For example, we interestingly show that in the 30N-50N band where the DOFS is the largest (See Fig.2(b) in the manuscript), this contribution reaches ~85% from which only ~30% originate from the stratosphere (Fig. S4(b)) and ~55% from the troposphere (Fig. S6(b) and Fig.1(b) here below). This is now specifically mentioned in the last paragraph of Section 2 of the revised manuscript and in the Supplementary materials.

This further supports the findings that IASI is able to detect a large part of the real variability of O_3 in the N.H. troposphere, and that the increase in the observed concentrations and variability in the mid-latitudes N.H. during spring-summer likely indicate a photochemical production of O_3 associated with anthropogenic precursor emissions (Cfr. Section 4.1 of the manuscript).

Nevertheless, and as mentioned at the end of Section 2 of the manuscript and in conclusions of the Supplementary materials, we acknowledge that both the apriori and the stratospheric contributions resulting from the limited sensitivity of IASI partly mask the variability of tropospheric ozone measured by IASI and may bias the real trend in tropospheric O_3.

[3] Regarding the general performance of the fitting procedure: the figure (Fig. 4) is hard to read. Later in the study, the residuals are shown to actually be quite large (Figs 9 and 10): does this mean that significant processes are not considered? The performance should be better described and discussed at the beginning of section 4.2, with a dedicated figure.]
The figure has been provided at a high resolution and is in our opinion fully readable. The performance of the model is described throughout the manuscript, in Section 4.2 in terms of the covariates with the associated uncertainties, in Section 4.3.1 in terms of temporal sampling effect (daily vs monthly) and in Section 4.3.2 in terms of trend uncertainties.

As mentioned in Section 2, model residuals are less than 10% of the IASI O_3 measurements and good correlation coefficients between the IASI and the regression model time series (0.70-0.95) are obtained for all layers and all latitude bands. The residuals represent generally around 30-60% of the deseasonalised O_3 time series. This is now specifically mentioned in Section 4.3.1. This might seem quite large but this has to be mitigated by the fact that the non-seasonal variations are only minor contributors. Similar residuals have been reported in previous studies, suggesting that the regression model and the method applied here on IASI time series perform generally well.

We acknowledge however, that the model could be improved in several ways (e.g. including Eliassen-palm flux, EESC proxies) to further reduce the regression residuals. Further investigations on the regressors uncertainties and the total error on ozone measurements should be performed as well. This is now indicated in the Conclusion.

[4] Another point that needs to be improved: throughout the paper, the authors attribute enhanced lower tropospheric ozone to ozone production from anthropogenic emissions. But there are not only anthropogenic emissions that will contribute to lower tropospheric production, biogenic emissions and fires, for example, will also emit significant O3 precursors. This attribution to anthropogenic activities is not really demonstrated. The comparisons to MOZART-4 simulations in the supplemental material is not that convincing: constant anthropogenic emissions are used, but with daily fire emissions. For the 'realism of anthropogenic emissions', the authors should provide some numbers on previous model evaluations against surface networks. Are there more uncertainties on anthropogenic emissions than on natural emissions? What about stratosphere-troposphere exchanges: is it well simulated by models? Has it been evaluated?]
Previous studies showed good evidence for an increase in tropospheric ozone downwind industrialized areas of the N.H. with a summer maximum and argue that this is due to high photochemical activity associated with anthropogenic emissions of NO, hydrocarbons and CO from combustion of fossil fuels (e.g. Logan et al., 1985; Fusco and Logan, 2003; Dufour et al., 2010; Cooper et al., 2010; Wilson, et al., 2012; Safieddine et al., 2013). Even if it is hard to reconcile the trends in tropospheric ozone with changes in emissions of ozone precursor, trends in emissions have already been able to qualitatively explain measured ozone trends over some

regions although the magnitude of the trend is not consistent with that from model simulations (e.g. Cooper et al., 2010; Logan et al., 2012; Wilson et al., 2012). This has been specifically added in the last paragraph of Section 4.3.2.

The anthropogenic emissions for NO_x and CO are much larger than the fires and biogenic emissions, and they have the largest contributions in industrialized regions of the N.H. (Europe, US, China). In the POLMIP emissions used in this study, the anthropogenic NO_x emissions represent 72% of the total NO_x (see Emmons et al. ACP, 2015) while the fire and soil NO_x emissions only represent 11% and 12% of the total, respectively. For CO, the anthropogenic emissions are also larger than the biomass and the biogenic emissions (~60% *vs* ~30% and <10%, respectively). On the contrary, the biogenic NMVOC (non-methane organic volatile compounds) emissions represent the largest contribution to the total NMVOC (~80%). This is added in Section 4.1.

The MOZART4-GEOS5 model has been evaluated against surface, ozonesondes and aircraft measurements in previous studies (e.g. Emmons et al., 2010; 2013; 2015; Pfister et al., 2008; Wespes et al., 2012). Result indicated that MOZART-4 is slightly biased low by around 5-15%, but that it reproduces generally well the variability of observations in space and time. This is now indicated in the Supplement.

The stratosphere-troposphere exchange is well known to be a common problem in global chemistry-transport models. However, we showed on Fig. S1 of the supplement that the concentrations, the amplitudes of the seasonal cycles and the timing of the maxima are well captured in MOZART4 in the UTLS region for all bands between 50S-50N. We also note that the stratospheric contributions are calculated to be the lowest in the bands south of 50° of the N.H. (~20% in summer in 30°N-50°N; See Fig. S4(b) of the Supplement) and that the stratosphere-troposphere exchanges are usually the weakest during the summer. As a consequence, this even reinforces the conclusion made about the ability of IASI to detect the variations in O_3 MLT columns, particularly in mid-latitudes of the N.H. This has been now specifically mentioned in Section 4.1.

[5) My final main comment is that the discussions generally lack quantitative comparisons to other studies. It is generally written that there is a 'good agreement' in trends but it would be interesting to provide orders of magnitude: maybe with a final table comparing results depending on the method chosen?]
As suggested by referee#1, when comparing to the previous publications of the trend analysis, "in agreement with previous studies" has been replaced by "comparable to the results published in the previous studies" throughout the paper. Quantitative comparisons cannot be made considering the different time period in our study with respect to others.

In addition, as suggested by the referee in his specific comments below, trend values and temporal resolutions of measurements from previous studies have been added in the discussion in Section 4.3.2 and we also now provide comparisons between trends inferred from a subsampled IASI dataset to match the temporal sampling of FTIR. The results are added in Table 4 of the revised manuscript. These new results show that fitted trends inferred from IASI and from FTIR are within the uncertainties of each other and that those associated with the

subsampled IASI datasets are significantly larger than those obtained from the daily ones, leading to statistically non-significant trends. This gives further evidences for the ability of IASI, thanks to its high temporal sampling, to detect statistically apparent trends even on short periods.

Specific comments:

[1) Introduction:
a) P. 27577, l. 21: Why are there warnings? Only because too many unknowns or are their specific reasons?
b) P. 27578: 1st paragraph: It would be helpful to provide a few numbers for trends identifies in previous studies. Are the signs consistent? What were these studies based on? Observations at what resolution? etc.]
a) Warnings are mostly related to possible underestimation of the true uncertainties in the ozone trends that can be attributed to decreasing EESC. This has been added in the revised text.
b) It has been added. Numbers for trends from previous papers are now given later in the manuscript in Section 4.3.

[2) Section 2: Cf. main comment: a better evaluation of vertical correlations is the observations is required. Also provide information on the a priori used for the retrieval. The last sentence is disturbing and does not really help the reader. . . It would be good to confront each result to the identified sources of uncertainties in the discussion parts.]
See responses to general comment 2) above. The last sentence has been changed accordingly. The apriori and stratospheric contribution are now discussed as well in the discussion Section 4.1.

Information on the a priori has been added in Section 2:
"The a priori information (a priori profile and a priori covariance matrix) is built from the Logan/Labow/McPeters climatology (McPeters et al., 2007) and only one single O_3 a priori profile and variance-covariance matrix are used."

[3) Section 3:
a) Define ODS
b) l.12-13, P.27582: I am not an expert in this type of statistical analysis but I just don't get what this means. Maybe a little bit more explanations would be helpful.
c) Table 1 and corresponding text: the source of the data used should be detailed for all proxies: are they from model simulations? reanalyses? observations?
d) Sentence btw P. 27584-P. 27585: Would be good to detail briefly why harmonic and linear trends are appropriate for these effects, since these are among the main targeted features of the analysis.]
a) ODS is defined in Section 1.
b) We calculated the uncertainty of the fitted parameters by computing the standard error with an effective sample size (n*) of independent information based on the lag-1 autocorrelation coefficient correlation of the noise residual ($n^* = n \cdot \frac{1-\Phi}{1+\Phi}$) as in Santer al. (2000).This is now better explained in Section 3.1 of the revised version with the Eq. (3).
c) Details for the proxies have been added in the text.

d) The choice of using “statistical” harmonic and linear terms instead of “physical” proxies in the backward elimination approach is widely applied in previous ozone regression studies (e.g. Mäder et al., 2007; 2010). Physical proxies for the Equivalent Effective stratospheric chlorine (EESC) and for the Eliassen-Palm (EP) flux could be used for describing changes in ozone depleting bromine and chlorine substance and in the Brewer-Dobson circulation instead of the linear trend and harmonic terms. As explained in Section 3.2, the use of the EESC proxy could be an interesting alternative, in particular for the measurements starting before the turnaround point for the ozone hole recovery in 1996/1997. This would avoid adjusting two LT terms (one before and one after the turnaround).

[4) Section 4:
a) Also, the discussion should include reminders about expected uncertainties (that had to be kept in mind). For example P. 27586, last paragraph about the results in the tropics: what about the large contribution from the a priori? Does it matter in this discussion of the variability?
b) Several mention of the impact of anthropogenic emissions that has not been demonstrated: what about other sources? (Cf. comments above)
c) Section 4.2: Cf comments above about the residual. A lot of the processes have already been identified in the previous description of the O3 variability. This description could be a lot shorter, avoiding repetition. More importantly, it would be helpful to clearly explain why the regression is performed and what we learn with the coefficients plotted, what we learn in terms of O3 variability.
d) P.27589, last sentence: this statement seems really strong and is not well demonstrated. MOZART4-GEOS5 has probably already been compared to surface observations of O3 and NO2 in many regions, very probably providing a better evaluation of the quality of the anthropogenic emissions. Authors could provide a few numbers from the literature here.
e) P.27590, l. 13-14: Unless I missed it, this is the 1st mention of these numbers regarding the performance of IASI. This should be in section 2. And in this section, the authors should explain if the findings are still relevant considering this uncertainty (bias in this case).
f) It would be helpful to add a short conclusion at the end of section 4.2 to clearly explain how/if the multivariate regression approach provided original information, or if it is mainly used to get rid of other factors than the trends the authors are aiming at identifying.
g) Section 4.3.1: Results only discussed here for the US layer. What about other layers? Similar conclusions (I guess) or less critical to have daily obs? What about previous studies cited throughout the paper: what temporal resolution are they using?
h) Section 4.3.2: Provide numbers for trends obtained in the literature (cf general comment above).
i) Section 4.3.3: Are trends consistent if the full IASI dataset or IASI at the FTIR location is used? Hence: do we really need such high coverage to conclude? For regions where trends are insignificant if inferred from FTIR: same result if IASI used only when FTIR observation is available?]
a) We thank the referee for pointing that out. The discussion related to Fig.4 has been now extended to include the effect of the a priori contribution:
“A lower tropospheric column (e.g. ground-700 hPa) can generally not well be decorrelated because of the weak sensitivity of IASI in the lowermost layers (Section 2). However, the measurements in northern mid-latitudes in spring-summer are characterized by a larger

sensitivity. In the ground-700hPa columns, we find that the apriori contributions do not exceed 40% and they range between 10% and 20% over the continental regions…."
"This certainly helps in detecting the real variability of O_3 in the N.H. troposphere, and, the increase in the observed concentrations and the variability may likely indicate a photochemical production of O_3 associated with anthropogenic precursor emissions."

b) Cfr responses to general comment 4) above. The small contributions from fires and biogenic emissions are now mentioned in the revised Section 4.1.
c) Please refer to responses to general comments 1) and 3).
d) Cfr responses to general comments 2) and 4).
e) Actually, this bias was already mentioned in Section 2. The bias is supposed to only affect the constant terms by ~10-15% in UTLS in the mid-latitudes and in the tropics, not the ozone variations. The sentence has been rewritten.
f) This has been added. Please refer to response to main comment 1) above.
g) We thank the referee for this comment. Section 4.3.1 and Figure 9 have been revised to clarify the discussion. The averaged relative residuals are now indicated in the middle panels in the revised Figure 9 which now also includes the differences between the both models (with and without the linear trend term) to highlight the offset which corresponds well to a trend over the IASI period. We also note that this offset is observed for most of layers and latitudinal bands particularly where either O_3 recovery or solar effect is important, consistently with the decrease in trend uncertainty. This is illustrated in Figure 2 below (same as Figure 9 of the manuscript) which shows one additional example (MLST in 30°S-50°S) of model adjustment, characterized by a large significant negative trend in both daily and monthly data (see Table 2 of the manuscript) and, as a result, by a large offset between the two regression models.

We add in the text: "The same conclusions can be drawn from the fits in other layers and latitude bands, especially those where the solar cycle variation of ozone is largest (MLST and UTLS) or where the ozone recovery occurs (UST). A larger trend uncertainty associated with the monthly data *vs* daily data is found in all situations (see Table 2, Section 4.3.2)."

Thanks to the high temporal sampling of the instrument, obtaining daytime daily measurements from IASI in the other layers is not critical at all, except for polar regions where daytime measurements are not possible during the polar night (data are only available during February-October and October-April over 70N-90N and 70S-90S, respectively; See Table 2).

To the best of our knowledge, the previous studies which focused on an analysis of inter-annual variability and long term trend in O_3 (total, stratospheric or tropospheric columns, either on regional or global scales) have all applied a regression model on monthly time series, not on daily measurements.

h) Cfr responses to General comment 5) and to Specific comment 1b). Trend values from previous studies have been added in the revised text for comparison.
i) We thank the referee for this comment.
As one can expect from the FTIR measurements illustrated on Figure 10 of the manuscript, IASI time series with the same sampling as the one of the FTIR leads to non-significant trends. This has been tested by applying the regression models on subsampled IASI dataset with the same

temporal resolution as that of the FTIR datasets. In all cases, we observe that the fitted trends inferred from IASI and FTIR are within the uncertainties of each other and that the uncertainties associated with the subsampled IASI datasets are significantly larger than the ones with the full daily dataset. These trend values have been added in Table 4 of the manuscript and this is mentioned in the revised Section 4.3.3.

Even if validating the IASI fitted trends with independent datasets is challenging due to the short-time period of available IASI measurements and the insufficient number of usable correlative measurements over such a short period, our results in Section 4.3.2 give convincing evidences for the ability of IASI to measure changes in O_3 records and sustain the need for continuous and high temporal frequency measurements.

[5) Conclusions:
a) P. 27598, l. 19: 'reasonably independent' is too vague considering that it is critical. It needs to be better evaluated.
b) Last sentence: I have not really seen this conclusion clearly appearing in the results.
c) P. 27599: I do not really agree with the conclusion on anthropogenic emissions as well since it is not really demonstrated here, and not referenced.]
a) Cfr general comment 2) and 4). The IASI vertical sensitivity in the MLT has been better evaluated throughout the manuscript.
b) As indicated in Section 1, only the MetOp-A measurements have been used. The extension of the O_3 records with the successive IASI instruments -B (2012) and –C (2018), and with IASI successor on EPS-SG after 2021, will allow assessing consistent trends in the different atmospheric layers.
c) See responses to General comment 4).

[6) Supplemental material
a) Information on the O3 tagging technique should be briefly provided in the S.1 section.
b) I do not agree with the conclusions provided. I do not see how the authors conclude that it's a problem due to anthropogenic emissions.
c) 2: The contribution from STE exchange does not really help with the problem of IASI's vertical resolution (Cf. comment above). A comparison of simulated contributions with and without smoothing would provide some indication on both aspects.]
a) Detailed information on the tagging procedure and all the photolysis and kinetic reactions used in MOZART4 for the tagged species can be found in Emmons et al. (2012). This has been mentioned in Section S1 of the Supplement.
b) Please refer to General comment 4) above.
c) Please refer to General comment 2) above.

Technical comments:

[1) Table 3: why 'Feb.-Oct' and 'Oct-Apr'? What do blank lines correspond to? (only '-')]
These time periods correspond to periods of available daytime IASI observations for the polar zonal bands. Because only daytime IASI observations (determined with a solar zenithal angle to the sun < 80°) are used in this study since they are characterized by a better vertical sensitivity to

the troposphere, we do not have measurement during the polar night (indicated by '-' in Table 3 of the manuscript). This is now mentioned in the revised text.

[2) Figure 4: No (a) and (b) in this Figure. . . The lines for the partial columns are hard to read, I suggest adding a specific figure. Small black titles in the figures are hard to read, real titles would be clearer.]
Titles have been enlarged and (a) and (b) have been added. A higher resolution of the figure has been provided.

[3) Figure 6: Color scale could be adjusted for the bottom plot since magnitudes change for each plot.]
It has been scaled

All the other technical corrections have been included in the revised version.

Figure Caption

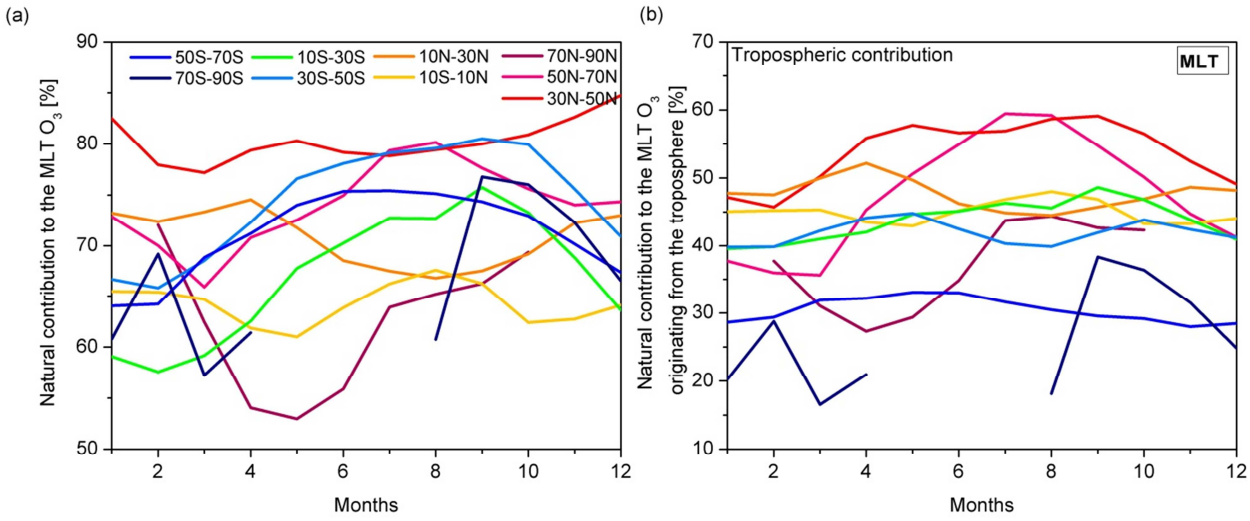

Figure 1: Contribution to the IASI MLT O_3 columns (%) (a) of the natural variability (troposphere and stratosphere) and (b) from the troposphere.

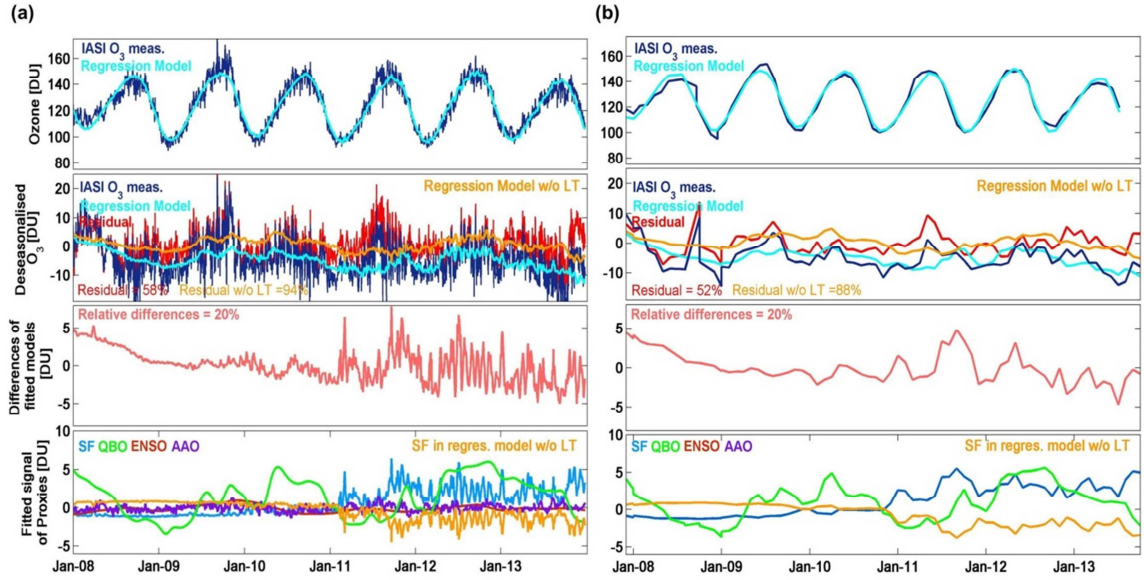

Figure 2. Daily (a) and monthly (b) time series of O_3 measurements and of the fitted regression model in the UST in the 30°S-50°S latitude band (top row), of the deseasonalised O_3 (2^d row), of the difference of the fitted models with and without the linear term (3^d row), and of the fitted signal of proxies ([regression coefficients*Proxy]): SF (blue), QBO (QBO^{10} + QBO^{30}; green), ENSO (red) and AAO (purple) (bottom) (given in DU). The averaged relative residuals are also indicated (%).

List of relevant changes in the manuscript and in the supplement:

- US→UST and MLS→ MLST have been changed throughout the manuscript and the supplement. Cfr reviewer#1 (general comment 3).

Abstract:
- l18: time development → temporal evolution; cfr reviewer#2, specific comment 1b.
- l28: … consistent with "other studies suggesting" … has been added. Cfr reviewer#2 (specific comment 1c).

Introduction:
- l46: "present" → "undergoes". Cfr reviewer#2 (specific comment 2a).
- l59: "for various reasons" → "because of possible underestimation of the true uncertainties in the ozone trends attributed to decreasing Effective Equivalent Stratospheric Chlorine (EESC)". Cfr reviewer#3 (specific comment 1a).
- l71: "(mostly from ground-based and satellite observations)" has been added.
- l75: "GCOS" → "a Global Climate Observing System (GCOS)".
- l85-86 has been rephrased → "This is further strengthened by the possibility of using IASI measurements to discriminate O_3 distributions …". Cfr reviewer#2 (specific comment 2b).

Section 2:
- l122-124 has been added: "The a priori information (a priori profile and a priori covariance matrix) is built from the Logan/Labow/McPeters climatology (McPeters et al., 2007) and only one single O_3 a priori profile and variance-covariance matrix are used.". Cfr reviewer#3 (specific comment 2).

- l135: "… (determined with a solar zenith angle to the sun < 80°)" … has been added. Cfr reviewer#3 (technical comment 3).

- l150-152: "The sharp decrease of sensitivity down to the surface is inherent to nadir thermal IR sounding in cases of low surface temperature or low thermal contrast and indicates that the retrieved information principally comes from the a priori in the lowest layer." has been added; Cfr reviewer 1 (specific comment 2).

- l170-179: the last two sentences have been rewritten: "We show that the stratospheric contribution to the MLT columns measured by IASI varies between 30% and 60%, depending on latitude and season (Fig. S5). The limited vertical sensitivity of IASI contributes to this by a smaller part (~10%-20%) than the natural stratospheric influence (~20% to 45%) (See Fig. S4 and S5). In addition, we find that the contribution of the natural variability (from both the troposphere and the stratosphere) on the MLT O_3 columns is larger than 50% everywhere. In the 30N-50N band where the DOFS is the largest (See Fig.2 (b)), this contribution reaches ~85% from which ~25-35% originates from the stratosphere and ~55% from the troposphere (Fig.S6 (a) and (b)). Nevertheless, the contamination of IASI MLT O_3 with variations in stratospheric O_3 has to be kept in mind when analyzing IASI MLT O_3". Cfr reviewer#1 (Supplemental material), reviewer#2 (General comment 3 and specific comment 3b) and reviewer#3 (General comment 2 and specific comment 2).

Section 3:

- The first sentence has been rephrased: "In order to characterize the changes in ozone measured by IASI and to allow a proper separation of trend, we use a multiple linear regression model accounting for a linear trend and for inter-annual, seasonal and non-seasonal variations related to physical processes that are known to affect the ozone records". Cfr reviewer#2 (Specific comment 3a).

- l197-203: Details on how the correction for the autocorrelation is applied to uncertainties have been added: " … as discussed in Santer et al. (2000) and references therein:

$$\sigma_e^2 = (Y^T Y)^{-1} \cdot \frac{\sum_t [O_3(t) - yY(t)]^2}{n-m} \cdot \frac{1+\Phi}{1-\Phi} \quad (3)$$

Where Y is the matrix with the covariates ($trend, \cos(n\omega t), \sin(n\omega t), X_{norm,j}$) sorted by column, y is the vector of the regression coefficients corresponding to the columns of Y, n is the number of daily (or monthly) data points in the time series, m is the number of the fitted parameters, and Φ is the lag-1 autocorrelation of the residuals". Cfr reviewer#1 (Specific comment 1), reviewer#2 (specific comment 3b) and reviewer 3 (specific comment 3b).

- l205: adequate → robust; cfr reviewer#2, Specific comment 3c.

- l225-229: "The F10.7 cm solar radio flux is an excellent indicator of solar activity and is commonly used to represent the 11 year solar cycle. It is available from continuous routine consistent measurements at the Penticton Radio Observatory in British Columbia which are corrected for the variable Sun-Earth distance resulting from the eccentric orbit of the Earth around the Sun." has been added. Cfr reviewer#3, Specific comment 3c.

- l233: "both components" → "the solar flux and linear trend terms". Cfr reviewer#2 (Specific comment 3e).

- l244-246: the sentence has been rephrased: "…orthogonal zonal winds measured at 10 hPa (Fig.3a; orange) and 30 hPa (Fig.3a; green) by the ground-station in Singapore have been considered here …". Cfr reviewer#3 (Specific comment 3c).

- l247-254: This sentence has been added: "The El Niño/Southern Oscillation is represented by the 3-month running mean of Sea Surface Temperature (SST) anomalies (in degrees Celsius) in the Niño region 3.4 (region bounded by 120°W-170°W and 5°S- 5°N). Raw data are taken from marine ships and buoys observations. The North Atlantic and Antarctic Oscillations are described by the daily (or monthly) NAO and AAO indices which are constructed from the daily (or monthly) mean 500-hPa height anomalies in the 20°N-90°N region and 700-hPa height anomalies in the 20°S-90°S region, respectively. Detailed information for these proxies can be found in http://www.cpc.ncep.noaa.gov/". Cfr reviewer#3 (Specific comment 3c).

- l262-265: This sentence has been added: "We have verified that including a typical time-lag relation between ozone and the ENSO variable from 0 to 4 months did not improve the regression model in terms of residuals and uncertainty of the fitted parameters. As a

consequence, a time-lag has not been taken into account in our study". Cfr reviewer#2 (General comment 1).

Section 4

- l300-306: The first paragraph has been rewritten: "…The performance of the multiple linear model is evaluated in subsection 4.2 in terms of residuals errors, regression coefficients and associated uncertainties determined from the regression procedure (Sect. 3). Based on this, we characterize the principal physical processes that affect the IASI ozone records. Finally, the ability of IASI to derive apparent trends is examined in Sect. 4.3.". Cfr reviewer#3 (General comment 1).

- 341-355: This paragraph has been added: "… the latter being larger than the total retrieval error (less than 25%, see Fig. 4 (b)). The lower tropospheric column (e.g. ground-700 hPa) can generally not well be discriminated because of the weak sensitivity of IASI in the lowermost layers (Section 2). However, the measurements in northern mid-latitudes in spring-summer are characterized by a larger sensitivity. In the ground-700hPa columns, we find that the apriori contributions do not exceed 40% and they range between 10% and 20% over the continental regions. In addition, the stratosphere-troposphere exchanges are usually the weakest in summer. The stratospheric contributions into the IASI MLT columns are estimated to be the lowest in the summer mid-latitudes N.H. (e.g. ~35% in the 30°N-50°N band; See Fig. S5 (b) of the Supplement) and, as mentioned in Section 2, the real natural contribution originating from the troposphere reaches ~55% (cfr Fig. S6 (b) in Supplement). This certainly helps in detecting the real variability of O_3 in the N.H. troposphere, and, the increase in the observed concentrations and in the variability may likely indicate a photochemical production of O_3 associated with anthropogenic precursor emissions (e.g. Logan et al., 1985; Fusco and Logan, 2003; Dufour et al., 2010; Cooper et al., 2010; Wilson, et al., 2012; Safieddine et al., 2013).". Cfr reviewer#3, (General comment 4 and Specific comment 4a).

- l355-360: This has been added: "Changes in biomass and biogenic emissions of NO_x, CO and non-methane organic volatile compounds (NMVOC) may also play a role. However, they only represent a small part of the total emissions for NO_x and CO (e.g. ~23% *vs* 72% for the anthropogenic NO_x emissions and ~40% *vs* 60% for the anthropogenic CO emissions from the emissions dataset used in the Supplement), while the biogenic emissions of NMVOC represent the largest contribution to the total (~80%)". Cfr reviewer#3 (General comment 4 and Specific comment 4b).

- l369: The sentence has been rewritten: "The fact that the patterns at ~10km are similar to those at ~20 km mainly reflects the low sensitivity of IASI to that level compared to the others". Cfr reviewer#1 (Specific comment 3).

- l386-389: This has been added: "The regression model explains a large fraction of the variance in the daily IASI data over the troposphere (~85%-95%) and the stratosphere (~85%-95% in all cases, except for the UST with ~70-95%), as estimated from $\frac{\sigma\left(O_3^{Fitted\ model}(t)\right)}{\sigma\left(O_3(t)\right)}$ where σ is the standard deviation relative to the fitted regression model and to the IASI O_3 time series". Cfr reviewer#3 (General comment 1).

- l396-397: this has been added: " … or with the missing time-lags in the regression model between the QBO and ENSO variables and the response of mid-latitude lower stratospheric ozone (Neu et al., 2014)". Cfr Reviewer#2 (General comment 1 and Specific comments 4e and 4g).

- l449-452: The sentence has been rewritten: "Note that the constant terms in the UTLS region in the mid-latitudes and in the tropics are certainly affected by the fact that the FORLI-O_3 profiles are biased high by ~10-15% in this layer and latitude bands …". Cfr reviewer#3 (Specific comment 4e).

- l461-467: This has been added: "A positive (or negative) sign of the coefficients indicates that the associated variables are correlated (or anti-correlated) with the IASI O_3 time series. Note that if the uncertainty is larger than its associated estimate (i.e. larger than 100%, corresponding to an error bar overlapping the zero line), it means that the estimate becomes statistically non-significant when accounting for the autocorrelation in the noise residuals at the end of the elimination process. This is summarized in Table S1 of the Supplement". Cfr reviewer#1 (Specific comment 4c).

- l467-469, this has been added: "The contribution of the fitted variables into the IASI O_3 variations is estimated as $\frac{\sigma\left(\left[a_n; b_n; x_j\right]\left[\cos(n\omega t); \sin(n\omega t); X_{norm,j}\right]\right)}{\sigma\left(O_3(t)\right)}$ where σ is the standard deviation relative to the fitted signal of harmonic or proxy terms and to the IASI O_3 time series. From Figure 8, we …". Cfr reviewer#3 (General comment 1).

- l475-480 has been added: "The annual term contributes importantly around 45%-85% of the observed O_3 variations, except in the 10°N-30°N and equatorial bands (10%-30%), while the influence of the semi-annual variation on O_3 is smaller (10%-25%) and highly variable between the bands. In the UST, the amplitudes vary only slightly (around -5% to 5%) and account for the weak summer maximum. The contributions of the annual harmonic term are estimated between 5%-30%". Cfr reviewer#3 (General comment 1).

- l486-487: "… (scaled coefficients of 10%–15% in UTLS and contributions up to 75% and 21% for QBO and SF, respectively)" has been added. Cfr reviewer#3 (General comment 1).

- l494-496: the sentence has been rewritten: "(<10% and <5%, respectively), with scaled coefficients lower than 5%, and, in many cases for the NAO/AAO proxies, they are even not statistically significant when taking into account the correlation in the noise residuals (see Table S1 in Supplement)". Cfr reviewer#3 (General comment 1).

- l498-499: this sentence has been added: "The negative ENSO coefficient in the tropical UTLS is consistent with results from Neu et al. (2014)". Cfr reviewer#2 (Specific comment 4h).

- l504-507: This sentence has been added: "We note that the non-representation of time-lags in the proxy time series may be underestimating the role of some geophysical variables on O_3 variations, in particular that of ENSO and QBO in zonal bands outside the regions where these

geophysical quantities are measured (i.e. Niño region 3.4 for ENSO and Singapore for QBO)". Cfr reviewer#2 (General comment 1 and Specific comment 4g).

- l513-515: This sentence has been added in the conclusion of the Section 4.2: "As a general feature, the results demonstrate the representativeness of the fitted models in each layer and latitude band. This good performance of the regression procedure allows examination of the adjusted linear trend term in Section 4.3 below". Cfr reviewer#3 (General comment 1 and Specific comment 4f).

- l536-537: We have added: "… calculated by subtracting the model seasonal cycle from the time series, ….". Cfr reviewer#1, Specific comment 5a.

- l537-539: "The averaged residuals relative to the deseasonalised IASI time series strongly vary with the layers and latitudinal bands and usually range between 30% and 60%" has been added. Cfr reviewer#3, General comment 3.

- l543: "not compensated" → "only partly compensated". Cfr reviewer#1, Specific comment 4a.

- l543-552: this part has been rewritten for clarification: "This leads to an offset between the fitted O_3 time series resulting from the both regression models (with and without the linear term), which corresponds well to a trend over the IASI period, and, consequently, to larger residuals (e.g. 80% without *vs*. 44% with the linear term for this example and 94% without *vs* 58% with the linear term for the 30°S-50°S band in the MLST illustrated in Fig. S1 of the Supplement). This offset is observed for a lot of layers and latitudinal bands. On the contrary, the linear term can largely be compensated by the solar flux term in the monthly averages: the offset is weak and the difference between the both fitted models is smaller (averaged differences relative to the deseasonalised IASI time series of 10% in monthly data *vs* 17% in daily data for this example) ." Cfr reviewer#1 (General comment 2, Specific comments 4b and 5a,b) and reviewer#3 (Specific comment 4g).

- l554-559: This sentence has been rewritten for clarification: "This effective co-linearity of the linear and the monthly solar flux terms translates to larger model fit residuals (44% in daily averages *vs* 60% in monthly averages in UST, relative to the deseasonalised IASI time series), to smaller relative differences between both regression models (with and without the linear term) (17% in daily vs 10% in monthly data), and to larger uncertainty on the trend coefficients when using the monthly data in comparison with the daily data". Cfr reviewer#1 (General comment 2) and reviewer#3 (Specific comment 4g).

- l563-566: This paragraph has been added: "The same conclusions can be drawn from the fits in other layers and latitude bands, especially those where the solar cycle variation of ozone is large (MLST and UTLS, see Fig. 8) or where the ozone recovery would occur (UST). A larger trend uncertainty associated with monthly data *vs* daily data is found in all situations (see Table 2, Section 4.3.2 below)". Cfr reviewer#1 (General comment 2) and reviewer#3 (Specific comment 4g).

- l577-579: This has been added: “In the northern and southern polar regions, the polar night period is not covered because only IASI observations during sunlight (over Feb-Oct and Oct-Apr for N.H. and S.H., respectively) are used in this study (See Sect. 2)”. Cfr reviewer#3 (Specific comment 4g).

- l584-587: We have added: “ … the use of daily median strongly helps in reducing everywhere the uncertainty associated with the trends for the reasons discussed above (Sect. 4.3.1). This is particularly observed in the UST where the ozone hole recovery would occur, but also in the MLST and the UTLS where the solar cycle variation of ozone is the largest (see Figure 8). As a consequence, the UST …”. Cfr reviewer#1 (General comment 1).

- l604-612: Numbers and kind of observations have been included: “… Kÿrola et al. (2013) and Laine et al. (2014) report for instance a change of up to 10%/decade in O_3 trends between 1997-2011 *vs.* 1984-1997. Positive trends in the UST are consistent with many previous observations if one considers the fact that the period covered by IASI is later than those reported in previous studies and that the recovery rate seems to heighten since the beginning of the turnaround (Knibbe et al. (2014) reports a factor of two increase in the recovery rate between 1997–2010 with ~0.7DU/yr and 2001–2010 with ~1.4DU/yr in the S.H.) They could indicate a leveling off of the negative trends that were observed since the second half of the 1990’s mostly from satellites and ground-based monthly mean data …”. Cfr reviewer#3 (General comment 5 and Specific comment 1b).

- l611: “was”→”were”. l620: “conducting” →”leading”. l623: “in Table 3” → “in winter (Table 3)”. L625: “in summer N.H…. in winter S.H.”. Cfr reviewer#3 (Specific comments 7,8,9,10).

- l66-674: This paragraph has been rewritten: “… As a consequence, it is hard to reconcile the trends in tropospheric ozone with changes in emissions of ozone precursors. However, trends in emissions have already been able to qualitatively explain measured ozone trends over some regions but with inconsistent magnitude between observations and model simulations (e.g. Cooper et al., 2010; Logan et al., 2012; Wilson et al., 2012). It is also worth to keep in mind that due to medium sensitivity of IASI to the troposphere, the a priori contribution and ozone variations in stratospheric layers may largely influence the trends seen by IASI in the MLT layer (*cfr*. Sect. 2 and Supplement)”. Cfr reviewer#1 (Specific comments 12a,b) and reviewer#3 (General comments 4).

- l691-692: Numbers have been included: “These values are consistent with those reported in Knibbe et al. (2014) for the 2001-2010 period in spring in the Antarctic (around 3-5 DU/yr)…”. Cfr reviewer#3 (General comment 5 and Specific comment 1b).

- l713-719: This paragraph has been added: “In order to better characterize the effect of the temporal frequency on determining statistical trends, the IASI time series have been subsampled to match the temporal resolution of FTIR. The associated trend values are also indicated in Table 4 (2^d row). In any cases, we observe that the fitted trends inferred from both IASI and FTIR with the same temporal samplings are within the uncertainties of each other and that those associated with the subsampled IASI datasets are significantly larger than those obtained with the daily

ones, leading to statistically non-significant trends." Cfr reviewer#2 (General comments 2 and Specific comment 4k) and reviewer#3 (General comments 5 and specific comment 4i).

- l721-723: This sentence has been added in the conclusion of Section 4.3.3: "Even if validating the IASI fitted trends with independent datasets is challenging due to the short-time period of available IASI measurements and the insufficient number of usable correlative measurements over such a short period, …". Cfr reviewer#2 (General comments 2) and reviewer#3 (General comments 5).

Summary and Conclusions

- l777-780: This has been added at the end of the conclusion section: "… for changes in the Brewer-Dobson circulation, as well as including time lags in ENSO and QBO proxies) will have to be explored. Further investigation on the regressors uncertainties and on the total error on ozone measurements should be performed as well to understand on the unexplained variations in IASI O_3 records." Cfr reviewer#2 (General comments 1) and reviewer#3 (General comments 5).

Tables

- **"…** accounting for the autocorrelation in the noise residuals …" has been added in the Title of Table 2
- "…(successive rows for different time intervals). Italic values (2^d row) refer to trends inferred from subsampled IASI data and …" has been added in the title of Table 4. Cfr reviewer#2 (General comments 2) and reviewer#3 (General comments 5).

Figure captions

- Fig. 5: "expressed as $[\sigma(O_3(t))/O_3(t)].100\%$" has been corrected. Cfr reviewer#1 (Technical comment).
- Fig.9 includes an additional row. The caption has been changed accordingly: "…of the deseasonalised O_3 (2^d row), of the difference of the fitted models with and without the linear term (3^d row), and of the fitted signal of proxies ([regression coefficients*Proxy]): SF (blue), QBO (QBO^{10} + QBO^{30}; green), ENSO (red) and AAO (purple) (bottom) (given in DU). The averaged residuals relative to the deseasonalised IASI time series are also indicated (%)." Cfr reviewer#1 (General comment 2) and reviewer#3 (Specific comment 4g).

Supplementary Materials

- l5-7: "This supporting information provides, in Table S1, a tabulated summary of the variables that are kept in the statistical model at the 95% level at the end of the iterative backward selection for each 20° latitude bands and for each partial column analyzed in the manuscript". Cfr reviewer#1 (Specific comment 4c).

- l27-42: The description of the emissions dataset has been extended: "The emissions inventory used here is the same as in Wespes et al. (2012) and in Duflot et al. (2015). The anthropogenic emissions are from the inventory provided by D. Streets (Argonne National Lab) and University of Iowa for ARCTAS (http://bio.cgrer.uiowa.edu/arctas/emission.html; http://bio.cgrer.uiowa.edu/arctas/arctas/07222009/). It is a composite dataset of regional emissions representative of emissions for 2008: it is built upon the INTEX-B Asia inventory (Zhang et al.,2009) with the US NEI (National Emission Inventory) 2002 and CAC 2005 for

North America and the EMEP (European Monitoring and Evaluation Programme) 2006 for Europe inventory to make up NH emissions (see http://bio.cgrer.uiowa.edu/arctas/emission.html and Emmons et al. 2015 for an evaluation of the inventory with several models in the frame of the POLARCAT Model Intercomparison Program (POLMIP)). Emissions from EDGAR (Emissions Database for Global Atmospheric Research) were used for missing regions and species. The anthropogenic emissions are constant over years with no monthly variations. Daily biomass burning emissions are taken from the global Fire INventory from NCAR (FINN, Wiedinmyer et al., 2011). They vary with year. The oceanic emissions are taken from the POET emissions dataset (Granier et al., 2005) and the biogenic emissions from MEGANv2 (Model of Emissions of Gases and Aerosols from Nature) inventory (Guenther et al., 2006).” Cfr reviewer#2 (specific comments 6a,d,g).

- l47-49: This sentence has been added: “Results have shown that MOZART-4 is slightly biased low over the troposphere (around 5-15%), but that it reproduces generally well the variability of observations in space and time”. Cfr reviewer#3 (General comment 4).

- l54-58: “following the formalism of Rodgers (2000):

$$X_{Model\_Smoothed}=X_a+\mathbf{A}(X_{Model}-X_a) \quad \text{(S1)}$$

where X_{Model} represents the O_3 profile modeled by MOZART-4 which is first vertically interpolated to the pressure levels of the a priori profiles (Xa) used in the FORLI-O_3 retrieval algorithm” has been added.

- l103-104: “(see Emmons et al. (2012) for detailed information on the “tagging” approach and on the photolysis and kinetic reactions for the tagged species)” has been added. Cfr reviewer#3 (Specific comment 6a).

- Section S3 has been completely rewritten for clarification: “It represents the natural stratospheric influence into the MLT columns as modeled by MOZART-4 and it ranges between ~20% to 45% with, as expected, the largest contribution above the winter southern latitudes. Fig. S5 is the same as Fig. S4 but the model time series account for the IASI vertical sensitivity by applying the averaging kernels of each specific IASI observations to the corresponding gridded MOZART-4 profile (see Eq. S1), similarly to Wespes et al. (2012). Eq. S1 can be expressed as :

$$X_{Model\_Smoothed} = [\mathbf{A}X_{O3\_tagged\_NOx}] + [\mathbf{A}(X_{Model} - X_{O3\_tagged\_NOx})] + [X_a - \mathbf{A}(X_a)] \quad \text{(S2)}$$

where the first two terms represent the contributions from all the tropospheric odd nitrogen sources and from the stratosphere smoothed by the averaging kernels, respectively. The third component represents the contribution from the a priori to the ozone columns due to the limited vertical sensitivity of the IASI instrument. These terms are represented in Fig. S5 (a) and (b) for the MLT. The second term which is illustrated as a percentage of the total O_3 in Fig. S5 (b) (solid lines), simulates the stratospheric part as seen by IASI in the troposphere. This IASI stratospheric contribution, which is amplified by the limited vertical sensitivity of the instrument in the MLT when compared with the MOZART-4 stratospheric influence (Fig. S4 (b)), ranges between 30 and 65% depending on latitude and season. The largest contributions are calculated for the highest latitudes in winter-spring and they are attributed to both descent of stratospheric air mass into the polar vortex and to less IASI sensitivity over the poles. The low contribution above the South polar region (~25%) is explained by a loss of IASI sensitivity which translates to a large a priori contribution (40%). The smallest stratospheric contributions are calculated in the low

latitude bands. The difference between the stratospheric contributions simulated by MOZART-4 (Fig. S4 (b)) and those as seen by IASI (Fig. S5 (b)) is the stratospheric portion due to the IASI limited sensitivity and it reflects the smoothing error from the IASI measurements. It ranges between 10%-20% (except for the polar bands). This suggests that the limited vertical sensitivity of IASI, which artificially mixes stratospheric and tropospheric air masses, contributes to a lesser extent to the IASI MLT than the stratosphere-troposphere exchanges. The smoothing error translates also to an *a priori* contribution (dashed lines, Fig. S5 (b)) which, as expected from the analysis of the IASI vertical sensitivity (see Section 2 of the manuscript), is anti-correlated with the stratospheric contribution to some extent. It ranges between ~5% and ~20%. These results suggest that the variability of tropospheric ozone measured by IASI (Section 4.3.2 of the manuscript) is partly masked by the *a priori* and the stratospheric contributions". Cfr reviewer#1 (Specific comment 13), reviewer#2 (General comment 3) and reviewer#3 (General comment 2).

- l140-150: This paragraph has been added: "The total portion of the natural variability (from both the troposphere and the stratosphere) into the MLT O_3 measured by IASI can be estimated by subtracting from the IASI O_3 time series the *a priori* contribution and the stratospheric one due to the IASI limited sensitivity. This is illustrated in Fig.S6 (a). This natural contribution is larger than 50% of the IASI MLT O_3 column everywhere. Interestingly, the 30°N-50°N band shows the highest detectable natural portion (~80-85%) in the MLT columns, from which ~25-35% originates from the stratosphere (Fig. S4 (b)), and~50-60% from the troposphere (Fig.S6 (b)). It is also worth to note that the positive bias of MOZART-4 *vs.* IASI in the MLT (see Section S2) should not affect the calculated tropospheric contribution in the IASI MLT columns and that the stratospheric contribution for the 30°N-50°N band should be well estimated from MOZART-4 since the model matches very well the IASI observations in the upper layers for this band (Fig. S2 and S3)." Cfr reviewer#1 (Specific comment 13), reviewer#2 (General comment 3) and reviewer#3 (General comment 2).

- l175-181: Conclusion section has been partly rewritten for clarification: "Our results suggest that even if a large part of the IASI O_3 MLT measurements in the N.H. originates from the troposphere (40-60%), the apparent negative trend in the troposphere observed by IASI in the N.H. summer (see Tables 2 and 3 in Section 4.3.2 of the manuscript) is partly masked by the influence of the stratosphere and of the medium vertical sensitivity of IASI. In other words, the decrease of tropospheric O_3, which could be attributed to decline of O_3 precursor emissions, is likely attenuated by the positive changes in O_3 variations detected in upper layers. This would mean that the negative trend deduced from IASI could in reality be more important …"

- Table S1 has been added. Cfr reviewer#1 (Specific comment 4c).

- Figures S1 (Cfr reviewer#1, General comment 2), S4 and S6 (Cfr reviewer#1, Specific comment 13; reviewer#2, General comment 3, and reviewer#3, General comment 2) have been added.

Ozone variability in the troposphere and the stratosphere from the first six years of IASI observations (2008-2013)

C. Wespes[1], D. Hurtmans[1], L.K. Emmons[2], S. Safieddine[3], C. Clerbaux[1,3], D. P. Edwards[2] and P.-F. Coheur[1]

[1]Spectroscopie de l'Atmosphère, Service de Chimie Quantique et Photophysique, Université Libre de Bruxelles (U.L.B.), Brussels, Belgium

[2]National Center for Atmospheric Research, Boulder, CO, USA

[3]Sorbonne Universités, UPMC Univ. Paris 06; Université Versailles St-Quentin; CNRS/INSU, LATMOS-IPSL, Paris, France

*Now at Department of Civil and Environmental Engineering, Institute of Technology, Cambridge, Massachusetts, United States

Abstract

In this paper, we assess how daily ozone (O_3) measurements from the Infrared Atmospheric Sounding Interferometer (IASI) on the MetOp-A platform can contribute to the analyses of the processes driving O_3 variability in the troposphere and the stratosphere and, in the future, to the monitoring of long-term trends. The ~~time development~~temporal evolution of O_3 during the first 6 years of IASI (2008-2013) operation is investigated with multivariate regressions separately in four different layers (ground-300 hPa, 300-150 hPa, 150-25 hPa, 25-3 hPa), by adjusting to the daily time series averaged in 20° zonal bands, seasonal and linear trend terms along with important geophysical drivers of O_3 variation (e.g. solar flux, quasi biennial oscillations). The regression model is shown to perform generally very well with a strong dominance of the annual harmonic terms and significant contributions from O_3 drivers, in particular in the equatorial region where the QBO and the solar flux contribution dominate. More particularly, despite the short period of IASI dataset available to now, two noticeable statistically significant apparent trends are inferred from the daily IASI measurements: a positive trend in the upper stratosphere (e.g. 1.74±0.77DU/yr between 30°S-50°S) which is consistent with ~~the~~other studies suggesting a

turnaround for stratospheric O_3 recovery, and a negative trend in the troposphere at the mid-and high northern latitudes (e.g. -0.26±0.11 DU/yr between 30°N-50°N), especially during summer and probably linked to the impact of decreasing ozone precursor emissions. The impact of the high temporal sampling of IASI on the uncertainty in the determination of O_3 trend has been further explored by performing multivariate regressions on IASI monthly averages and on ground-based FTIR measurements.

1 Introduction

Global climate change is one of the most important environmental problems of today and monitoring the behavior of the atmospheric constituents (radiatively active gases and those involved in their chemical production) is key to understand the present climate and apprehend future climate changes. Long-term measurements of these gases are necessary to study the evolution of their abundance, changing sources and sinks in the atmosphere.

As a reactive trace gas present simultaneously in the troposphere and in the stratosphere, O_3 plays a significant role in atmospheric radiative forcing, atmospheric chemistry and air quality. In the stratosphere, O_3 is sensitive to changes in (photo-)chemical and dynamical processes and, as a result, ~~present~~undergoes large variations on seasonal and annual time scales. Measurements of O_3 total column have indicated a downward trend in stratospheric ozone over the period from 1980s to the late 1990s relative to the pre-1980 values, which is due to the growth of the reactive bromine and chlorine species following anthropogenic emissions during that period (WMO, 2003). In response to the 1987 Montreal Protocol and its amendments, with a reduction of the Ozone-Depleting Substances (ODS; Newchurch et al., 2003), a recovery of stratospheric ozone concentrations to the pre-1980 values is expected (Hofmann, 1996). While earlier works have debated a probable turnaround for the ozone hole recovery (e.g. Hadjinicolaou et al., 2005; Reinsel et al., 2002; Stolarski and Frith, 2006), WMO already indicated in 2007 that the total ozone in the 2002-2005 period was no longer decreasing, reflecting such a turnaround. Since then several studies have shown successful identification of ozone recovery over Antarctica and over northern latitudes (e.g. Mäder et al., 2010; Salby et al., 2011; WMO, 2011; Kuttippurath et al., 2013; Knibbe et al., 2014; Shepherd et al., 2014). Nevertheless, the most recent papers as

well as the WMO 2014 ozone assessment have warned ~~for various reasons~~, because of possible underestimation of the true uncertainties in the ozone trends attributed to decreasing Effective Equivalent Stratospheric Chlorine (EESC), against overly optimistic conclusions with regard to a possible increase in Antarctic stratospheric ozone (Kramarova et al., 2014; WMO, 2014; Knibbe et al., 2014; de Laat et al., 2015; Kuttippurath et al., 2015; Varai et al., 2015). The causes of the observed stratospheric O_3 changes are hard to isolate and remain uncertain precisely considering the contribution of dynamical variability to the apparent trend and the limitations of current chemistry-climate models to reproduce the observations. The assessment of ozone trends in the troposphere is even more challenging due to the influence of many simultaneous processes (e.g. emission of precursors, long-range transport, stratosphere-troposphere ~~–STE–~~ exchanges~~), –~~ STE–), which are all strongly variable temporally and spatially (e.g. Logan et al., 2012; Hess and Zbinden, 2013; Neu et al., 2014). Overall, there are still today large differences in the value of the O_3 trends determined from independent studies and datasets (mostly from ground-based and satellite observations) in both the stratosphere and the troposphere (e.g. Oltmans et al., 1998; 2006; Randel and Wu, 2007; Gardiner et al., 2008; Vigouroux et al., 2008; Jiang et al., 2008; Kyrölä et al., 2010; Vigouroux et al., 2014). In order to improve on this and because O_3 has been recognized as ~~an GCOS~~a Global Climate Observing System (GCOS) Essential Climate Variables (ECVs), the scientific community has underlined the need of acquiring high quality global, long-term and homogenized ozone profile records from satellites (Randel and Wu, 2007; Jones et al., 2009; WMO, 2007; 2011; 2014). This specifically has resulted in the ESA Ozone Climate Change Initiative (O_3-CCI; http://www.esa-ozone-cci.org/).

The Infrared Atmospheric Sounding Interferometer (IASI) onboard the polar orbiting MetOp, with its unprecedented spatiotemporal sampling of the globe, its high radiometric stability and the long duration of its program (3 successive instruments to cover 15 years) provides in principle an excellent means to contribute to the analyses of the O_3 variability and trends. This is further strengthened by the possibility of using IASI measurements to discriminate ~~well with IASI, the~~ O_3 distributions and variability in the troposphere and the stratosphere, as shown in earlier studies (Boynard et al., 2009; Wespes et al., 2009; Dufour et al, 2010 ; Barret et al., 2011; Scannell et al., 2012; Wespes et al., 2012; Safieddine et al., 2013). Here, we use the first 6 years

(2008-2013) of the new O_3 dataset provided by IASI on MetOp-A to perform a first analysis of the O_3 time development in the stratosphere and in the troposphere. This is achieved globally by using zonal averages in 20° latitude bands and a multivariate linear regression model which accounts for various natural cycles affecting O_3. We also explore in this paper to which extent the exceptional temporal sampling of IASI can counterbalance the short period of data available for assessing trends in partial columns.

In Sect. 2, we give a short description of IASI and of the O_3 retrieved columns used here. Section 3 details the multivariate regression model used for fitting the time series. In Sect. 4, we evaluate how the ozone natural variability is captured by IASI and we present the time evolution of the retrieved O_3 profiles and of four partial columns (Upper Stratosphere –~~US –~~;UST-; Middle-Low Stratosphere –~~MLS~~MLST–; Upper Troposphere Lower Stratosphere –UTLS–; Middle-Low Troposphere –MLT–) using 20-degree latitudinal averages on a daily basis. The apparent dynamical and chemical processes in each latitude band and vertical layer are then analyzed on the basis of the multiple regression results using a series of common geophysical variables. The "standard" contributors in the fitted time series, as well as a linear trend term, are analyzed in the specified altitude layers. Finally, the trends inferred from IASI are compared against those from FTIR for six stations in the northern hemisphere.

2 IASI measurements and retrieval method

IASI measures the thermal infrared emission of the Earth-atmosphere between 645 and 2760 cm^{-1} with a field of view of 2×2 circular pixels on the ground, each of 12 km diameter at nadir. The IASI measurements are taken every 50 km along the track of the satellite at nadir, but also across-track over a swath width of 2200 km. IASI provides a global coverage twice a day with overpass times at 09:30 and 21:30 mean local solar time. The instrument is also characterized by a high spectral resolution which allows the retrieval of numerous gas-phase species (e.g. Clerbaux et al., 2009; Clarisse et al., 2012).

Ozone profiles are retrieved with the Fast Optimal Retrievals on Layers for IASI (FORLI) software developed at ULB/LATMOS. FORLI relies on a fast radiative transfer and on a

retrieval methodology based on the Optimal Estimation Method (Rodgers, 2000). In the version used in this study (FORLI-O_3 v20100815), the O_3 profile is retrieved for individual IASI measurement on a uniform 1 km vertical grid on 40 layers from surface up to 40 km. The a priori information (a priori profile and a priori covariance matrix) is built from the Logan/Labow/McPeters climatology (McPeters et al., 2007) and only one single O_3 a priori profile and variance-covariance matrix are used. The retrieval parameters and performances are detailed in Hurtmans et al. (2012). The FORLI-O_3 profiles and/or total and partial columns have undergone validation using available ground-based, aircraft, O_3 sonde and other satellite observations (Anton et al., 2011; Dufour et al., 2012; Gazeaux et al., 2012; Parrington et al., 2012; Pommier et al., 2012; Scannell et al., 2012; Oetjen et al., 2014). Generally, the results show good agreements between FORLI-O_3 and independent measurements with a low bias (<10%) in the total column and in the vertical profile, except in UTLS where a positive bias of 10-15% is reported (Dufour et al., 2012; Gazeaux et al., 2012; Oetjen et al., 2014).

In this study, only daytime O_3 IASI observations from good spectral fits (RMS of the spectral residual lower than 3.5×10^{-8}W/cm^2.sr.cm^{-1}) have been analyzed. Daytime IASI observations (determined with a solar zenith angle to the sun < 80°) are characterized by a better vertical sensitivity to the troposphere associated with a higher surface temperature and a higher thermal contrast (Clerbaux et al., 2009; Boynard et al., 2009). Furthermore, cloud contaminated scenes with cloud cover < 13% (Hurtmans et al., 2012) were removed using cloud information from the Eumetcast operational processing (August et al., 2012).

An example of typical FORLI-O_3 averaging kernel functions for one mid-latitude observation in July (45°N/66°E) is represented on Fig.1. The layers have been defined as: ground-300 hPa (MLT), 300-150 hPa (UTLS), 150-25 hPa (~~MLS~~MLST) and above 25 hPa (~~US~~UST), so that they are characterized by a DOFS (Degrees Of Freedom for Signal) close to 1 with a maximum sensitivity approximatively in the middle of the layers, except for the 300-150 hPa layer which has a reduced sensitivity. Taken globally, the DOFS for the entire profile ranges from ~2.5 in cold polar regions to ~4.5 in hot tropical regions, depending mostly on surface temperature, with a maximum sensitivity in the upper troposphere and in the lower stratosphere (Hurtmans et al.,

2012). In the MLT, the maximum of sensitivity peaks around 4–8 km altitude for almost all situations (Wespes et al., 2012). The sharp decrease of sensitivity down to the surface is inherent to nadir thermal IR sounding in cases of low surface temperature or low thermal contrast and indicates that the retrieved information principally comes from the a priori in the lowest layer. Figure 2 presents July 2010 global maps of averaged FORLI-O_3 partial columns for two partial layers (MLT and ~~MLS~~MLST), and of the associated DOFS and *a priori* contribution (calculated as X_a-AX_a, where X_a is the *a priori* profile and A, the averaging kernel matrix, following the formalism of Rodgers (2000)). The two layers exhibit different sensitivity patterns: in the MLT, the DOFS typically range from 0.4 in the cold polar regions to 1 in regions characterized by high thermal contrast with medium humidity, such as the mid-latitude continental Northern Hemisphere (N.H.) (Clerbaux et al., 2009). Lower DOFS values in the intertropical belt are explained by ~~an~~ overlapping ~~from~~ water vapor lines. In contrast, the DOFS for the ~~MLS~~MLST are globally almost constant and close to one, with only slightly lower values (0.9) over polar regions. The *a priori* contribution is anti-correlated with the sensitivity, as expected. It ranges between a few % to ~30% and does not exceed 20% on 20° zonal averages in the troposphere (see Supporting Information; Fig. S3, dashed lines), while the a priori contribution is smaller than ~12% in the middle stratosphere. These findings indicate that the IASI ~~MLS~~MLST time series should accurately represent stratospheric variations, while the time series in the troposphere may reflect to some extent variations from the upper layers in addition to the real variability in the troposphere. In order to quantify this effect, the contribution of the stratosphere into the tropospheric ozone as seen by IASI has been estimated with a global 3-D chemical transport model (MOZART-4).~~We show that it varies between 30 and 60% depending on latitude and season.~~ Details of the model-observation comparisons can be found in the Supplement (see Figs. S2 and S3). ~~The fact that~~ We show that the stratospheric contribution to the MLT columns measured by IASI varies between 30% and 60%, depending on latitude and season (Fig. S5). The limited vertical sensitivity of IASI contributes to this by a smaller part (~10%-20%) than the natural stratospheric influence (~20% to 45%) (See Fig. S4 and S5). In addition, we find that the contribution of the natural variability (from both the troposphere and the stratosphere) on the MLT O_3 columns is ~~"contaminated" to a significant extend~~ larger than 50% everywhere. In the 30N-50N band where the DOFS is the largest (See Fig.2 (b)), this contribution reaches ~85%

from which ~25-35% originates from the stratosphere and ~55% from the troposphere (Fig.S6 (a) and (b)). Nevertheless, the contamination of IASI MLT O_3 with variations in stratospheric O_3 ~~should~~has to be kept in mind when analyzing IASI MLT O_3.

3 Fitting method

3.1. Statistical model

In order to characterize the changes in ozone measured by IASI and to allow a proper separation of trend ~~due to ODS from trend due to other processes~~, we use a multiple linear regression model accounting for a linear trend and for inter-annual, seasonal and non-seasonal variations related to ~~dynamical~~physical processes ~~and solar flux~~that are known to affect the ozone records. More specifically, the time series analysis is based on the fitting of daily (or monthly) median partial columns in different latitude band following:

$$O_3(t) = Cst + x_1 \cdot trend + \sum_{n=1,2}\left[a_n \cdot \cos(n\omega t) + b_n \cdot \sin(n\omega t)\right] + \sum_{j=2}^{m} x_j X_{norm,j}(t) + \varepsilon(t) \quad (1)$$

where t is the number of days (or months), x_1 is the 6-year trend coefficient in the data, ω = $2\pi/365.25$ for the daily model (or $2\pi/12$ for the monthly model) and $X_{norm,j}$ are independent geophysical variables, the so-called "explanatory variables" or "proxies", which are in this study normalized over the period of IASI observation (2008-2013), as:

$$X_{norm}(t) = 2\left[X(t) - X_{median}\right] / \left[X_{\max} - X_{\min}\right] \quad (2)$$

$\varepsilon(t)$ in Eq. (1) represents the residual variation which is not described by the model and which is assumed to be autoregressive with time lag of 1 day (or 1 month). The constant term (Cst) and the coefficients a_n, b_n, x_j are estimated by the least-squares method and their standard errors (σ_e) are calculated from the covariance matrix of the coefficients and corrected to take into account the uncertainty due to the autocorrelation of the noise residual~~.~~ as discussed in Santer et al. (2000) and references therein:

$$\sigma_e^2 = (Y^T Y)^{-1} \cdot \frac{\sum_t \left[O_3(t) - yY(t)\right]^2}{n-m} \cdot \frac{1+\Phi}{1-\Phi} \quad (3)$$

Where Y is the matrix with the covariates ($trend, \cos(n\omega t), \sin(n\omega t), X_{norm,j}$) sorted by column, y is the vector of the regression coefficients corresponding to the columns of Y, n is the number of daily (or monthly) data points in the time series, m is the number of the fitted parameters, and Φ is the lag-1 autocorrelation of the residuals.

The median is used as a statistical average since it is more ~~adequate~~robust against the outliers than the normal mean (Kyrölä et al., 2006; 2010). Note that, similarly to Kyrölä et al. (2010), the model has been applied on O_3 mixing ratios rather than on partial columns but without significant improvement on the fitting residuals and R values.

3.2. Geophysical variables

In Eq. (1), harmonic time series with a period of a year and a half year are used to account for the Brewer-Dobson circulation and the solar insolation (a_1 and b_1 coefficients), and for the meridional circulation (a_2 and b_2 coefficients), respectively (Kyrölä et al., 2010), these effects being of a periodic nature. The geophysical variables (X_j) are used here to parameterize the ozone variations on non-seasonal timescales. The chosen proxies are $F_{10.7}, QBO^{10}, QBO^{30}, ENSO$, *NAO/AAO*, the first three being the most commonly used ("standard") proxies to describe the natural ozone variability, i.e. the solar radio flux at 10.7 cm and the quasi-biennial oscillation (*QBO*) which is represented by two orthogonal zonal components of the equatorial stratospheric wind measured at 10 hPa and 30 hPa, respectively (e.g. Randel and Wu, 2007). The three other proxies, *ENSO*, *NAO* and *AAO*, are used to account for other important fluctuating dynamical features: the El Niño/Southern Oscillation, the North Atlantic Oscillation and the Antarctic Oscillation, respectively. Table 1 lists the selected proxies, their sources and their resolutions. The time series of these proxies normalized over the 2000-2013 period following Eq. 2 are shown in Fig. 3a and b and they are shortly described hereafter:

~~- *Solar flux*: over the period 2008 -~~ - *Solar flux*: The F10.7 cm solar radio flux is an excellent indicator of solar activity and is commonly used to represent the 11 year solar cycle. It is available from continuous routine consistent measurements at the Penticton Radio Observatory

in British Columbia which are corrected for the variable Sun-Earth distance resulting from the eccentric orbit of the Earth around the Sun. Over the period 2008-2013, the radio solar flux increases from about 65 units in 2008 to 180 units in 2013 and is characterized by a specific daily "fingerprint" (see Fig. 3a). Note that because the period of IASI observations does not cover a full 11 year solar cycle, it could affect the determination of the trend in the regression procedure. The difficulty in discriminating ~~both components~~the solar flux and linear trend terms is a known problem for such multivariate regression: it feeds into their uncertainties and it can lead to biases in the coefficients determination (e.g. Soukharev et al., 2006).

- *QBO terms*: The QBO of the equatorial winds is a main component of the dynamics of the tropical stratosphere (Chipperfield et al., 1994; 2003; Randel and Wu, 1996; 2007; Logan et al., 2003; Tian et al., 2006; Fadnavis and Beig, 2009; Hauchecorne et al., 2010). It strongly influences the distributions of stratospheric O_3 propagating alternatively westerly and easterly with a mean period of 28 to 29 months. Positive and negative vertical gradients alternate periodically. At the top of the vertical QBO domain, there is a predominance of easterlies, while, at the bottom, westerly winds are more frequent. In order to account for the out-of-phase relationship between the QBO periodic oscillations in the upper and in the lower stratosphere, orthogonal ~~QBO time series~~zonal winds measured at 10 hPa (Fig. 3a; orange) and 30 hPa (Fig. 3a; green) ~~based on observed stratospheric winds at~~by the ground-station in Singapore have been considered here (Randel and Wu, 1996; Hood and Soukharev, 2006).

- *NAO, AAO and ENSO*: The El Niño/Southern Oscillation is represented by the 3-month running mean of Sea Surface Temperature (SST) anomalies (in degrees Celsius) in the Niño region 3.4 (region bounded by 120°W-170°W and 5°S- 5°N). Raw data are taken from marine ships and buoys observations. The North Atlantic and Antarctic Oscillations are described by the daily (or monthly) NAO and AAO indices which are constructed from the daily (or monthly) mean 500-hPa height anomalies in the 20°N-90°N region and 700-hPa height anomalies in the 20°S-90°S region, respectively. Detailed information for these proxies can be found in http://www.cpc.ncep.noaa.gov/. These proxies describe important dynamical features which affect ozone distributions in both the troposphere and the lower stratosphere (e.g. Weiss et al., 2001~~;~~, Frossard et al., 2013; Rieder et al., 2013; and references therein). The daily or 3-monthly average indexes used to parameterize these fluctuations are shown in Fig. 3b. The NAO and

AAO indexes are used for the N.H. and the S.H. (Southern Hemisphere), respectively (both are used for the equatorial band). These proxies have been included in the statistical model for completeness even if they are expected to only have a weak apparent contribution to the IASI ozone time series due to their large spatial variability in a zonal band (e.g. Frossard et al., 2013; Rieder et al., 2013). We have verified that including a typical time-lag relation between ozone and the ENSO variable from 0 to 4 months did not improve the regression model in terms of residuals and uncertainty of the fitted parameters. As a consequence, a time-lag has not been taken into account in our study.

- *Effective equivalent stratospheric chlorine (~~EESC): the~~): The* EESC is a common proxy used for describing the influence of the ODS in O_3 variations. However, because the IASI time series starts several years after the turnaround for the ozone hole recovery in 1996/1997 (WMO, 2010), their influence is not represented by a dedicated proxy but is rather accounted for by the linear trend term.

Even if some of the above proxies are only specific to processes occurring in the stratosphere, we adopt the same approach (geophysical variables, model and regression procedure) for adjusting the IASI O_3 time series in the troposphere. This proves useful in particular to account for the stratospheric contribution to the tropospheric layer (~30-60%; see Sect. 2 and Supplement, Fig. S~~3~~5) due to stratosphere-troposphere exchanges (STE) and to the fact that this tropospheric layer is not perfectly decorrelated from the stratosphere. This has to be kept in mind when analyzing the time series in the troposphere in Sect. 4. Specific processes in the troposphere such as emissions of ozone precursors, long-range transport and in situ chemical processing are taken into account in the model in the harmonic and the linear trend terms of the Eq. 1 (e.g. Logan et al., 2012). Including harmonic terms having 4- and 3-month periods in the model has been tested to describe O_3 dependency on shorter scales (e.g. Gebhardt et al., 2014), but this did not improved the results in terms of residuals and uncertainty of correlation coefficients.

3.3. Iterative backward variable selection

Similarly to previous studies (e.g. Steinbrecht et al., 2004; Mäder et al., 2007, 2010; Knibbe et al., 2014), we perform an iterative stepwise backward elimination approach, based on p-values of

293 the regression coefficients for the rejection, to select the most relevant combination of the above
294 described regression variables (harmonic, linear and explanatory) to fit the observations. The
295 minimum p-value for a regression term to be removed (exit tolerance) is set at 0.05, which
296 corresponds to a significance of 95%. The initial model which includes all regression variables is
297 fitted first. Then, at each iteration, the variables characterized by p-values larger than 5% are
298 rejected. At the end of the iterative process, the remaining terms are considered to have
299 significant influence on the measured O_3 variability while the rejected variables are considered to
300 be non-significant. The correction accounting for the autocorrelation in the noise residual is then
301 applied to give more confidence in the coefficients determination.
302
303 **4 Ozone variations observed by IASI**
304 In this section, we first examine the ozone variations in IASI time series during 2008-2013 in the
305 four layers defined in the troposphere and the stratosphere to match the IASI sensitivity (Sect. 2).
306 The performance of the multiple linear model is evaluated in subsection 4.2 in terms of residuals
307 errors, regression coefficients and associated uncertainties determined from the ~~multiple linear~~
308 regression procedure (Sect. 3~~) are analyzed in Sect. 4.2. The~~). Based on this, we characterize the
309 principal physical processes that affect the IASI ozone records. Finally, the ability of IASI to
310 derive apparent trends is examined in Sect. 4.3.
311
312 **4.1 O_3 time series from IASI**
313 Figure 4a shows the time development of daily O_3 number density over the entire altitude range
314 of the retrieved profiles based on daily medians. The time series cover the six years of available
315 IASI observations and are separated in three 20-degree latitude belts: 30°N-50°N (top panel),
316 10°N-10°S (middle panel) and 30°S-50°S (bottom panel). The figure shows the well-known
317 seasonal cycle at mid-latitudes in the troposphere and the stratosphere with maxima observed in
318 spring-summer and in winter-spring, respectively, and a strong stability of ozone layers with
319 time in the equatorial belt. At high latitudes of both hemispheres, the high ozone concentrations
320 and the large amplitude of the seasonal cycle observed in ~~LS~~MLST and UTLS are mainly the
321 consequence of the large-scale downward poleward Brewer-Dobson circulation which is
322 prominent in ~~later~~late winter below 25 km.

Figure 4b presents the estimated statistical uncertainty on the O_3 profiles retrieved from FORLI. This total error depends on the latitude and the season, reflecting, amongst other, the influence of signal intensity, of interfering water lines and of thermal contrast under certain conditions (e.g. temperature inversion, high thermal contrast at the surface). It usually ranges between 10 and 30% in the troposphere and in the UTLS (Upper Troposphere-Lower Stratosphere), except in the equatorial belt due to the low O_3 amounts (see Fig. 4a) which leads to larger relative errors. The retrieval errors are usually less than 5% in the stratosphere.

The relative variability (given as the standard deviation) of the daily median O_3 time series presented in Fig. 4a is shown in Fig. 5, as a function of time and altitude. It is worth noting that, except in the UTLS over the equatorial band, the variability is larger than the estimated retrieval errors of the FORLI-O_3 data (~25% *vs*. ~15% and ~10% *vs*. ~5%, on average over the troposphere and the stratosphere, respectively), reflecting that the high natural temporal variability of O_3 in zonal bands is well captured with FORLI (Dufour et al., 2012; Hurtmans et al., 2012). The standard deviation is larger in the troposphere and in the stratosphere below 20 km where dynamic processes play an important role. The largest values (> 70% principally in the northern latitudes during winter) are measured around 9-15 km altitude. They highlight the influence of tropopause height variations and the STE processes. In the stratosphere, the variability is always lower than 20% and becomes negligible in the equatorial region. Interestingly, the lowest troposphere of the N.H. (below 700 hPa; < 4 km) is marked by an increase in both O_3 concentrations (Fig. 4a) and standard deviations (between ~30% and ~45%) in spring-summer~~. This likely indicates~~, the latter being larger than the total retrieval error (less than 25%, see Fig. 4 (b)). The lower tropospheric column (e.g. ground-700 hPa) can generally not well be discriminated because of the weak sensitivity of IASI in the lowermost layers (Section 2). However, the measurements in northern mid-latitudes in spring-summer are characterized by a larger sensitivity. In the ground-700hPa columns, we find that the apriori contributions do not exceed 40% and they range between 10% and 20% over the continental regions. In addition, the stratosphere-troposphere exchanges are usually the weakest in summer. The stratospheric contributions into the IASI MLT columns are estimated to be the lowest in the

summer mid-latitudes N.H. (e.g. ~35% in the 30°N-50°N band; See Fig. S5 (b) of the Supplement) and, as mentioned in Section 2, the real natural contribution originating from the troposphere reaches ~55% (cfr Fig. S6 (b) in Supplement). This certainly helps in detecting the real variability of O_3 in the N.H. troposphere, and, the increase in the observed concentrations and in the variability may likely indicate a photochemical production of O_3 associated with anthropogenic precursor emissions (e.g. Logan et al., 1985; ~~Dufour et al., 2010; Safieddine et al., 2013).~~ Fusco and Logan, 2003; Dufour et al., 2010; Cooper et al., 2010; Wilson, et al., 2012; Safieddine et al., 2013). Changes in biomass and biogenic emissions of NO_x, CO and non-methane organic volatile compounds (NMVOC) may also play a role. However, they only represent a small part of the total emissions for NO_x and CO (e.g. ~23% *vs* 72% for the anthropogenic NO_x emissions and ~40% *vs* 60% for the anthropogenic CO emissions from the emissions dataset used in the Supplement), while the biogenic emissions of NMVOC represent the largest contribution to the total (~80%).

The zonal representation of the O_3 variability seen by IASI is given in Fig. 6. It shows the daily number density at altitude levels corresponding to maximum of sensitivity in the four analyzed layers in most of the cases (600 hPa - ~6 km; 240 hPa - ~10 km; 80 hPa - ~20 km; 6 hPa - ~35 km) (Sect. 2). The top panel (~35 km) reflects well the photochemical O_3 production by sunlight with the highest values in the equatorial belt during the summer (~3×10^{12} molecules.cm^{-3}). The middle panels (~20 km and ~10 km) shows the transport of ozone rich-air to high latitudes in late winter (up to ~6×10^{12} molecules.cm^{-3} in the N.H.) which is induced by the Brewer-Dobson circulation. The fact that the patterns at ~10km are similar ~~in ~10~~to those at ~20 km mainly reflects the low sensitivity of IASI to that level compared to the others. Finally, the lower panel (~6 km) presents high O_3 levels in spring at high latitudes (~1.4×10^{12} molecules.cm^{-3} in the N.H.), which likely reflects both the STE processes and the contribution from the stratosphere due to the medium IASI sensitivity to that layer (cfr. Sect. 2 and Supplement), and a shift from high to middle latitudes in summer which could be attributed to anthropogenic O_3 production. The MLT panel also reflects the seasonal oscillation of the Inter-Tropical Convergence Zone (ITCZ) around the Equator and the large fire activity in spring around 20°S-40°S.

4.2 Multivariate regression results: Seasonal and explanatory variables

Figure 4a shows superimposed on the time series of the IASI ozone concentration profile, those of the partial columns (dots) for the 4 layers (color ~~scale~~contours). The adjusted daily time series to these columns with the regression model defined by Eq. 1 is also overlaid and shown by colored lines. The model represents reasonably well the ozone variations in the four layers, with, as illustrated for three latitude bands, good coefficient correlations (e.g. R_{MLT}=0.94; R_{UTLS}=0.91; R_{MLST}=0.90 and R_{UST}=0.91 for the 30°N-50°N band) and low residuals (< 8 %) in all cases. The regression model explains a large fraction of the variance in the daily IASI data over the troposphere (~85%-95%) and the stratosphere (~85%-95% in all cases, except for the UST with ~70-95%), as estimated from $\frac{\sigma\left(O_3^{Fitted\ model}(t)\right)}{\sigma\left(O_3(t)\right)}$ where σ is the standard deviation relative to the fitted regression model and to the IASI O_3 time series.

However, note that the fit fails to reproduce the highest ozone values (> 5×10^{12} molecules.cm^{-3}) above the seasonal maxima for 30°N-50°N latitude band, especially in the ~~MLS~~MLST during the springs 2009 and 2010. This could be associated with occasional downward transport of upper atmospheric NO_x-rich air occurring in winter and spring at high latitudes (Brohede et al., 2008) following the strong subsidence within the intense Arctic vortex in 2009-2010 (Pitts et al., 2011) or with the missing time-lags in the regression model between the QBO and ENSO variables and the response of mid-latitude lower stratospheric ozone (Neu et al., 2014).

Figure 7 displays the annual cycle averaged over the 6 years recorded by IASI (dots) for the studied layers and bands, as well as that from the fit of the daily O_3 columns (lines). The regression model follows perfectly the O_3 variations in terms of timing of O_3 maxima and of amplitude of the cycle. The fit is generally characterized by low residuals (<10%) and good correlation coefficients (0.70-0.95), which indicates that the regression model is suitable to describe the zonal variations. Exception is found over the Southern latitudes (residual up to 15% and R down to 0.61) probably because of the variation induced by the ozone hole formation which is not parameterized in the regression model, and because of the low temporal sampling of daytime IASI measurements in this region.

From Figure 7, the following general patterns in the O_3 seasonal cycle can be isolated from the zonally averaged IASI datasets:

1- In ~~US~~UST (top left panel), the maxima is in the equatorial belt, around 4.7×10^{18} molecules.cm^{-2} throughout the year and the amplitudes are small compared to the averaged O_3 values. The largest amplitude in the annual cycle is found in the N.H. between 30°N and 50°N where O_3 peaks in July after the highest solar elevation (in June) following a progressive buildup during spring-summer. In agreement with FTIR observations (e.g. Steinbrecht et al., 2006; Vigouroux et al., 2008), a shift of the O_3 maximum from spring (March–April) to late summer (August–September) is found as one moves from high to low latitudes in the N.H. In the S.H., the general shape of the annual cycle which shows a peak in October–November before the highest solar elevation (in December), results from loss mechanisms depending on annual cycle of temperatures and other trace gases. Other effects such as changing Brewer–Dobson circulation, light absorption and tropical stratopause oscillations may also considerably impact on the cycle in this layer (Brasseur and Solomon, 1984; Schneider et al., 2005).

2- In the lower stratosphere (MLST and UTLS, top right and bottom left panels), the pronounced amplitudes of the annual cycle is dominated by the influence of the Brewer Dobson circulation with the highest O_3 values observed over polar regions (reaching ~6×10^{18} molecules/cm^2 on average *vs.* ~2×10^{18} molecules/cm^2 on average in the equatorial belt). The maximum is shifted from late winter at high latitudes to spring at lower latitudes.

3- In MLT (bottom right panel), we clearly see a large hemispheric difference with the highest values over the N.H. (also in UTLS). Maxima are observed in spring, reflecting more effective STE processes. A particularly broad maximum from spring to late summer is observed in the 30°N-50°N band. It probably points to anthropogenic production of O_3. This has been further investigated in the Supplement through MOZART4-IASI comparison by using constant anthropogenic emissions in the model settings (see Fig. S2). The results show clear differences between the modeled and the observed MLT seasonal cycles, which highlights the need for further investigation of the role of anthropogenically produced O_3 and the realism of anthropogenic emissions inventories.

Figure 8 presents all the fitted regression parameters included in Eq. 1 (Sect. 3) in the four layers as a function of latitude. The uncertainty in the 95% confidence limits which accounts for the autocorrelation in the noise residual is given by error bars. The constant term (Fig. 8a) is found to be statistically significant (uncertainty<10%) in all cases. It captures the two ozone maxima in the stratosphere: one over the Northern Polar regions in the ~~MLS~~MLST and one at equatorial latitudes in the ~~US~~UST (~4.5×10^{18} molecules.cm^{-2}), the important decrease of O_3 in the lower stratospheric layers (UTLS and ~~MLS~~MLST) moving from high to equatorial latitudes, and the weak negative and strong positive gradients in the Northern MLT and in the ~~US~~UST, respectively. The sum of the constant terms of the four layers varies between 7.50×10^{18} (equatorial region) and 9.50×10^{18} molecules.cm^{-2} (polar regions) and is similar to the one of the fitted total column (relative differences < 3.5%) (red line). ~~When analyzing~~ Note that the constant terms~~, it is worth keeping in mind that FORLI-O3 profiles are biased high~~ in the UTLS region ~~by ~10%–15%~~ in the mid-latitudes and in the tropics are certainly affected by the fact that the FORLI-O_3 profiles are biased high by ~10-15% in this layer and latitude bands (Dufour et al., 2012; Gazeaux et al., 2012). The representativeness of the 20° zonal averages in terms of spatial variability has been examined by fitting the IASI time series for specific locations in the N.H. (results shown with stars in Fig. 8a): the constant terms are found to be consistent, within their uncertainties, with those averaged per latitude bands in all cases. Over the polar region where O_3 shows a large natural variability, the regression coefficient is characterized by a large uncertainty.

The regression coefficients for other variables (harmonic and proxy terms) which are retained in the regression model by the stepwise elimination procedure are shown in Fig. 8b. They are scaled by the fitted constant term and the error bars represent the uncertainty in the 95% confidence limits accounting for the autocorrelation in the noise residual. ~~We~~A positive (or negative) sign of the coefficients indicates that the associated variables are correlated (or anti-correlated) with the IASI O_3 time series. Note that if the uncertainty is larger than its associated estimate (i.e. larger than 100%, corresponding to an error bar overlapping the zero line), it means that the estimate becomes statistically non-significant when accounting for the autocorrelation in the noise residuals at the end of the elimination process. This is summarized in Table S1 of the

Supplement. The contribution of the fitted variables into the IASI O_3 variations is estimated as $\frac{\sigma([a_n; b_n; x_j][\cos(n\omega t); \sin(n\omega t); X_{norm,j}])}{\sigma(O_3(t))}$ where σ is the standard deviation relative to the fitted signal of harmonic or proxy terms and to the IASI O_3 time series. From Figure 8, we find that:

1- The annual harmonic term (upper left) is the main driver of the O_3 variability and largely dominates (scaled a_1+b_1 around ±40 %) over the semi-annual one (upper right; scaled a_2 +b_2 around ±15 %). In UTLS and ~~MLS~~MLST, its amplitude decreases from high to low latitudes likely following the cycle induced by the Brewer-Dobson circulation (*cfr.* Fig. 6 and Fig. 7) and the sign of the coefficient accounts for the winter-spring maxima in both hemispheres (negative values in the S.H. and positive ones in the N.H). ~~In the US, they vary only slightly (around −5% to 5 %) and account for the weak summer maximum~~The annual term contributes importantly around 45%-85% of the observed O_3 variations, except in the 10°N-30°N and equatorial bands (10%-30%), while the influence of the semi-annual variation on O_3 is smaller (10%-25%) and highly variable between the bands. In the UST, the amplitudes vary only slightly (around -5% to 5%) and account for the weak summer maximum. The contributions of the annual harmonic term are estimated between 5%-30%. As expected, the uncertainties associated with the annual terms are very weak and most of the harmonic terms (annual and seasonal) are statistically significant.

2- The QBO and solar flux proxies are generally minor (scaled coefficients < 10%) and they are often statistically non-significant contributors to O_3 variations after accounting for the autocorrelation in the noise residual~~,~~ (see Table S1 in the Supplement), except ~~for the UTLS~~ in equatorial region (scaled coefficients of 10%–15% in UTLS and contributions up to 75% and 21% for QBO and SF, respectively) where they are important drivers of O_3 variations (e.g. Logan et al., 2003; Steinbrecht et al., 2006b; Soukharev and Hood, 2006; Fadnavis and Beig, 2009). Previous studies have indeed supported the solar influence on the lower stratospheric equatorial dynamics (e.g. Soukharev and Hood, 2006; McCormack et al., 2007). Note that the QBO[30] proxy (data not shown) has negative coefficients for the mid-latitudes, which is in line with Frossard et al. (2013).

3- The contributions described by the ENSO and NAO/AAO proxies are generally very weak~~,~~ (<10% and <5%, respectively), with scaled coefficients lower than 5%, and, in many cases~~,~~ for the NAO/AAO proxies, they are even not statistically significant when taking into account the correlation in the noise residuals~~.~~ (see Table S1 in Supplement). Despite of this, it is worth pointing out that their effects to the O_3 variations are ~~in agreement with~~ comparable to the results published in the previous studies~~, which~~. The negative ENSO coefficient in the tropical UTLS is consistent with results from Neu et al. (2014). Rieder et al. (2013) and Frossard et al. (2013) have also shown large regions of negative coefficients for NAO North of 40°N, and large regions of positive and negative coefficient estimates for ENSO, North of 30°N and South of 30°S, respectively ~~(Rieder et al., 2013; Frossard et al., 2013).~~.

We note that the non-representation of time-lags in the proxy time series may be underestimating the role of some geophysical variables on O_3 variations, in particular that of ENSO and QBO in zonal bands outside the regions where these geophysical quantities are measured (i.e. Niño region 3.4 for ENSO and Singapore for QBO).Finally, we see in Fig. 8b, large uncertainties associated with the regression coefficients in UTLS in comparison with other layers, and in polar regions in comparisons with other bands. We interpret this as an effect from the high natural variability of O_3 measured by IASI in UTLS (see Fig.5) and from missing parameterizations and low temporal sampling of daytime IASI measurements over the poles, respectively.

As a general feature, the results demonstrate the representativeness of the fitted models in each layer and latitude band. This good performance of the regression procedure allows examination of the adjusted linear trend term in Section 4.3 below.

4.3 Multivariate regression results: trend over 2008-2013

An additional goal of the multivariate regression method applied to the IASI O_3 time series is to determine the linear trend term and its associated uncertainty. Despite the fact that more than 10 years of observations, corresponding to the large scale of solar cycle, is usually required to perform such a trend analysis, we could argue that statistically relevant trends could possibly be

derived from the first six years of IASI observations, owing to the high spatio-temporal frequency (daily) of IASI global observations, to the daily "fingerprint" in the solar flux (see Figure 3 (a)), possibly making it distinguishable from a linear trend, and to its weak contribution to O_3 variations (see section 4.2. and references therein). To verify the specific advantage of IASI in terms of frequency sampling, we compare, in the subsections below, the statistical relevance of the trends when retrieved from the monthly averaged IASI datasets *vs* the daily averages as above, in the 20° zonal bands for the 4 partial and the total columns.

4.3.1. Regressions applied on daily *vs* monthly averages

Figure 9 (top) provides, as an example, the 6-year time series of ~~the~~ IASI O_3 ~~partial column in the US (dark blue), for~~ daily averages (left panels, dark blue) ~~vs~~ compared to the monthly averages (right panels, dark blue) for the 30°S-50°S latitude band in the UST (dark blue), along with the results from the regression procedure (light blue). Note that either daily or monthly F10.7, NAO and AAO proxies (see Table 1) are used depending on the frequency of the IASI O_3 averages to be adjusted. The ~~middle panels provide~~second row in Fig.9 provides the deseasonalised IASI and fitted time series, calculated by subtracting the model seasonal cycle from the time series, as well as the residuals (red curves). The averaged residuals relative to the deseasonalised IASI time series strongly vary with the layers and latitudinal bands and usually range between 30% and 60%. The fitted signal in DU of each proxy is shown on the bottom panels. The O_3 time series and the solar flux signal resulting from the adjustment without the linear term trend in the regression model are also represented (orange lines in ~~middle~~ 2^d and bottom panels, respectively). When it is not included in the regression model, the linear trend term is ~~not~~only partly compensated by the solar flux term in the daily averages~~, which~~. This leads to an offset between the fitted O_3 time series resulting from the both regression models (with and without the linear term), which corresponds well to a trend over the IASI period, and, consequently, to larger residuals (e.g. 80% without *vs*. 44% with the linear term for this example and 94% without *vs* 58% with the linear term for the 30°S-50°S band in the MLST illustrated in Fig. S1 of the Supplement~~), while it~~). This offset is observed for a lot of layers and latitudinal bands. On the contrary, the linear term can largely be compensated by the solar flux term in the monthly averages ~~(75% without~~: the offset is weak and the difference between the both fitted

models is smaller (averaged differences relative to the deseasonalised IASI time series of 10% in monthly data *vs*~~. 60% with the linear term).~~ 17% in daily data for this example). In this example, the linear and solar flux terms are even not simultaneously retained in the iterative stepwise backward procedure when applied on the monthly averages while they are when applied on daily averages. This effective co-linearity of the linear and the monthly solar flux terms translates to ~~a large~~larger model fit residuals (44% in daily averages *vs* 60% in monthly averages in UST, relative to the deseasonalised IASI time series), to smaller relative differences between both regression models (with and without the linear term) (17% in daily vs 10% in monthly data), and to larger uncertainty ~~for~~on the trend ~~coefficient in~~ coefficients when using the monthly data ~~and~~in comparison with the daily data. This even leads, in this specific example, to a not statistically significant linear term of 1.21±1.30DU/yr when derived from monthly averages *vs*. a significant trend of 1.74±0.77DU/yr from daily averages.

The same conclusions can be drawn from the fits in other layers and latitude bands, especially those where the solar cycle variation of ozone is large (MLST and UTLS, see Fig. 8) or where the ozone recovery would occur (UST). A larger trend uncertainty associated with monthly data *vs* daily data is found in all situations (see Table 2, Section 4.3.2 below).

This brings us to the important conclusion that, thanks to the unprecedented sampling of IASI, apparent trends can be detected in FORLI-O_3 time series even on a short period of measurements. This supports the need for regular and high frequency measurements for observing ozone variations underlined in other studies (e.g. Saunois et al., 2012). The O_3 trends from the daily averages of IASI measurements are discussed and compared with results from the monthly averages in the subsection below.

4.3.2. O_3 trends from daily averages

Table 2 summarizes the trends and their uncertainties in the 95% confidence limit, calculated for each 20° zonal band and for the 4 partial and the total columns. In the northern and southern polar regions, the polar night period is not covered because only IASI observations during sunlight (over Feb-Oct and Oct-Apr for N.H. and S.H., respectively) are used in this study (See

Sect. 2). For the sake of comparison, the trends are reported for both the daily (top values) and the monthly (bottom values) averages, and their uncertainties account for the auto-correlation in the noise residuals considering a time lag of 1-day or 1-month, respectively. We show that the daily and monthly trends in all layers and all latitude bands fall within each other uncertainties, but that the use of daily median strongly helps in reducing everywhere the uncertainty associated with the trends for the reasons discussed above (Sect. 4.3.1). This is particularly observed in the UST where the ozone hole recovery would occur, but also in the MLST and the UTLS where the solar cycle variation of ozone is the largest (see Figure 8). As a consequence, the UST trends in monthly averages are shown to be mostly non-significant in comparison with those from daily averages ~~for the reasons discussed above (Sect. 4.3.1).~~ Table 3 summarizes the trends in the daily averages for two 3-month periods: June-July-August (JJA) and December-January-February (DJF).

From Tables 2 and 3, we observe very different trends according to the latitude and the altitude. From Table 2, we find for the total columns that the trends derived from the daily medians are only significant at high northern latitudes and that they are interestingly of the same order as those obtained from other satellites and assimilated satellite data (Weatherhead and Anderson, 2006; Knibbe et al., 2014) or from ground-based measurements (Vigouroux et al., 2008) calculated over longer time periods. The non-significant trends calculated for the mid- and low latitudes of the N.H. are also ~~in agreement with~~comparable to the results published in the previous studies (Reinsel et al., 2005; Andersen ~~and Knudsen, 2006~~et al., 2006a; Vigouroux et al., 2008). Regarding the individual layers, we find the following:

1- In the US, significant positive trends are observed in both hemispheres from the daily medians, particularly over the mid- and high latitudes of both hemispheres (e.g. 1.74±0.77DU.yr−1 in the 30°S–50°S band, i.e., 12%/decade) where the changes in ozone trends before and after the turnaround in 1997 ~~is~~have been found to be the highest ~~(~~. Kÿrola et al~~.,~~. (2013~~;~~) and Laine et al~~.,~~. (2014~~).~~) report for instance a change of up to 10%/decade in O_3 trends between 1997-2011 *vs*. 1984-1997. Positive trends in the ~~US~~UST are ~~in agreement~~consistent with many previous observations if one considers the fact that the period covered by IASI is later than those reported in previous studies and that the recovery rate

seems to heighten since the beginning of the turnaround (Knibbe et al. (2014) reports a factor of two increase in the recovery rate between 1997–2010 with ~0.7DU/yr and 2001–2010~~), and they~~ with ~1.4DU/yr in the S.H.). They could indicate a leveling off of the negative trends that ~~was existing~~were observed since the second half of the 1990's mostly from satellites and ground-based monthly mean data (e.g. WMO 2006, 2011; Randel and Wu, 2007; Vigouroux et al., 2008; Steinbrecht et al., 2009; Jones et al., 2009; McLinden et al., 2009; Laine et al., 2014; Nair et al., 2014). The causes of this "turnaround" remain, however, uncertain. If the compensating impact of decreasing chlorine in recent years and maximum solar cycle (over 2011-2012 in the period studied here) is probably part of the answer (e.g. Steinbrecht et al., 2004), the effects of changing stratospheric temperatures and Brewer~~-~~-Dobson circulation (Salby et al., 2002; Reinsel et al., 2005; Dhomse et al., 2006; Manney et al., 2006) could also contribute and should be further investigated. The long-lasting cold winter/spring 2011 in the Arctic ~~conducting~~leading to unprecedented ozone loss (Manney et al., 2011), could explain the non-significant trend in the 70°N-90°N band. This is supported by the results in winter (Table 3~~, which shows a significant positive trend when derived from the summer data.~~). From Table 3, we generally find significant positive trends in summer N.H. and weaker positive or even non-significant trends in winter S.H.. A non-significant trend is also calculated for the 70°S-90°S band in spring (data not shown). This could indicate the strong influence of changing stratospheric temperatures on ozone depletion from year to year (e.g. Dhomse et al., 2006), leading to larger uncertainties in our trends estimations and larger fitting residuals (see Sect. 4.2) due to the fact that the stratospheric temperature is not taken into account as an explanatory variable in the model.

2- In the ~~MLS~~MLST, one can see that, except in the high latitude bands, the trends are either non-significant or significantly negative. This is in agreement with the trend analysis of Jones et al. (2009) for the 20–25 km altitude range over the 1997–2008 period, as well as with other studies at N.H. latitudes, which investigated O_3 changes in the 18–25 km range between 1996 and 2005 (Miller et al., 2006; Yang et al., 2006; Kivi et al., 2007). The results derived separately for summer and winter in Table 3 are also in line with those of Kivi et al. (2007) which reported contrasted trends in the Arctic ~~MLS~~MLST depending on season.

3- In the UTLS, negative trends are calculated in the tropics and significant positive trends are found in the mid- and high latitudes of N.H., these latter falling within the uncertainties of those reported by Kivi et al. (2007) for the tropopause-150 hPa layer between 1996 and 2003. The large positive trends calculated at Northern latitudes (e.g. 1.28±0.82 DU/year in the 70°N-90°N band) contribute for ~ 30% to the positive trend for the total column. This result is ~~in agreement~~consistent with Yang et al. (2006) which reported that UTLS contributes 50% to positive trends for the total columns measured in the mid-latitudes of the N.H. from ozonesondes. In that study, these positive trends were linked to changes in atmospheric dynamics either related to natural variability induced by potential vorticity and tropopause height variations or related to anthropogenic climate change. Hence, the apparent increase in total ozone in the mid-latitudes of the N.H. seen by IASI would reflect the combined contribution of dynamical variability and declining ozone-depleting substances (e.g. Weatherhead and Andersen, 2006; WMO, 2006; Harris et al., 2008; Nair et al., 2014). It is worth to keep in mind that these effects are not independently accounted for in the regression model. Previous studies reported, however, that dynamical and chemical processes are physically coupled in the atmosphere, making difficult to define unambiguously such drivers in a statistical model (e.g. Mäder et al., 2007; Harris et al., 2008). On a seasonal basis (see Table 3), the trends seen by IASI at Northern latitudes in summer are all significantly positive and increasing towards the pole. Note that the trends in upper layers may contribute to the ones calculated in UTLS due to the medium IASI sensitivity to that layer (*cfr.* Sect. 2).

4- In the MLT, most of the trends are significantly negative (Tables 2 and 3). The non-significant trends in polar regions could be partly related to the lack of IASI sensitivity to tropospheric O_3 (see Sect. 2, Fig. 2). On a seasonal basis, we see that the negative trends are more pronounced during the JJA period (around -0.25±0.10DU.yr^{-1}) for all bands except between 30°N and 10°S. In the N.H., these results tend to confirm the leveling off of tropospheric ozone observed in recent years during the summer months (Logan et al., 2012). This trend, however, remains difficult to interpret because it could be linked to a variety of processes including most importantly: the decline of anthropogenic emissions of ozone precursors, the increase of UV-induced O_3 destruction in the troposphere and STE processes (Isaksen et al., 2005; Logan et al., 2012; Parrish et al., 2012; Hess and Zbinden, 2013). As ~~for~~

~~the upper layers, our results for the Arctic are~~ a consequence, it is hard to reconcile the trends in ~~agreement~~ tropospheric ozone with ~~the findings~~changes in emissions of ~~Kivi et al. (2007) which reported an increase of ozone in the ground-400 hPa layer~~ozone precursors. However, trends in ~~summer~~emissions have already been able to qualitatively explain measured ozone trends over ~~the 1996–2003 period following changes in the Arctic Oscillation.~~some regions but with inconsistent magnitude between observations and model simulations (e.g. Cooper et al., 2010; Logan et al., 2012; Wilson et al., 2012). It is also worth to keep in mind that due to medium sensitivity of IASI to the troposphere, the a priori contribution and ozone variations in ~~upper~~stratospheric layers may largely influence the trends seen by IASI in ~~that~~the MLT layer (*cfr.* Sect. 2 and Supplement).

4.3.3. O_3 trends from IASI *vs* FTIR data

In order to validate the trends inferred from IASI in the ~~US~~UST and in the total columns, we compare them with those obtained from ground-based FTIR measurements at several NDACC stations (Network for the Detection of Atmospheric Composition Change, available at http://www.ndsc.ncep.noaa.gov/data/data_tbl/) by using the same fitting procedure and taking into account the autocorrelation in the noise residuals. A box of 1°×1° centered on the stations has been used for the collocation criterion. The regression model is applied on the daily FTIR data for a series of time periods starting after the turnaround point (from 1998 for mid-latitude stations and from 2000 for polar stations), as well as for the same periods as recently studied in Vigouroux et al. (2014) for the sake of comparison. Note that because we are not interested here in validating the IASI columns which was achieved in previous papers (e.g. Dufour et al., 2014; Oetjen et al., 2014) but in validating the trends obtained from IASI, we did not correct biases between IASI and FTIR due to different vertical sensitivity and *a priori* information. The results are given in DU/year in Table 4. We see large significant positive total column trends from IASI at middle and polar stations (e.g. 5.26±4.72 DU/yr at Ny-Alesund), especially during spring ~~and which~~. These values are ~~in agreement~~consistent with ~~the trends~~those reported in Knibbe et al. (2014) for the 2001-2010 period~~.~~ in spring in the Antarctic (around 3-5 DU/yr). This trend is not obtained from the FTIR data for which trends are found to be mostly non-significant (even not retained in the stepwise elimination procedure in some cases) as reported in Vigouroux et al.

(2014), except at Jungfraujoch which shows a trend of 5.28±4.82DU/yr over the 2008–2012 period. For the periods starting before 2000, we calculated from FTIR, in agreement with Vigouroux et al. (2014), a significantly negative trend at Ny-Alesund for the total column and significantly positive trends at polar stations for the US. In addition, we see from Table 4 a leveling off of O_3 at polar stations in the ~~US~~UST after 2003, as~~–~~ previously reported in Vigouroux et al. (2014), which was explained by a compensation effect between the decrease of solar cycle after its maximum in 2001-2002 and a positive trend. These trends are, however, non-significant and inferred only from few FTIR measurements (see Number of days column, Table 4).

From IASI, it is worth to point out that, in all cases, positive trends are calculated in the ~~US~~UST (even if some are not significant) and that these trends are consistent with those calculated from FTIR data covering a ~11-year period and starting after the turnaround (e.g. at Thule; 1.24±1.09 DU/yr from IASI for the period 2008-2013 *vs*. 1.42±0.78 DU/yr from the FTIR over 2001-2012). This is illustrated for three stations (Ny-Alesund, Thule and Kiruna) in Fig.10 which compares the time series from IASI (2008-2013, in red) with those from FTIR covering periods starting after the turnaround (in blue). Their associated trends as well as the trend calculated from FTIR covering the IASI period (in green) are also indicated.

In order to better characterize the effect of the temporal frequency on determining statistical trends, the IASI time series have been subsampled to match the temporal resolution of FTIR. The associated trend values are also indicated in Table 4 (2^{d} row). In any cases, we observe that the fitted trends inferred from both IASI and FTIR with the same temporal samplings are within the uncertainties of each other and that those associated with the subsampled IASI datasets are significantly larger than those obtained with the daily ones, leading to statistically non-significant trends.

Even if validating the IASI fitted trends with independent datasets is challenging due to the short-time period of available IASI measurements and the insufficient number of usable correlative measurements over such a short period, the results obtained for ~~trends inferred from~~

IASI *vs*. FTIR tend to confirm the conclusion drawn in Sects. 4.3.1 and 4.3.2, that the high temporal sampling of IASI provides good confidence in the determination of the trends even on periods shorter than those usually required from other observational means.

6 Summary and conclusions

In this study, we have analyzed 6 years of IASI O_3 profile measurements as well as the total O_3 columns based on the profile. Four layers have been defined following the ability of IASI to provide reasonably independent information on the ozone partial columns: the mid-lower troposphere (MLT), the upper troposphere – lower stratosphere (UTLS), the mid-lower stratosphere (~~MLS~~MLST) and the upper stratosphere (~~US~~UST). Based on daily values of these four partial or of the total columns in 20° zonal averages, we have demonstrated the capability of IASI for capturing large scale ozone variability (seasonal cycles and trends) in these different layers. We have presented daytime vertical and latitudinal distributions for O_3 as well as their evolution with time and we have examined the underlying dynamical or chemical processes. The distributions were found to be controlled by photochemical production leading to a maximum in summer at equatorial region in the ~~US~~UST, while they reflect the impact of the Brewer-Dobson circulation with maximum in winter-spring at mid- and high latitude in the ~~MLS~~MLST and in the troposphere. The effect of the photochemical production of O_3 from anthropogenic precursor emissions was also observed in the troposphere with a shift in the timing of the maximum from spring to summer in the mid-latitudes of the N.H.

The dynamical and chemical contributions contained in the daily time development of IASI O_3 have been analyzed by fitting the time series in each layer and for the total column with a set of parameterized geophysical variables, a constant factor and a linear trend term. The model was shown to perform well in term of residuals (< 10%), correlation coefficients (between 0.70 and 0.99) and statistical uncertainties (< 7%) for each fitted proxies. The annual harmonic terms (seasonal behavior) were found to be largely dominant in all layers but the US, with fitted amplitudes decreasing from high to low latitudes in agreement with the Brewer-Dobson circulation. The QBO and solar flux terms were calculated to be important only in the equatorial

768 region, while other dynamical proxies accounted for in the regression (ENSO, NAO, AAO) were
769 found negligible.
770
771 Despite the short time period of available IASI dataset used in this study (2008-2013) and the
772 potential ambiguity between the solar and the linear trend terms, statistically significant trends
773 were derived from the six first years of daily O_3 partial columns measurements (on the contrary
774 to monthly averages which lead to mostly non-significant trends). This result which was
775 strengthened from comparisons with the regression applied on local FTIR measurements, is
776 remarkable as it demonstrates the added value of IASI exceptional frequency sampling for
777 monitoring medium to long-term changes in global ozone concentrations. We found two
778 important apparent trends:
779 1) Significant positive trends in the upper stratosphere, especially at high latitudes in both
780 hemispheres (e.g. 1.74±0.77DU/yr in the 30°S-50°S band), which are consistent with a probable
781 "turnaround" for upper stratospheric O_3 recovery (even if the causes of such a turnaround are
782 still under investigations). In addition, the trends calculated for some local stations are in line
783 with those calculated from FTIR measurements after the turnaround.
784 2) Negative trends in the troposphere at mid- and high Northern latitudes, especially during
785 summer (e.g. -0.26±0.11DU/yr in the 30°N-50°N band) which are in line with the decline of
786 ozone precursor emissions.
787
788 To confirm the above findings beyond the 6 first years of IASI measurements and to better
789 disentangle the effects of dynamical changes, of the 11-year solar cycle and of the equivalent
790 effective stratospheric chlorine (EESC) decline on the O_3 time series, further years of IASI
791 observations will be required, and more complete fitting procedures (including, among others,
792 proxies to account for the decadal trend in the EESC, for the ozone hole formation, for changes
793 in the Brewer-Dobson circulation, as well as including time lags in ENSO and QBO proxies) will
794 have to be explored. Further investigation on the regressors uncertainties and on the total error on
795 ozone measurements should be performed as well to understand on the unexplained variations in
796 IASI O_3 records.
797

This will be achievable with the long-term homogeneous records obtained by merging measurements from the three successive IASI instruments on MetOp-A (2006); -B (2012) and –C (2018), and by IASI successor on EPS-SG after 2021 (Clerbaux and Crevoisier, 2013; Crevoisier~~,~~ et al., 2014).

Acknowledgments

IASI has been developed and built under the responsibility of the Centre National d'Etudes Spatiales (CNES, France). It is flown onboard the MetOp satellites as part of the EUMETSAT Polar System. The IASI L1 data are received through the EUMETCast near real time data distribution service. Ozone data used in this paper are freely available upon request to the corresponding author. We acknowledge support from the O_3-CCI project funded by ESA and by the O3M-SAF project funded by EUMETSAT. P.-F. Coheur and C. Wespes are, respectively, Senior Research Associate and Postdoctoral Researcher with F.R.S.-FNRS. The research in Belgium was also funded by the Belgian State Federal Office for Scientific, Technical and Cultural Affairs and the European Space Agency (ESA Prodex IASI Flow and BO_3MSAF). The National Center for Atmospheric Research is funded by the National Science Foundation.

References

Andersen, S. B. and Knudsen, B. M.: The influence of polar vortex ozone depletion on NH mid-latitude ozone trends in spring, Atmos. Chem. Phys., 6, 2837–2845, 2006a.

Andersen, S. B., Weatherhead, E. C., Stevermer, A., Austin, J., Brühl, C, Fleming, E. L., de Grandpré, J., Grewe, V., Isaksen, I., Pitari, G., Portmann, R. W., Rognerud, B., Rosenfield, J. E., Smyshlyaev, S., Nagashima, T., Velders, G. J. M., Weisenstein, D. K., and Xia, K.: Comparison of recent modeled and observed trends in total column ozone, J. Geophys. Res., 111, D02303, doi:10.1029/2005JD006091, 2006b.

Anton, M., D. Loyola, C. Clerbaux, M. Lopez, J. Vilaplana, M. Banon, J. Hadji-Lazaro, P. Valks, N. Hao, W. Zimmer, P. Coheur, D. Hurtmans, and L. Alados-Arboledas: Validation of the Metop-A total ozone data from GOME-2 and IASI using reference ground-based measurements at the Iberian peninsula, Remote Sensing of Environment, 115, 1380-1386, 2011.

August, T., D. Klaes, P. Schlüssel, T. Hultberg, M. Crapeau, A. Arriaga, A., O'Carroll, A., Coppens, D., Munro, R., Calbet, X.: IASI on Metop-A: Operational Level 2 retrievals after five years in orbit. Journal of Quantitative Spectroscopy and Radiative Transfer, 114(11), 1340–1371, 2012.

Barret, B., Le Flochmoen, E., Sauvage, B., Pavelin, E., Matricardi, M., and Cammas, J. P.: The detection of post-monsoon tropospheric ozone variability over south Asia using IASI data, Atmos. Chem. Phys., 11, 9533-9548, doi:10.5194/acp-11-9533-2011, 2011.

Bourassa, A. E., D. A. Degenstein, W. J. Randel, J. M. Zawodny, E. Kyrölä, C. A. McLinden, C. E. Sioris, and C. Z. Roth: Trends in stratospheric ozone derived from merged SAGE II and Odin-OSIRIS satellite observations, Atmos. Chem. Phys., 14, 6983–6994, doi:10.5194/acp-14-6983-2014, 2014.

Boynard, A., C. Clerbaux, P.-F. Coheur, D. Hurtmans, S. Turquety, M. George, J. Hadji-Lazaro, C. Keim, and J. Meyer-Arnek: Measurements of total and tropospheric ozone from IASI: comparison with correlative satellite, ground-based and ozonesonde observations, Atmos. Chem. Phys., 9, 6255-6271, 2009.

Brohede, S., McLinden, C. A., Urban, J., Haley, C. S., Jonsson, A. I., and Murtagh, D.: Odin stratospheric proxy NOy measurements and climatology, Atmos. Chem. Phys., 8, 5731–5754, doi:10.5194/acp-8-5731 2008, 2008.

Brasseur, G. and Solomon, S: Aeronomy of the Middle Atmosphere, 441 pp., D. Reidel Publishing Company, Dordrecht, The Netherlands, 1984.

Chipperfield, M. P., Kinnersley, J. S., and Zawodny, J.: A two-dimensional model study of the QBO signal in SAGE II NO_2 and O_3, Geophys. Res. Lett., 21, 589–592, 1994.

Chipperfield, M. P.: A three-dimensional model study of longterm mid-high latitude lower stratosphere ozone changes, Atmos. Chem. Phys., 3, 1253–1265, 2003.

Clarisse L., D. Hurtmans, C. Clerbaux, J. Hadji-Lazaro, Y. Ngadi, P.-F. Coheur: Retrieval of sulphur dioxide from the infrared atmospheric sounding interferometer (IASI) Atmospheric Measurement Techniques 5, 3, 581-594, 2012.

Clerbaux, C., A. Boynard, L. Clarisse, M. George, J. Hadji-Lazaro, H. Herbin, D. Hurtmans, M. Pommier, A. Razavi, S. Turquety, C. Wespes, and P.-F. Coheur: Monitoring of atmospheric composition using the thermal infrared IASI/MetOp sounder, Atmos. Chem. Phys., 9, 6041-6054, 2009.

Clerbaux C. and C. Crevoisier: New Directions: Infrared remote sensing of the troposphere from satellite: Less, but better, Atmospheric Environment, 72, 24-26, 2013.

Coheur, P.-F., B. Barret, S. Turquety, D. Hurtmans, J. Hadji-Lazaro, and C. Clerbaux: Retrieval and characterization of ozone vertical profiles from a thermal infrared nadir sounder, J. Geophys. Res., 110, D24, 303, doi:10.1029/2005JD005845, 2005.

Cooper, O., Parrish, D., Stohl, A., Trainer, M., Nédélec, P., Thouret, V., Cammas, J., Oltmans, S., Johnson, B., and Tarasick, D.: Increasing springtime ozone mixing ratios in the free troposphere over western North America, Nature, 463, 344–348, doi:10.1038/nature08708, 2010.

Crevoisier, C., Clerbaux, C., Guidard, V., Phulpin, T., Armante, R., Barret, B., Camy-Peyret, C., Chaboureau, J.-P., Coheur, P.-F., Crépeau, L., Dufour, G., Labonnote, L., Lavanant, L., Hadji-Lazaro, J., Herbin, H., Jacquinet-Husson, N., Payan, S., Péquignot, E., Pierangelo, C., Sellitto, P., and Stubenrauch, C. : Towards IASI-New Generation (IASI-NG): impact of improved spectral resolution and radiometric noise on the retrieval of thermodynamic, chemistry and climate variables, Atmos. Meas. Tech., 7, 4367-4385, 2014.

de Laat, A. T. J., R. J. van der A, and M. van Weele: Tracing the second stage of ozone recovery in the Antarctic ozone-hole with a “big data” approach to multivariate regressions, Atmos. Chem. Phys.,15, 79–97, doi:10.5194/acp-15-79-2015, 2015.

878 Dhomse, S., Weber, M., Wohltmann, I., Rex, M., and Burrows, J. P.: On the possible causes of
879 recent increases in northern hemispheric total ozone from a statistical analysis of satellite data
880 from 1979 to 2003, Atmos. Chem. Phys., 6, 1165–1180, doi:10.5194/acp-6-1165-2006, 2006.
881 Dufour, G., M. Eremenko, J. Orphal, and J.-M. Flaud: IASI observations of seasonal and day-to-
882 day variations of tropospheric ozone over three highly populated areas of China: Beijing,
883 Shanghai, and Hong Kong, Atmos. Chem. Phys., 10, 3787-3801, 2010.
884 Dufour, G., M. Eremenko, A. Griesfeller, B. Barret, E. LeFlochmoen, C. Clerbaux, J. Hadji-
885 Lazaro, P.-F. Coheur, and D. Hurtmans: Validation of three different scientific ozone products
886 retrieved from IASI spectra using ozonesondes, Atmos. Meas. Tech., 5, 611-630, 2012.
887 Fadnavis, S. and Beig, J.: Quasibiennial Oscillation in Ozone and Temperature over Tropics, J.
888 Atmos. Sol. Terr. Phys., 71, 1450–1455, doi:10.1016/j.jastp.2008.11.012, 2009.
889 Gardiner, T., Forbes, A., de Mazière, M., Vigouroux, C., Mahieu, E., Demoulin, P., Velazco, V.,
890 Notholt, J., Blumenstock, T., Hase, F., Kramer, I., Sussmann, R., Stremme,W., Mellqvist, J.,
891 Strandberg, A., Ellingsen, K., and Gauss, M.: Trend analysis of greenhouse gases over Europe
892 measured by a network of ground-based remote FTIR instruments, Atmos. Chem. Phys., 8,
893 6719–6727, 2008.
894 Frossard, L., H.E. Rieder, M. Ribatet, J. Staehelin, J. A, Maeder, S. Di Rocco, A. C. Davison, T.
895 Pete.: On the relationship between total ozone and atmospheric dynamics and chemistry at mid-
896 latitudes – Part 1: Statistical models and spatial fingerprints of atmospheric dynamics and
897 chemistry, Atmos. Chem. Phys., 13, 147–164, doi:10.5194/acp-13-147-2013, 2013.
898 Fusco, A. C. and Logan, J. A., Analysis of 1970–1995 trends in tropospheric ozone at Northern
899 Hemisphere midlatitudes with the GEOS-CHEM model, J. Geophys. Res., 108, 4449,
900 doi:10.1029/2002JD002742, 2003.
901 Gazeaux, J., C. Clerbaux, M. George, J. Hadji-Lazaro, J. Kuttippurath, P.-F. Coheur, D.
902 Hurtmans, T. Deshler, M. Kovilakam, P. Campbell, V. Guidard, F. Rabier, and J.-N. Thepaut:
903 Intercomparison of polar ozone profiles by IASI/Metop sounder with 2010 concordiasi
904 ozonesonde observations, Atmos. Meas. Tech., 5, 7923-7944, 2012.
905 Hadjinicolaou, P., Pyle, J. A., and Harris, N. R. P.: The recent turnaround in stratospheric ozone
906 over northern middle latitudes: A dynamical modeling perspective, Geophys. Res. Lett., 32,
907 L12821, doi:10.1029/2005GL022476, 2005.

908 Harris, N. R. P., E. Kyrö, J. Staehelin, D. Brunner, S.-B. Andersen, S. Godin-Beekmann, S.,
909 Dhomse, P. Hadjinicolaou, G. Hansen, I. Isaksen, A. Jrrar, A. Karpetchko, R. Kivi, B. Knudsen,
910 P. Krizan, J. Lastovicka, J. Maeder, Y. Orsolini, J. A. Pyle, M. Rex, K. Vanicek, M. Weber, I.
911 Wohltmann, P. Zanis and C. Zerefos: Ozone trends at northern mid- and high latitudes – a
912 European perspective. *Ann. Geophys*., 26, 1207-1220, 2008.
913 Hauchecorne, A., Bertaux, J. L., Dalaudier, F., Keckhut, P., Lemennais, P., Bekki, S., Marchand,
914 M., Lebrun, J. C., Kyrölä, E., Tamminen, J., Sofieva, V., Fussen, D., Vanhellemont, F., Fanton
915 d'Andon, O., Barrot, G., Blanot, L., Fehr, T., and Saavedra de Miguel, L.: Response of tropical
916 stratospheric O_3, NO_2 and NO_3 to the equatorial Quasi-Biennial Oscillation and to temperature as
917 seen from GOMOS/ENVISAT, Atmos. Chem. Phys. Discuss., 10, 9153–9171,
918 doi:10.5194/acpd-10-9153-2010, 2010.
919 Hess, P.G. and Zbinden, R.: Stratospheric impact on tropospheric ozone variability and trends:
920 1990–200, Atmos. Chem. Phys., 13, 649–674, 2013.
921 Hofmann, D.J.: Recovery of Antarctic ozone hole, Nature 384, 222-223 doi:10.1038/384222a0,
922 1996.
923 Hood, L. L. and Soukharev, B. E.: Solar induced variations of odd nitrogen: Multiple regression
924 analysis of UARS HALOE data, Geophys. Res. Lett., 33, L22805, doi:10.1029/2006GL028122,
925 2006.
926 Hurtmans, D., P. Coheur, C.Wespes, L. Clarisse, O. Scharf, C. Clerbaux, J. Hadji-Lazaro, M.
927 George, and S. Turquety: FORLI radiative transfer and retrieval code for IASI, Journal of
928 Quantitative Spectroscopy and Radiative Transfer, 113, 1391-1408, 2012.
929 Isaksen I. S. A., Zerefos, C. S., Kourtidis, K., Meleti, C., Dalsøren, S. B., Sundet, J. K., Grini, A.,
930 Zanis, P., and Balis, D.: Tropospheric ozone changes at unpolluted and semipolluted regions
931 induced by stratospheric ozone changes, J. Geophys. Res., 110, D02302,
932 doi:10.1029/2004JD004618, 2005.
933 Jiang, X., Pawson, S., Camp, C. D., Nielsen, E., Shia, R., Liao, T., Jeev, K., Limpasuvan, V., and
934 Yung, Y. L.: Interannual variability and trends in extratropical ozone. Part II: Southern
935 Hemisphere, J. Atmos. Sci., 65, 3030–3041, 2008.
936 Jones , A., J. Urban, D.P. Murtagh, P. Eriksson, S. Brohede, C. Haley, D. Degenstein, A.
937 Bourassa, C. von Savigny, T. Sonkaew, A. Rozanov, H. Bovensmann, and J. Burrows, Evolution

938 of stratospheric ozone and water vapour time series studied with satellite measurements, *Atmos.*
939 *Chem. Phys.*, *9* (16), 6055-6075, doi: 10.5194/acp-9-6055-2009, 2009.
940 Kuttippurath, J., F. Lefèvre, J.-P. Pommereau, H. K. Roscoe, F. Goutail, A. Pazmiño, and J. D.
941 Shanklin: Antarctic ozone loss in 1979–2010: First sign of ozone recovery, Atmos. Chem.
942 Phys.,1625–1635, 2013.
943 Kuttippurath, J., G. E. Bodeker, H. K. Roscoe, and P. J. Nair: A cautionary note on the use of
944 EESC-based regression analysis for ozone trend studies, Geophys. Res. Lett.,42, 162–168,
945 doi:10.1002/2014GL062142, 2015.
946 Kivi, R., Kyrö, E., Turunen, T., Harris, N. R. P., von der Gathen, P., Rex, M., Andersen, S. B.,
947 and Wohltmann, I.: Ozonesonde observations in the Arctic during 1989-2003: Ozone variability
948 and trends in the lower stratosphere and free troposphere, J. Geophys. Res., 112, D08306,
949 doi:10.1029/2006JD007271, 2007.
950 Knibbe J. S., R. J. van der A, and A. T. J. de Laat: Spatial regression analysis on 32 years of total
951 column ozone data, Atmos. Chem. Phys., 14, 8461–8482, 2014.
952 Kramarova, N.A., E. R. Nash, P. A. Newman, P. K. Bhartia, R. D. McPeters, D. F. Rault, C. J.
953 Seftor, P. Q. Xu, and G. J. Labow: Measuring the Antarctic ozone hole with the new Ozone
954 Mapping and Profiler Suite (OMPS), Atmos. Chem. Phys., 14, 2353–2361, 2014.
955 Kyrölä, E., Tamminen, J., Leppelmeier, G. W., Sofieva, V., Hassinen, S., Seppälä, A., Verronen,
956 P. T., Bertaux, J.-L., Hauchecorne, A., Dalaudier, F., Fussen, D., Vanhellemont, F., d'Andon, O.
957 F., Barrot, G., Mangin, A., Theodore, B., Guirlet, M., Koopman, R., Saavedra, L., Snoeij, P., and
958 Fehr, T.: Nighttime ozone profiles in the stratosphere and mesosphere by the Global Ozone
959 Monitoring by Occultation of Stars on Envisat, J. Geophys. Res., 111, D24306,
960 doi:10.1029/2006JD007193, 2006.
961 Kyrölä, E.; Tamminen, J.; Sofieva, V.; Bertaux, J. L.; Hauchecorne, A.; Dalaudier, F.; Fussen,
962 D.; Vanhellemont, F.; Fanton d'Andon, O.; Barrot, G.; Guirlet, M.; Fehr, T. and Saavedra de
963 Miguel, L.: GOMOS O_3, NO_2, and NO_3 observations in 2002–2008, Atmos. Chem. Phys., 10,
964 7723–7738, 2010, doi:10.5194/acp-10-7723-2010.
965 Kyrölä, E., Laine, M., Sofieva, V., Tukiainen, S., Tamminen, J., Päivärinta, S., Zawodny, J., and
966 Thomason, L.: Combined SAGE II-GOMOS ozone profile data set for 1984–2011 and trend

967 analysis of the vertical distribution of ozone, Atmos. Chem. Phys., 13, 10645–10658,
968 doi:10.5194/acp-13-10645-2013, 2013.
969 Laine, M. , N. Latva-Pukkila, and E. Kyrölä: Analysing time-varying trends in stratospheric
970 ozone time series using the state space approach, Atmos. Chem. Phys., 14, 9707–9725, 2014.
971 Logan, J. A.: Tropospheric Ozone: Seasonal behaviour, Trends, and Anthropogenic Influence, J.
972 Geophys. Res., 90(D6), 10 463–10 482, 1985.
973 Logan, J. A., Jones, D. B. A., Megretskaia, I. A., Oltmans, S. J. Johnson, B. J., V¨omel, H.,
974 Randel, W. J., Kimani, W., and Schmidlin, F. J.: Quasi-biennial oscillation in tropical ozone as
975 revealed by ozonesonde and satellite data, J. Geophys. Res., 108(D8), 4244,
976 doi:10.1029/2002JD002170, 2003
977 Logan, J. A., Staehelin, J., Megretskaia, I. A., Cammas, J.-P. , Thouret, V., Claude, H., De
978 Backer, H., Steinbacher, M., Scheel, H.-E., Stübi, R.,, Fröhlich, M., and Derwent R.: Changes in
979 ozone over Europe: Analysis of ozone measurements from sondes, regular aircraft (MOZAIC)
980 and alpine surface sites, J. Geophys. Res., 117, D09301, doi:10.1029/2011JD016952, 2012.
981 Mäder, J. A., Staehelin, J., Brunner, D., Stahel, W. A., Wohltmann, I., and Peter, T.: Statistical
982 modelling of total ozone: Selection of appropriate explanatory variables, J. Geophys. Res., 112,
983 D11108, doi:10.1029/2006JD007694, 2007.
984 Mäder, J.A., J. Staehelin, T. Peter, D. Brunner, H. E. Rieder, and W. A. Stahel: Evidence for the
985 effectiveness of the Montreal Protocol to protect the ozone layer, Atmos. Chem. Phys., 10,
986 12161-12171, 2010.
987 Manney, G. L., Santee, M. L., Froidevaux, L., Hoppel, K., Livesey, N. J., and Waters, J. W.:
988 EOS MLS observations of ozone loss in the 2004-2005 Arctic winter, Geophys. Res. Lett., 33,
989 L04802, doi:10.1029/2005GL024494, 2006.
990 Manney, G. Santee, M. L., Rex, M., Livesey, N. J., Pitts, M.C., Veefkind, P., Nash, E. N.,
991 Wohltmann, I., Lehmann, R., Froidevaux, L., Poole, L. R., Schoeberl, M. R., Haffner, D.P.,
992 Davies, J., Dorokhov, V., Gernandt, H., Johnson, B., Kivi, R., Kyrö, E., Larsen, N., Levelt, P. F.,
993 Makshtas, A., McElroy, C. T., Nakajima, H., Parrondo, M.C., Tarasick, D. W., von der Gathen,
994 P., Walker, K. A., and Zinoviev, N. S. : Unprecedented Arctic ozone loss in 2011, Nature, 478,
995 469–475, doi:10.1038/nature10556, 2011.

McCormack, J.P., D.E. Siskind and L.L. Hood: Solar-QBO interaction and its impact on stratospheric ozone in a zonally averaged photochemical transport model of the middle atmosphere, J. Geophys. Res., 112, D16109, doi:10.1029/2006JD008369, 2007.

McLinden, C.A., S. Tegtmeier, and V. Fioletov, Technical note: A SAGE-corrected SBUV zonal-mean ozone data set, *Atmos. Chem. Phys.*, *9* (20), 7963-7972, doi: 10.5194/acp-9-7963-2009, 2009.

McPeters, R. D., Labow, G. J., and Logan, J. A.: Ozone climatological profiles for satellite retrieval algorithms, J. Geophys. Res.-Atmos., 112, D05308, doi:10.1029/2005JD006823, 2007.

Miller, A. J., Cai, A., Tiao, G., Wuebbles, D. J., Flynn, L. E., Yang, S.-K., Weatherhead, E. C., Fioletov, V., Petropavlovskikh, I., Meng, X.-L., Guillas, S., Nagatani, R. M., and Reinsel, G. C.: Examination of ozonesonde data for trends and trend changes incorporating solar and Arctic oscillation signals, J. Geophys. Res., 111, D13305, doi:10.1029/2005JD006684, 2006.

Nair, P. J., S. Godin-Beekmann, J. Kuttippurath, G. Ancellet, F. Goutail, A. Pazmiño, L. Froidevaux, J. M. Zawodny, R. D. Evans, H. J. Wang, J. Anderson, and M. Pastel: Ozone trends derived from the total column and vertical profiles at a northern mid-latitude station, Atmos. Chem. Phys., 13, 10373–10384, 2013.

Neu, J.L., T. Flury, G. L. Manney, M. L. Santee, N. J. Livesey and J. Worden, Tropospheric ozone variations governed by changes in stratospheric circulation, Nat. Geosc., 7, 340–344, doi:10.1038/ngeo2138, 2014.

Newchurch, M.J., Yang, E-S., Cunnold, D.M., Reinsel, G.C. and Zawodny, J.M.: Evidence for slowdown in stratospheric ozone loss: first stage of ozone recovery, J. Geophys. Res. Atmos., 108, D16, doi:10.1029/2003JD003471, 2003.

Oetjen, H., Payne, V.H., Kulawik, S.S., Eldering, A., Worden, J., Edwards, D.P., Francis, G.L., Worden, H.M., Clerbaux, C., Hadji-Lazaro, J., Hurtmans, D. : Extending the satellite data record of tropospheric ozone profiles from Aura-TES to MetOp-IASI, Atmos. Meas. Tech. Discuss., 7, 7013–7051, 2014.

Oltmans, S. J., Lefohn, A. S., Scheel, H. E., Harris, J. M., Levy II., H., Galbally, I. E., Brunke, E., Meyer, C. P., Lathrop, J. A., Johnson, B. J., Shadwick, D. S., Cuevas, E., Schmidlin, F. J., Tarasick, D.W., Claude, H., Kerr, J. B., Uchino, O., and Mohnen, V.: Trends of ozone in the troposphere, Geophys. Res. Lett., 25, 139–142, doi:10.1029/97GL03505, 1998.

Oltmans, S. J., Lefohn, A. S., Harris, J. M., Galbally, I., Scheel, H. E., Bodeker, G., Brunke, E., Claude, H., Tarasick, D., Johnson, B. J., Simmonds, P., Shadwick, D., Anlauf, K., Hayden, K., Schmidlin, F., Fujimoto, T., Akagi, K., Meyer, C., Nichol, S., Davies, J., Redondas, A., and Cuevas, E.: Long-term changes in tropospheric ozone, Atmos. Environ., 40, 3156–3173, 2006.

Parrington, M., P. I. Palmer, D. K. Henze, D. W. Tarasick, E. J. Hyer, R. C. Owen, D. Helmig, C. Clerbaux, K. W. Bowman, M. N. Deeter, E. M. Barratt, P.-F. Coheur, D. Hurtmans, Z. Jiang, M. George, and J. R. Worden: The influence of boreal biomass burning emissions on the distribution of tropospheric ozone over north America and the north Atlantic during 2010, Atmos. Chem. Phys., 12, 2077-2098, doi: 10.5194/acp-12-2077-2012, 2012.

Parrish, D.D., K. S. Law, J. Staehelin, R. Derwent, O. R. Cooper,1, H. Tanimoto, A. Volz Thomas, S. Gilge,H.-E. Scheel, M. Steinbacher, and E. Chan: Long-term changes in lower tropospheric baseline ozone concentrations at northern mid-latitudes, Atmos. Chem. Phys., 12, 11485–11504, 2012.

Pitts, M. C., Poole, L. R., Dörnbrack, A., and Thomason, L. W.: The 2009–2010 Arctic polar stratospheric cloud season: a CALIPSO perspective, Atmos. Chem. Phys., 11, 2161–2177, doi:10.5194/acp-11-2161-2011, 2011.

Pommier, M., C. Clerbaux, K. S. Law, G. Ancellet, P. Bernath, P.-F. Coheur, J. Hadji- Lazaro, D. Hurtmans, P. Nedelec, J.-D. Paris, F. Ravetta, T. B. Ryerson, H. Schlager, and A. J.Weinheimer: Analysis of IASI tropospheric O_3 data over the arctic during POLARCAT campaigns in 2008, Atmos. Chem. Phys., 12, 7371-7389, doi:doi:10.5194/acp-12-7371-2012, 2012.

Randel, W. J. and Wu, F.: Isolation of the ozone QBO in SAGE II data by singular-value decomposition, J. Atmos. Sci., 53, 2546– 2559, 1996.

Randel, W. J. and Wu, F.: A stratospheric ozone profile data set for 1979-2005: Variability, trends, and comparisons with column ozone data, J. Geophys. Res.-Atmos., 112, D06313, doi:10.1029/ 2006JD007339, 2007.

Reinsel, G. C., Weatherhead, E. C. , Tiao, G. C., Miller, A. J., Nagatani, R. M., Wuebbles, D. J., and Flynn, L. E.: On detection of turnaround and recovery in trend for ozone, J. Geophys. Res., 107, D10, doi:10.1029/2001JD000500, 2002.

1055 Reinsel, G. C., Miller, A. J., Weatherhead, E. C., Flynn, L. E., Nagatani, R. M., Tiao, G. C., and
1056 Wuebbles, D. J.: Trend analysis of total ozone data for turnaround and dynamical contributions,
1057 J. Geophys. Res., 110, D16306, doi:10.1029/2004JD004662, 2005.
1058 Rodgers, C. D.: Inverse methods for atmospheric sounding: Theory and Practice, Series on
1059 Atmospheric, Oceanic and Planetary Physics, Vol. 2, World Scientific Publishing Co.,
1060 Singapore, 2000.
1061 Rieder, H. E., Frossard, L., Ribatet, M., Staehelin, J., Maeder, J. A., Di Rocco, S., Davison, A.
1062 C., Peter, T.,Weihs, P., and Holawe, F.: On the relationship between total ozone and atmospheric
1063 dynamics and chemistry at mid-latitudes – Part 2: The effects of the El Nino/Southern
1064 Oscillation, volcanic eruptions and contributions of atmospheric dynamics and chemistry to
1065 long-term total ozone changes, Atmos. Chem. Phys., 13, 165–179, doi:10.5194/acp-13- 165-
1066 2013, 2013.
1067 Safieddine S., Clerbaux C., George M., Hadji-Lazaro J., Hurtmans D., Coheur P.-F., Wespes C.,
1068 Loyola D., Valks P., Hao N.: Tropospheric ozone and nitrogen dioxide measurements in urban
1069 and rural regions as seen by IASI and GOME-2, J. Geophys. Res., 118, 18, 10555-10566, 2013.
1070 Salby, M., P. Callaghan, P. Keckhut, S. Godin, and M. Guirlet: Interannual changes of
1071 temperature and ozone: Relationship between the lower and upper stratosphere, J. Geophys.
1072 Res., 107(D18), 4342, doi:10.1029/2001JD000421, 2002.
1073 Salby, M., Titova, E., and Deschamps, L.: Rebound of Antarctic ozone, Geophys. Res. Lett., 38,
1074 L09702, doi:10.1029/2011GL047266, 2011.
1075 Santer, B.D., Wigley, T.M.L., Boyle, J.S., Gaffen, D.J., Hnilo, J.J., Nychka, D., Parker, D.E.,
1076 Parker, D.E. and Taylor, K.E.: Statistical significance of trends and trend differences in layer-
1077 average atmospheric temperature time series, J. Geophys. Res., 105(D6), 7337-7356, 2000.
1078 Saunois, M., Emmons, L., Lamarque, J.-F., Tilmes, S., Wespes, C., Thouret, V., and Schultz, M.:
1079 Impact of sampling frequency in the analysis of tropospheric ozone observations, Atmos. Chem.
1080 Phys., 12, 6757–6773, doi:10.5194/acp-12-6757-2012, 2012.
1081 Scannell, C., D. Hurtmans, A. Boynard, J. Hadji-Lazaro, M. George, A. Delcloo, A. Tuinder,
1082 P.F. Coheur, and C. Clerbaux: Antarctic ozone hole as observed by IASI/MetOp for 2008-2010,
1083 Atmos. Meas. Tech., 5, 123-139, 2012.

Schneider, M., Blumenstock, T., Hase, F., Höpfner, M., Cuevas, E., Redondas, A., and Sancho, J. M.: Ozone profiles and total column amounts derived at Izana Tenerife Island, from FTIR solar absorption spectra, and its validation by an intercomparison to ECC-sonde and Brewer spectrometer measurements, J. Quant. Spectros. Radiat. Transfer, 91, 3, 245–274, doi:10.1016/j.jqsrt.2004.05.067, 2005.

Shepherd, T.G., D. A. Plummer, J. F. Scinocca, M. I. Hegglin, V. E. Fioletov, M. C. Reader, E. Remsberg, T. von Clarmann, H. J. Wang: Reconciliation of halogen-induced ozone loss with the total-column ozone record, Nature Geoscience, 7, 443–449, doi:10.1038/ngeo2155, 2014.

Soukharev, B. E. and Hood, L. L.: Solar cycle variation of stratospheric ozone: Multiple regression analysis of long-term satellite data sets and comparisons with models, J. Geophys. Res.- Atmos., 111, D20314, doi:10.1029/2006JD007107, 2006.

Steinbrecht, W., Claude, H., and Winkler, P.: Enhanced upper stratospheric ozone: Sign of recovery or solar cycle effect?, J. Geophys. Res., 109, D02308, doi:10.1029/2003JD004284, 2004.

Steinbrecht, W., Claude, H., Schonenborn, F., McDermid, I. S., Leblanc, T., Godin, S., Song, T., Swart, D. P. J., Meijer, Y. J., Bodeker, G. E., Connor, B. J., Kampfer, N., Hocke, K., Calisesi, Y., Schneider, N., de la Noe, J., Parrish, A. D., Boyd, I. S., Brühl, C., Steil, B., Giorgetta, M. A., Manzini, E., Thomason, L. W., Zawodny, J. M., McCormick, M. P., Russell III, J. M., Bhartia, P. K., Stolarski, R. S., and Hollandsworth-Frith, S. M.: Long-term evolution of upper stratospheric ozone at selected stations of the Network for the Detection of Stratospheric Change (NDSC), J. Geophys. Res., 111, D10308, doi:10.1029/2005JD006454, 2006a.

Steinbrecht, W., Haßler, B., Br¨uhl, C., Dameris, M., Giorgetta, M. A., Grewe, V., Manzini, E., Matthes, S., Schnadt, C., Steil, B., and Winkler, P.: Interannual variation patterns of total ozone and lower stratospheric temperature in observations and model simulations, Atmos. Chem. Phys., 6, 349–374, doi:10.5194/acp-6-349-2006, 2006b.

Steinbrecht , W., H. Claude, F. Schönenborn, I.S. McDermid, T. Leblanc, S. Godin-Beekmann, P. Keckhut, A. Hauchecorne, J.A.E. Van Gijsel, D.P.J. Swart, G.E. Bodeker, A. Parrish, I.S. Boyd, N. Kämpfer, K. Hocke, R.S. Stolarski, S.M. Frith, L.W. Thomason, E.E. Remsberg, C. Von Savigny, A. Rozanov, and J.P. Burrows, Ozone and temperature trends in the upper

1113 stratosphere at five stations of the Network for the Detection of Atmospheric Composition
1114 Change, *Int. J. Remote Sens.*, *30*, 3875-3886, doi: 10.1080/01431160902821841, 2009.
1115 Stolarski, R. S. and Frith, S. M.: Search for evidence of trend slowdown in the long-term
1116 TOMS/SBUV total ozone data record: the importance of instrument drift uncertainty, Atmos.
1117 Chem. Phys., 6, 4057–4065, 2006.
1118 Tian, W., Chipperfield, M. P., Gray, L. J., and Zawodny, J. M.: Quasi-biennial oscillation and
1119 tracer distributions in a coupled chemistry-climate model, J. Geophys. Res., 111, D20301,
1120 doi:10.1029/2005JD006871, 2006.
1121 Varai, A., Homonnai, V., Jánosi, I.M., Müller, R. : Early signatures of ozone trend reversal over
1122 the Antarctic, Earth's Future, 3, 3, 95–109, doi:10.1002/2014EF000270, 2015.
1123 Vigouroux C., M. De Mazière, P. Demoulin, C. Servais, F. Hase, T. Blumenstock, I. Kramer, M.
1124 Schneider, J. Mellqvist, A. Strandberg, V. Velazco, J. Notholt, R. Sussmann, W. Stremme, A.
1125 Rockmann, T. Gardiner, M. Coleman, and P. Woods, Evaluation of tropospheric and
1126 stratospheric ozone trends over Western Europe from ground-based FTIR network observations,
1127 Atmos. Chem. Phys., 8 (23), 6865-6886, doi: 10.5194/acp-8-6865-2008, 2008.
1128 Vigouroux, C., T. Blumenstock, M. Coffey, Q. Errera, O. García, N. B. Jones, J. W. Hannigan,
1129 F. Hase, B. Liley, E. Mahieu, J. Mellqvist, J. Notholt, M. Palm, G. Persson, M. Schneider, C.
1130 Servais, D. Smale, L. Thölix, and M. De Mazière: Trends of ozone total columns and vertical
1131 distribution from FTIR observations at 8 NDACC stations around the globe, Atmos. Chem.
1132 Phys. Discuss., 14, 24623–24666, 2014.
1133 Weatherhead, E. C. and Andersen, S. B.: The search for signs of recovery of the ozone layer,
1134 Nature, 441, 39–45, doi:10.1038/nature04746, 2006.
1135 Weiss, A.K., J. Staehelin, C. Appenzeller, and N.R.P. Harris, Chemical and dynamical
1136 contributions to ozone profile trends of the Payerne (Switzerland) balloon soundings, *J.*
1137 *Geophys. Res.*, 106 (D19), 22685-22694, 2001.
1138 Wespes, C., Hurtmans, D., Clerbaux, C., Santee, M. L., Martin, R. V., and Coheur, P. F.: Global
1139 distributions of nitric acid from IASI/MetOP measurements, Atmos. Chem. Phys., 9, 7949–7962,
1140 doi:10.5194/acp-9-7949-2009, 2009.
1141 Wespes, C., L. Emmons, D. P. Edwards, J. Hannigan, D. Hurtmans, M. Saunois, P.-F. Coheur,
1142 C. Clerbaux, M. T. Coffey, R. L. Batchelor, R. Lindenmaier, K. Strong, A. J. Weinheimer, J. B.

Nowak, T. B. Ryerson, J. D. Crounse, and P. O. Wennberg: Analysis of ozone and nitric acid in spring and summer arctic pollution using aircraft, ground-based, satellite observations and mozart-4 model: source attribution and partitioning, Atmos. Chem. Phys., 12, 237-259, 2012.

Wilson, R. C., Fleming, Z. L., Monks, P. S., Clain, G., Henne, S., Konovalov, I. B., Szopa, S., and Menut, L.: Have primary emission reduction measures reduced ozone across Europe? An analysis of European rural background ozone trends 1996–2005, Atmos. Chem. Phys., 12, 437–454, doi:10.5194/acp-12-437-2012, 2012.

WMO: Scientific Assessment of Ozone Depletion: 2002, Global Ozone Research and Monitoring Project –Report No. 47, World Meteorological Organization, Geneva, Switzerland, 2003.

WMO: Scientific Assessment of Ozone Depletion: 2006, Global Ozone Research and Monitoring Project– Report 50, World Meteorological Organization, Geneva, Switzerland, 2007.

WMO: Scientific Assessment of Ozone Depletion: 2010, Global Ozone Research and Monitoring Project–Report 52, World Meteorological Organization), Geneva, Switzerland, 2011.

WMO : Scientific Assessment of Ozone Depletion: 2014, Global Ozone Research and Monitoring Project– Report 56, World Meteorological Organization, Geneva, Switzerland, 2014.

Yang, E.-S., Cunnold, D. M., Salawitch, R. J., McCormick, M. P., Russell, J., Zawodny, J. M., Oltmans, S., and Newchurch, M. J.: Attribution of recovery in lower-stratospheric ozone, J. Geophys. Res., 111, D17309, doi:10.1029/2005JD006371, 2006.

1173 **Table 1** List of the proxies used in this study and their sources

Proxy	Description (*resolution*)	Sources
F10.7	The 10.7 cm solar radio flux (*daily or monthly*)	NOAA National Weather Service Climate Prediction Center: ftp://ftp.ngdc.noaa.gov/STP/space-weather/solar-data/solar-features/solar-radio/noontime-flux/penticton/penticton_adjusted/listings/listing_drao_noontime-flux-adjusted_daily.txt or ftp://ftp.ngdc.noaa.gov/STP/space-weather/solar-data/solar-features/solar-radio/noontime-flux/penticton/penticton_adjusted/listings/listing_drao_noontime-flux-adjusted_monthly.txt
QBO^{10} **QBO^{30}**	Quasi-Biennial Oscillation index at 10hPa and 30hPa (*monthly*)	Free University of Berlin: www.geo.fu-berlin.de/en/met/ag/strat/produkte/qbo/
ENSO	El Niño /Southern Oscillation - Nino 3.4 Index (*3-monthly averages*)	NOAA National Weather Service Climate Prediction Center: http://www.cpc.noaa.gov/data/indices/
NAO	North Atlantic Oscillation index (*daily or monthly*)	ftp://ftp.cpc.ncep.noaa.gov/cwlinks/norm.daily.nao.index.b500101.current.ascii or http://www.cpc.ncep.noaa.gov/products/precip/CWlink/pna/norm.nao.monthly.b5001.current.ascii
AAO	Antarctic Oscillation index (*daily or monthly*)	ftp://ftp.cpc.ncep.noaa.gov/cwlinks/norm.daily.aao.index.b790101.current.ascii or http://www.cpc.ncep.noaa.gov/products/precip/CWlink/daily_ao_index/aao/monthly.aao.index.b79.current.ascii

1174
1175
1176
1177
1178
1179
1180
1181
1182
1183
1184
1185
1186
1187
1188
1189

Table 2 Ozone trends and associated uncertainties (95% confidence limits; accounting for the autocorrelation in the noise residuals), given in DU/year, for 20-degree latitude bands, based on daily (top values) and monthly (bottom values) medians over 6 years of IASI observations. Bold (underlined) values refer to significant (positive) trends. Values marked with a star (*) refer to trends which are rejected by the iterative backward elimination procedure†.

DU/ yr	**# Days**	**Ground-300hPa (MLT)**	**300-150hPa (UTLS)**	**150-25hPa (MLST)**	**25-3hPa (UST)**	**Total columns**
70°N-90°N (Feb-Oct)	1493	**-0.13±0.10** -0.03±0.29*	**1.28±0.82** 0.70±0.92*	**2.81±2.27** -0.04±2.60*	-0.16±0.97* -1.81±2.81*	**3.90±2.93** 1.37±3.62*
50°N-70°N	2103	-0.08±0.09 0.17±0.35*	**0.73±0.51** 1.24±1.24	0.97±1.30 2.28±4.24*	**0.55±0.36** 0.66±0.76	**1.93±1.71** 4.72±5.58
30°N-50°N	2105	**-0.19±0.05** **-0.15±0.13**	**0.34±0.18** 0.75±0.75	-0.34±0.77 -0.37±1.65*	**0.89±0.41** **0.87±0.52**	0.91±1.24 0.33±2.25*
10°N-30°N	2105	0.10±0.11 0.12±0.15*	-0.03±0.10* 0.05±0.12*	**-0.73±0.29** -0.55±0.62*	**0.95±0.65** **1.25±0.74**	0.21±0.30* 0.82±1.01
10°S-10°N	2104	**-0.41±0.12** **-0.25±0.14**	**-0.25±0.07** -0.08±0.10	-0.11±0.26* -0.11±0.64*	**0.44±0.19** 0.61±0.64	-0.16±0.34 0.13±0.83*
30°S-10°S	2106	**-0.22±0.10** **-0.15±0.13**	**-0.08±0.04** **-0.09±0.07**	**-0.61±0.26** **-0.45±0.36**	**0.89±0.58** 0.80±1.23	-0.04±0.31* -0.01±1.26*
50°S-30°S	2105	**-0.19±0.07** **-0.18±0.09**	**-0.22±0.08** **-0.27±0.12**	**-2.17±0.58** **-2.36±1.80**	**1.74±0.77** 1.21±1.30	-0.79±0.96 -0.64±1.45*
70°S-50°S	2105	**-0.13±0.05** *-0.22±0.12*	0.09±0.16 0.05±0.32*	0.56±0.82 0.02±1.15*	**0.54±0.29** 0.57±0.82	1.15±1.28 0.51±1.75*
90°S-70°S (Oct-Apr)	738	-0.15±0.21* -0.17±0.40*	0.01±0.61* 0.25±0.73*	0.00±2.36* 2.59±3.80*	**1.04±0.57** 0.91±2.10*	1.50±3.15* 3.28±5.12*

† The trend values result from the adjustment of the regression model where the linear term is kept whatever its p-value calculated during the iterative process.

Table 3 Same as Table 2 but for seasonal O_3 trends and associated uncertainties based on daily medians during JJA (top values) and DJF (bottom values) periods. Values marked with a star (*) refer to trends which are rejected by the iterative backward elimination procedure†.

DU/ yr	# Days	Ground-300hPa (MLT)	300-150hPa (UTLS)	150-25hPa (MLST)	25-3hPa (UST)	Total columns
70°N-90°N	613	**-0.18±0.08**	**1.13±0.65**	-0.91±1.52	**1.72±0.51**	**1.36±1.15**
(Feb-Oct)	48	-	-	-	-	-
50°N-70°N	551	**-0.23±0.07**	**1.03±0.37**	0.62±1.64	**1.67±0.48**	**3.01±1.64**
	527	-0.09±0.12*	**1.74±1.30**	0.73±1.73*	-0.66.±0.79	1.56±2.66*
30°N-50°N	551	**-0.30±0.10**	**0.42±0.30**	-0.30±0.65*	**0.84±0.25**	1.17±1.35
	529	**-0.24±0.09**	0.28±0.28	-0.82.±0.90	**0.62.±0.49**	-0.81.±1.05
10°N-30°N	551	-0.05±0.16*	**0.17±0.05**	**-0.34±0.30**	**0.36±0.27**	-0.09±0.54*
	529	**0.18±0.14**	0.01.±0.09*	**-1.05.±0.45**	0.49±0.54*	-1.14±0.44
10°S-10°N	551	-0.06.±0.10	0.04±0.05*	-0.84±0.86	0.32±0.42	-0.56±0.74
	529	**-0.70.±0.23**	**-0.32±0.10**	1.64±1.77	0.53±0.59	0.34±0.93*
30°S-10°S	551	**-0.26±0.09**	-0.06±0.07	**-0.56±0.40**	**1.06±0.55**	0.24±0.43
	530	**-0.15±0.11**	0.06±0.12*	-0.12±0.31*	**1.48±0.53**	**1.56±0.92**
50°S-30°S	551	**-0.21±0.05**	**-0.16±0.09**	-0.52±0.54	0.49±0.59	-0.44±0.83
	529	**-0.10±0.06**	**-0.14±0.06**	**-2.83±0.64**	**3.40±0.85**	0.47±0.52
70°S-50°S	551	**-0.25±0.06**	**1.03±0.60**	**2.63±1.65**	**0.98±0.62**	**3.44±2.47**
	529	**-0.10±0.04**	0.19±0.24*	**0.52±0.48**	**1.66±0.70**	**1.72±0.74**
90°S-70°S	-	-	-	-	-	-
(Oct-Apr)	523	**-0.21±0.20**	-0.46±0.80*	0.16±2.53*	**1.18±0.67**	0.98±3.27*

† The trend values result from the adjustment of the regression model where the linear term is kept whatever its p-value calculated during the iterative process.

Table 4 Ozone trends and associated uncertainties (95% confidence limits), given in DU/year over NDACC (Network for the Detection of Atmospheric Composition Change) stations in the N.H. based on daily medians of IASI (within a grid box of 1°x1° centered on stations, ~~top~~ two first rows) and FTIR observations~~.~~ (successive rows for different time intervals). Italic values (2d row) refer to trends inferred from subsampled IASI data and bold values refer to statistically significant trends. Values marked with a star (*) refer to trends which are rejected by the iterative backward elimination procedure†.

DU/yr	**Data periods**	**# days**	**25-3hPa (US)**	**Total columns**
Ny-Alesund (79°N) Mar-Sept	2008-2013	1239	0.56±0.73	**5.26±4.72**
	Subsamp. 2008-2012	*82*	*-0.29±4.58*	*6.26±18.11*
	2008-2012	84	-3.58±4.58	2.24±20.78*
	2003-2012	168	-0.17±0.70*	**-4.84±3.01**
	2000-2012	288	**0.64±0.60**	-1.02±2.40*
	1999-2012	320	**0.62±0.55**	**-2.35±1.40**
	1995-2012	383	**1.03±0.66**	1.31±2.39*
	1995-2003	167	**1.25±1.05**	3.33±3.41
Thule (77°N) Mar-Sept	2008-2013	1094	**1.24±1.09**	**4.97±4.72**
	Subsamp. 2008-2012	*231*	*1.31±2.69*	*0.10±7.36*
	2008-2012	340	-2.10±2.89	0.39±11.59*
	2003-2012	697	0.86±0.89	-2.77±2.99
	2000-2012	776	**1.33±0.86**	-1.29±1.73
	1999-2012	779	**1.69±0.88**	-1.25±1.74
	1999-2003	138	**3.73±2.90**	4.86±10.13*
Kiruna (68°N) Mar-Sept	2008-2013	1236	0.21±1.42	**4.41±4.00**
	Subsamp. 2008-2012	*226*	*0.97±4.05*	*3.78±6.03*
	2008-2012	254	-1.97±6.04*	-3.75±6.64*
	2003-2012	678	0.15±0.67*	2.26±3.68
	2000-2012	913	**1.60±1.29**	3.69±4.20
	1999-2012	984	**1.10±0.98**	-0.43±1.64*
	1996-2012	1183	**1.11±0.54**	**1.82±1.77**
	1996-2003	596	**1.26±1.21**	1.12±3.77*
Jungfraujoch (47°N)	2008-2013	1580	**2.95±0.61**	**5.64±3.15**
	Subsamp. 2008-2012	*524*	***3.72±1.14***	***5.61±5.11***
	2008-2012	565	1.60±1.80	**5.28±4.82**
	1998-2012	1582	0.10±0.35	-0.28±0.86*
	1995-2012	1771	0.02±0.33*	**0.85±0.79**

Zugspitze (47°N)	2008-2013	1729	**3.17±0.56**	**5.53±2.92**
	Subsamp.			
	2008-2012	*538*	***3.56±1.63***	***5.99±4.49***
	2008-2012	597	0.71±1.22	3.46±3.79
	1998-2012	1472	0.08±0.32*	0.81±0.98
	1995-2012	1525	0.23±0.32	**1.36±1.01**
Izana (28°N)	2008-2013	1803	0.56±0.65	**1.28±0.77**
	Subsamp.			
	2008-2012	*380*	*0.32±1.28*	*0.11±1.95*
	2008-2012	443	0.24±0.80*	0.91±2.44*
	1999-2012	1257	**0.46±0.25**	0.20±0.33*

† The trend values result from the adjustment of the regression model where the linear term is kept whatever its p-value calculated during the iterative process.

Figure captions

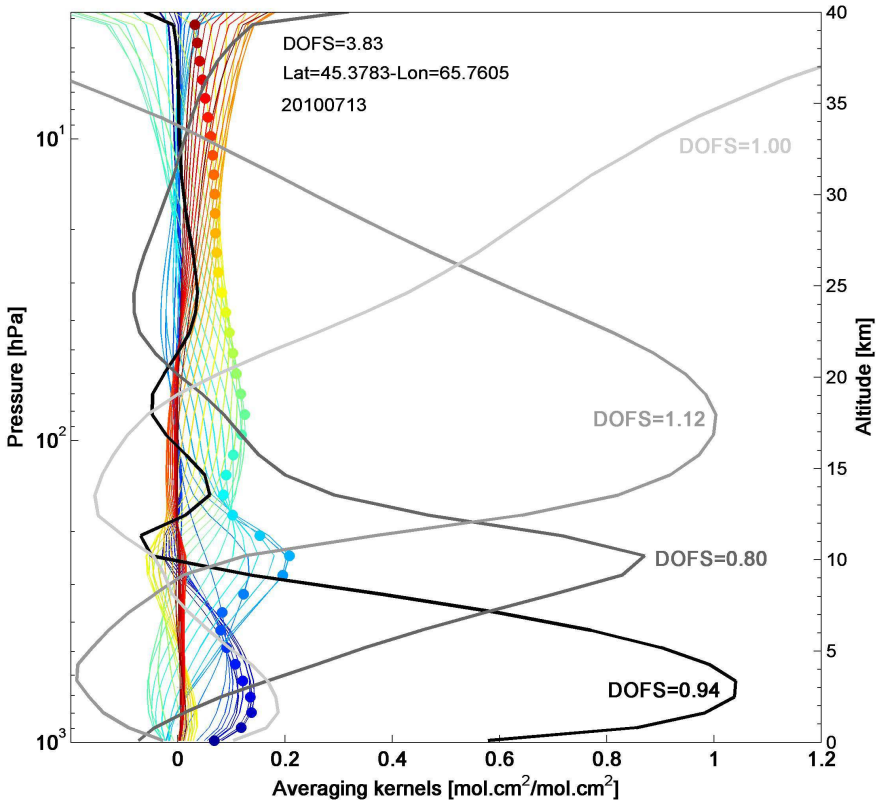

Figure 1. Typical IASI FORLI-O_3 averaging kernels, in partial column units, corresponding to one mid-latitude observation in July (45°N/66°E) for each 1 km retrieved layers from ground to 40 km altitude (color scale) and for 4 merged layers: ground-300 hPa; 300-150 hPa; 150-25 hPa; 25-3 hPa (grey lines). The total DOFS and the DOFS for each merged layers are also indicated.

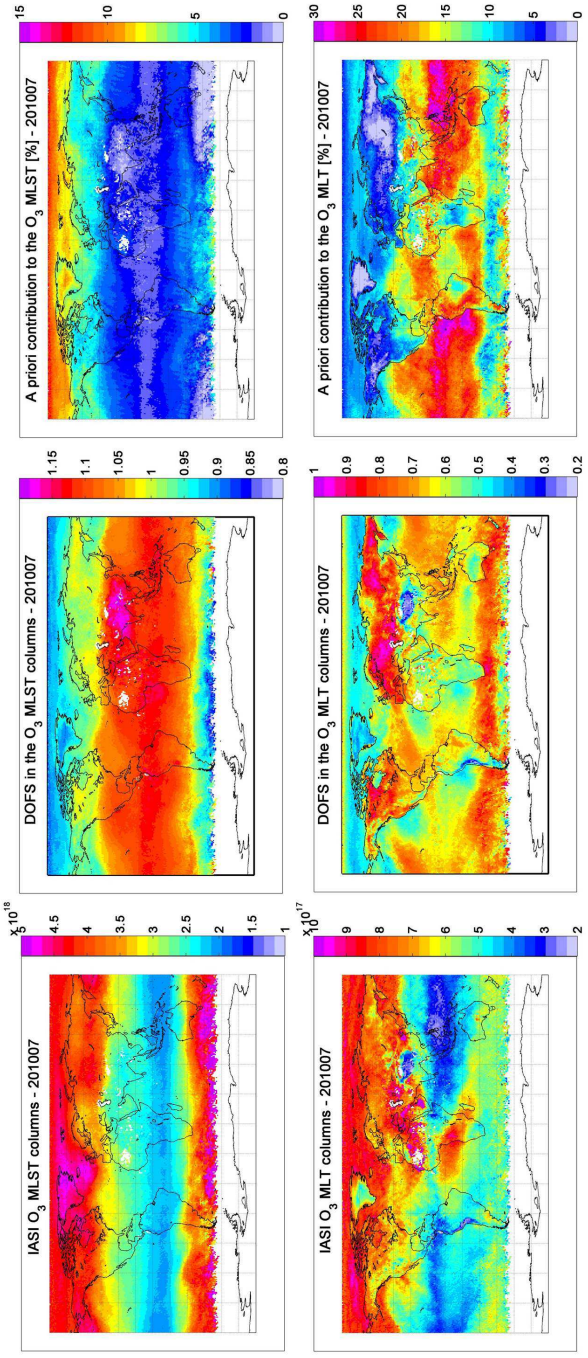

1253

1254 **Figure 2.** Distributions of (a) O_3 columns, (b) DOFS and (c) *a priori* contribution (given as a %)
1255 in the ground-300hPa (MLT) and 150-25hPa (MLST) layers for IASI O_3, averaged over July
1256 2010 daytime data. Note that the scales are different.

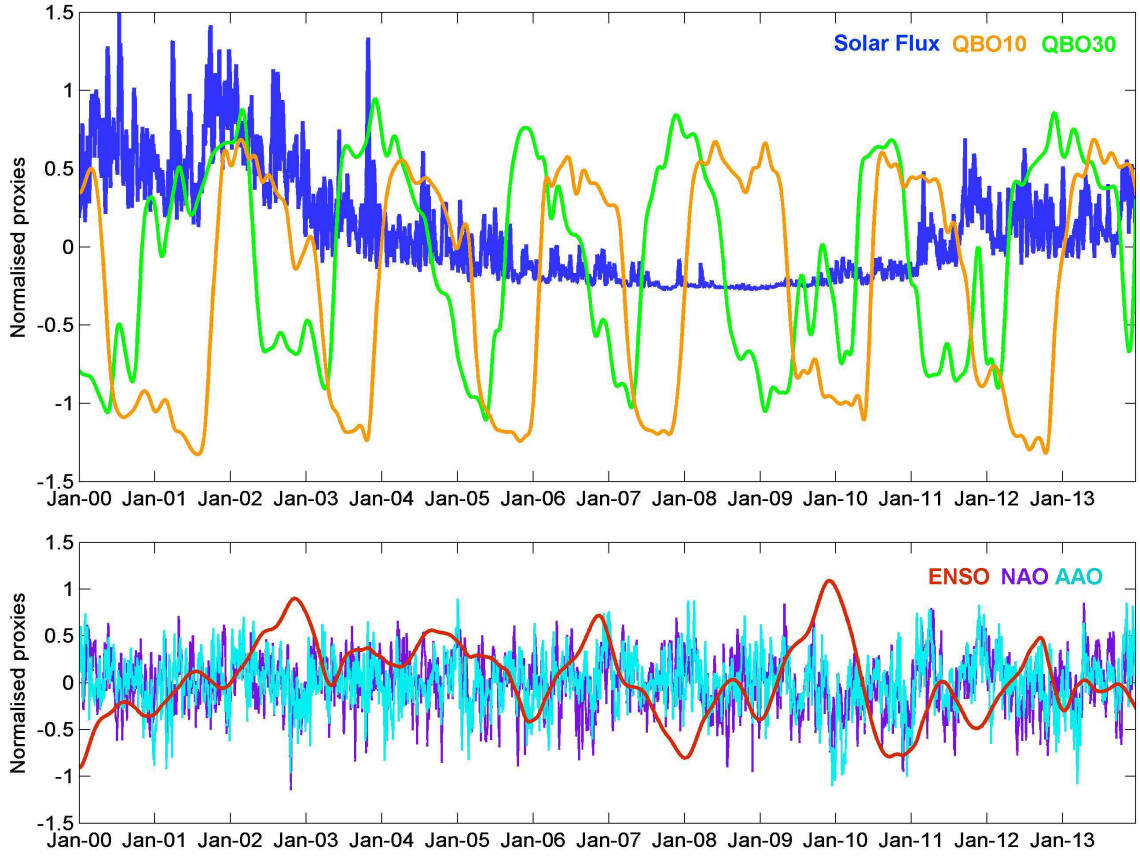

Figure 3. Normalized proxies as a function of time for the period 2000-2013 for the solar F10.7 cm radio flux (blue) and the equatorial winds at 10 (green) and 30 hPa (orange), respectively (top panel), and for the El Niño (red), north Atlantic oscillation (purple) and Antarctic oscillation (light blue) indexes (bottom panel).

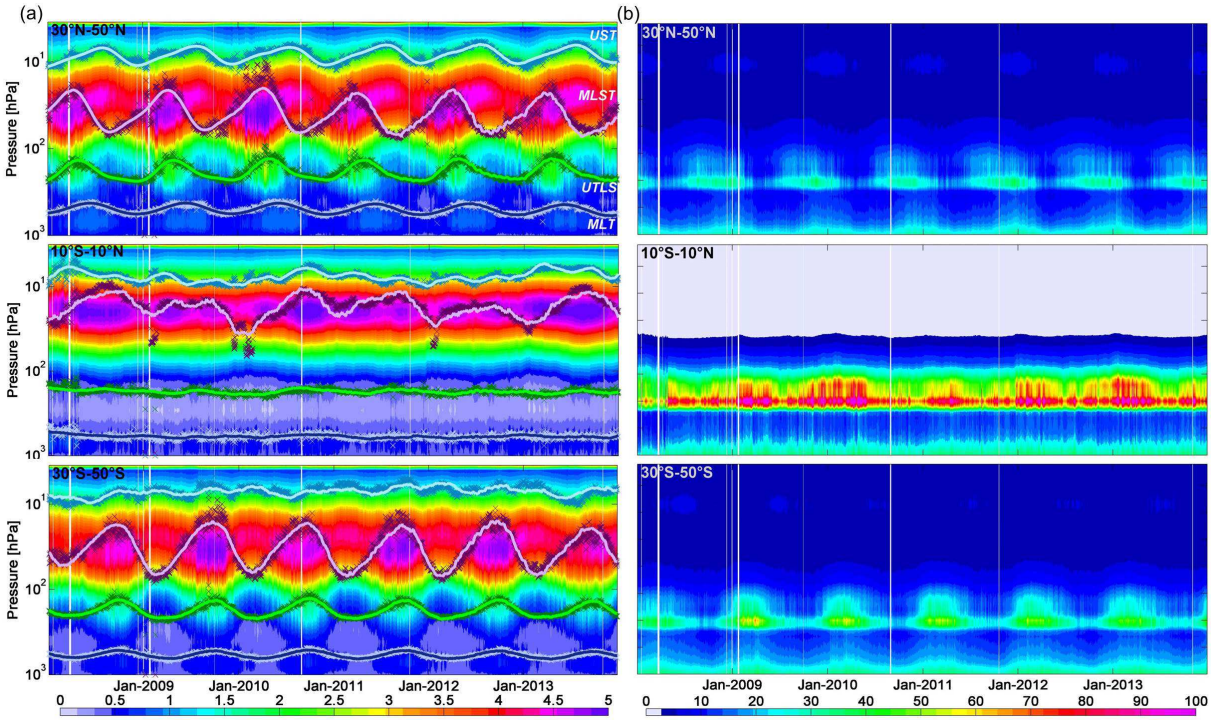

1266

1267 **Figure 4.** (a) Daily IASI O_3 profiles ($1x10^{12}$ molecules/cm^3) for the period 2008-2013 and over
1268 the range of the retrieved profiles as a function of time and altitude, in three latitude bands:
1269 30°N-50°N (top), 10°S-10°N (middle), 30°S-50°S (bottom). Superimposed daily IASI O_3 partial
1270 columns (scatters) and the associated fits (solid lines) from the multivariate regressions for the
1271 MLT (ground-300hPa), UTLS (300-150hPa), MLST (150-25hPa) and UST (above 25hPa)
1272 layers. The IASI measurements and the fits have been scaled for clarity. (b) Estimated total
1273 retrieval errors (%) associated with daily IASI O_3 profiles.

1274

1275

1276

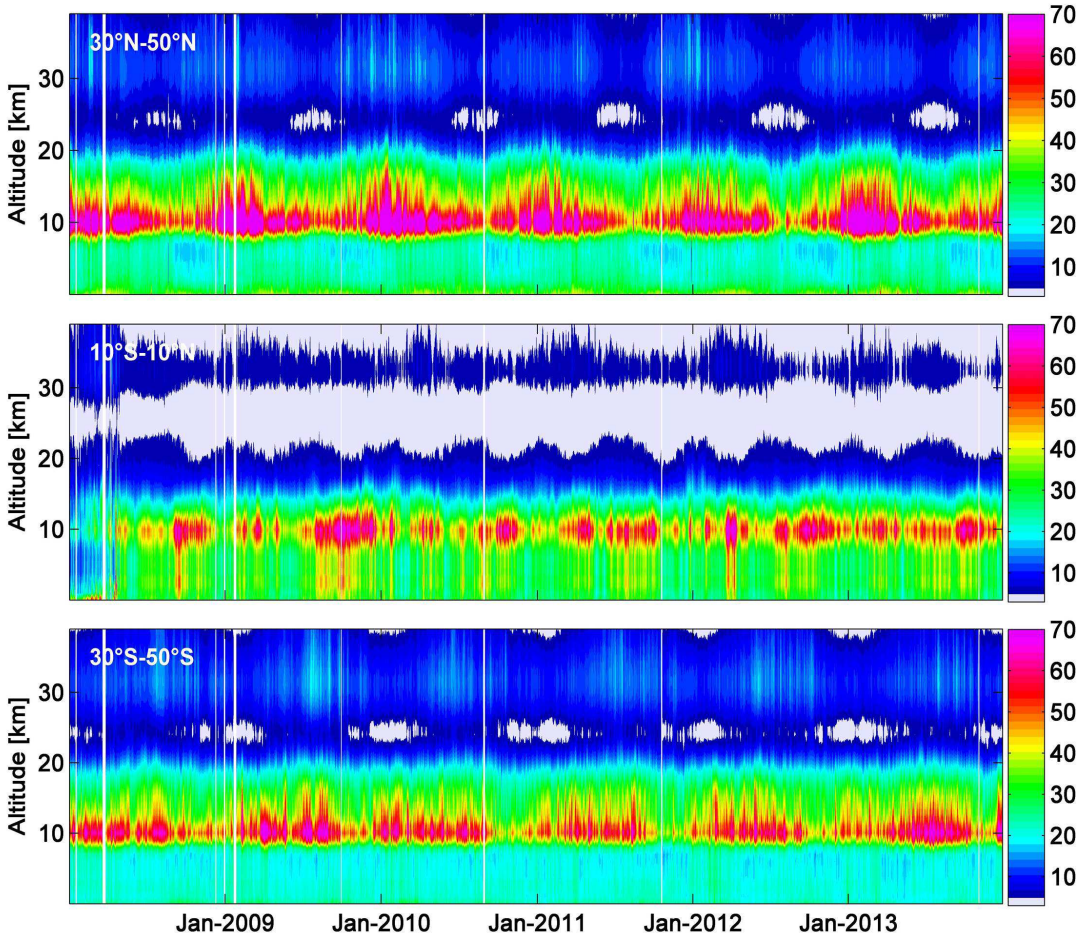

Figure 5. Daily IASI O_3 variability (%), expressed as ~~1xσ relative to the median values,~~ $[\sigma(O_3(t))/O_3(t)]100\%$, where σ is the standard deviation, as a function of time and altitude in three latitude bands: 30°N-50°N (top), 10°S-10°N (middle), 30°S-50°S (bottom).

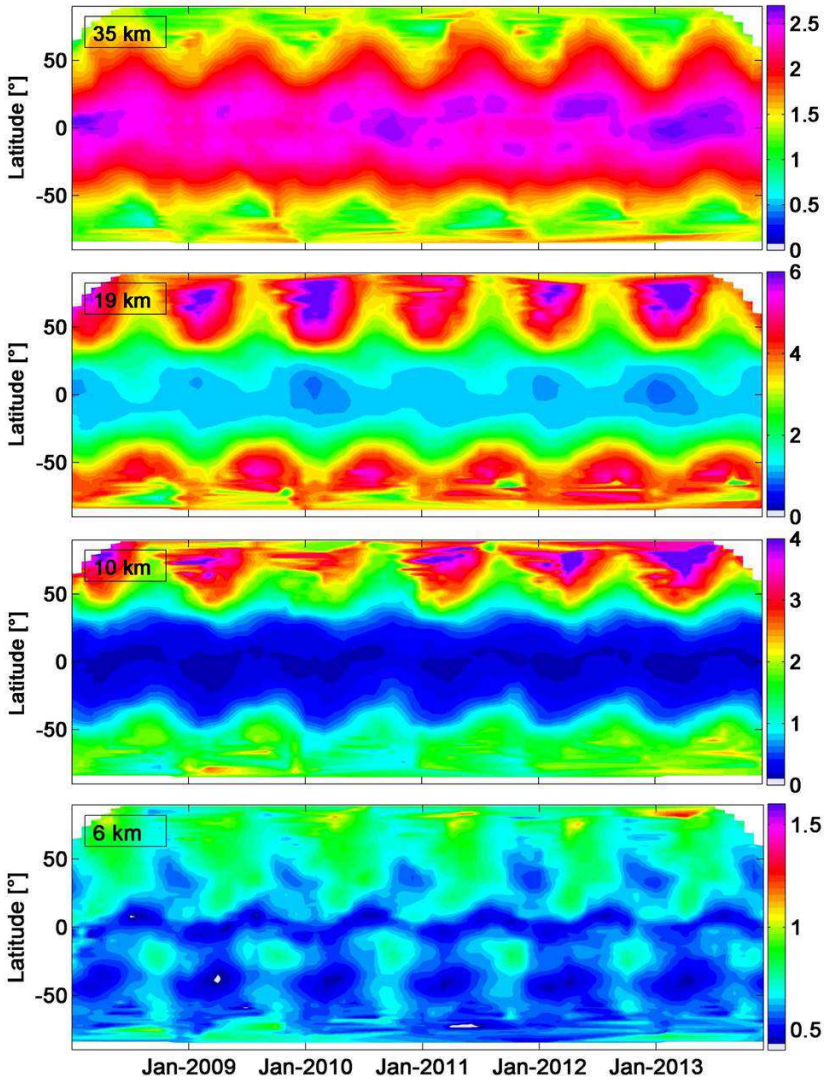

1285

1286 **Figure 6.** Daily IASI O_3 number density ($1x10^{12}$ molecules/cm^3) at 35 km (top row), 19 km
1287 (second row), 10 km (third row) and 6 km (bottom row) as a function of time and latitude. Note
1288 that the color scales are different.

1289

1290

1291

1292

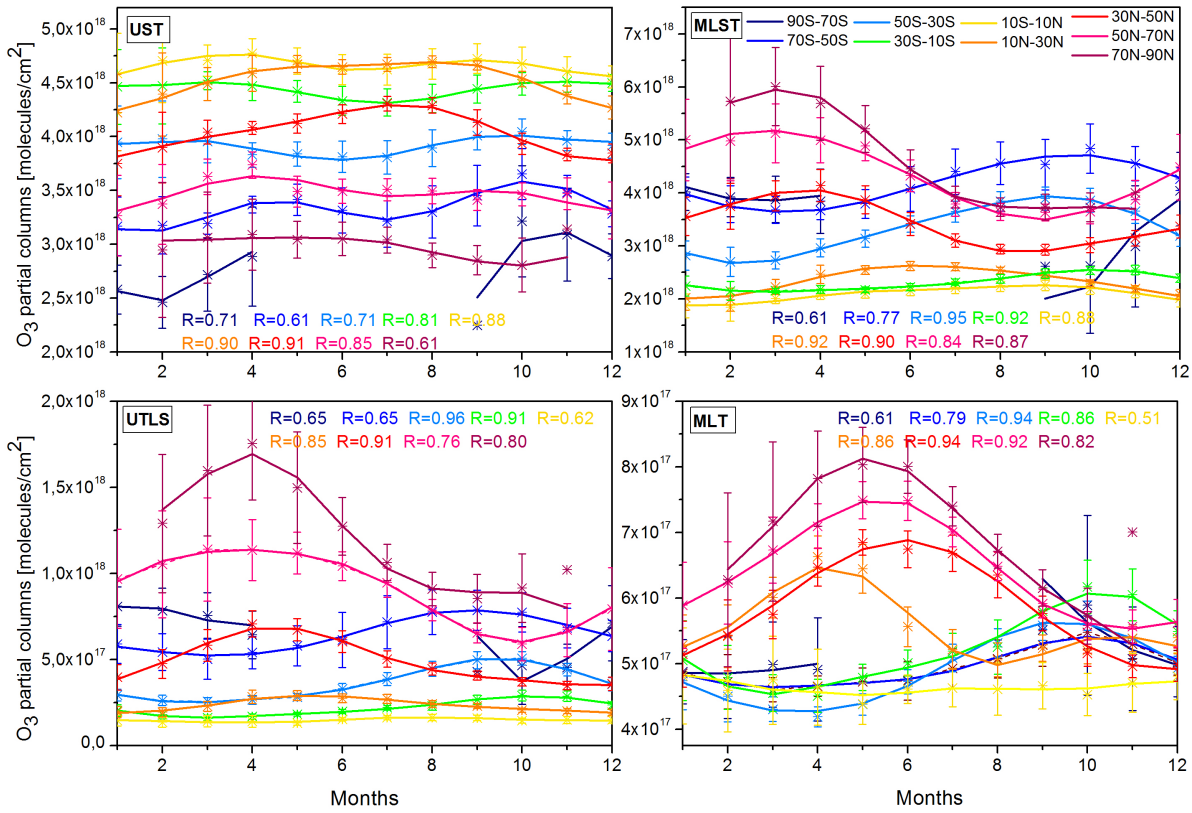

Figure 7. Monthly medians of measured (scatters) and of fitted (line) IASI O_3 columns averaged over the period 2008-2013, for the UST, MLST, UTLS and MLT layers and for each 20-degrees latitude bands (color scale~~).~~ in the top-right panel). The fit is based on daily medians. Error bars give the 1σ standard deviation relative to the monthly median values. Correlation coefficient (R) between the daily median observations and the fit are also indicated. Note that the scales are different.

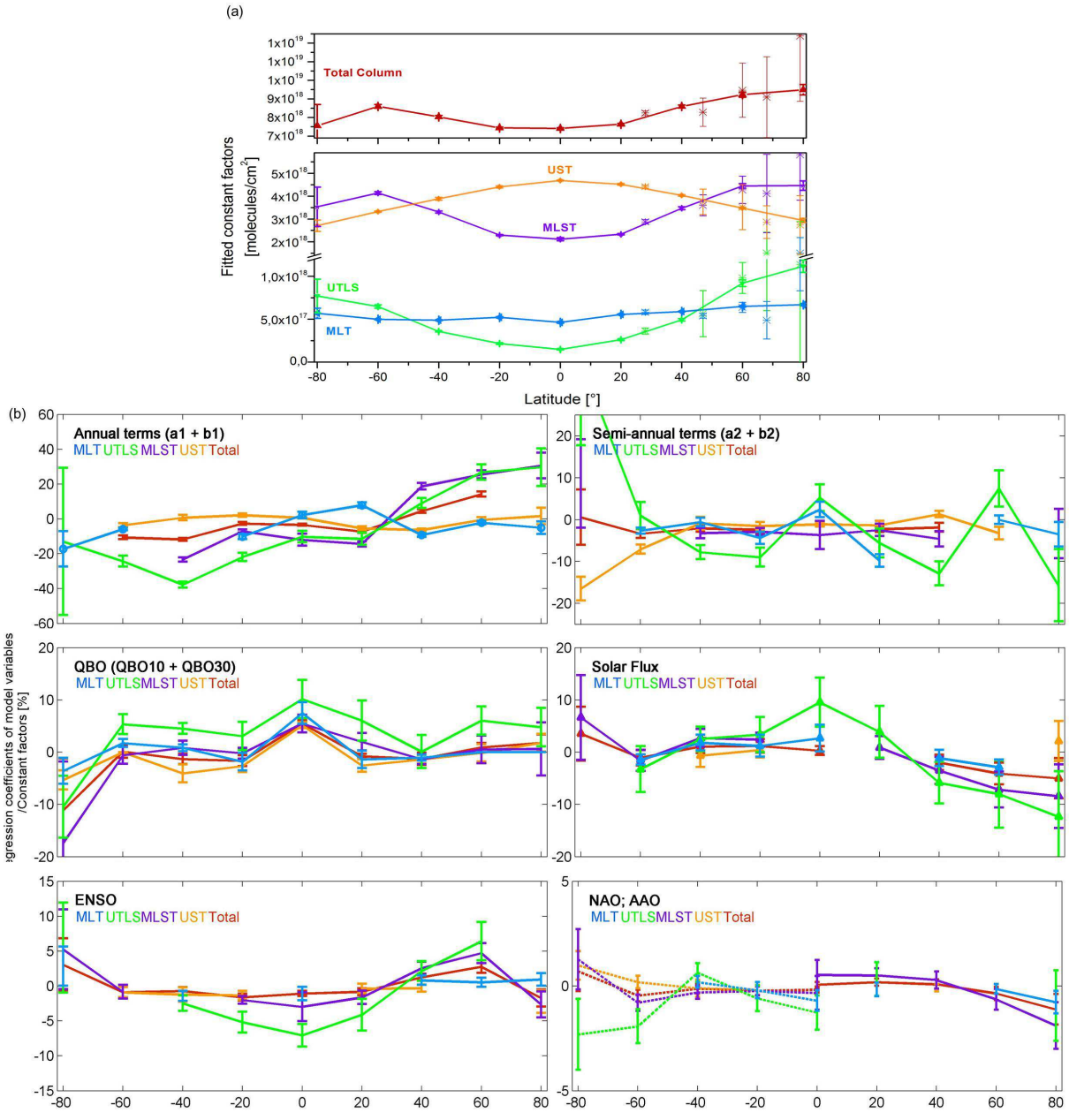

Figure 8. (a) Fitted constant factors (Cst, see Eq.1, Section 3) from the 6-years IASI daily O_3 time series for the 20-degree latitude belts, separately given for the 4 layers and for the total column. The stars correspond to the constant factors fitted above ground-based measurement stations: Ny-Ålesund (79°N), Kiruna (68°N), Harestua (60°N), Jungfraujoch (47°N), Izana (28°N). (b) Regression coefficients of the variables retained by the stepwise procedure, given in % as [(regression_coefficients])/fitted_Cst]x100%. Identification for the variables: Annual (top

left) and Semi-Annual variations (top right) terms, QBO at 10 and 30 hPa (bottom left), solar flux (bottom right). Note that the scales are different. The associated fitting uncertainties (95% confidence limits) are also represented (error bars).

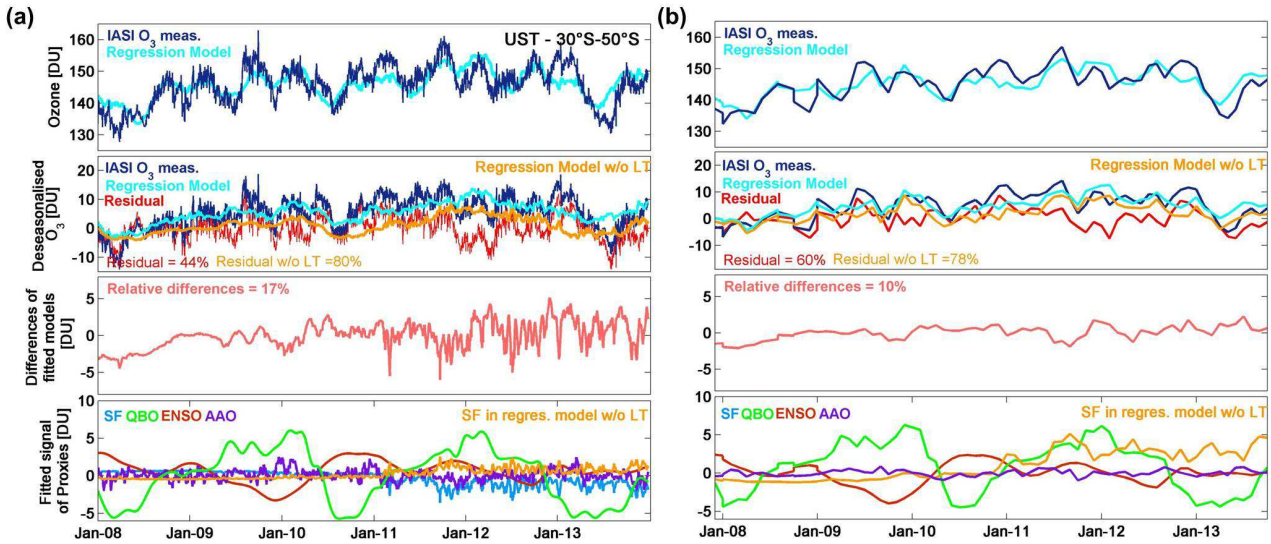

Figure 9. Daily (a) and monthly (b) time series of O_3 measurements and of the fitted regression model in the UST in the 30°S-50°S latitude band (top row), of the deseasonalised O_3 (2^d row), of the difference of the fitted models with and without the linear term (3^d row), and of the fitted signal of proxies ([regression coefficients*Proxy]): SF (blue), QBO (QBO^{10} + QBO^{30}; green), ENSO (red) and AAO (purple) (bottom) (given in DU). The averaged residuals relative to the deseasonalised IASI time series are also indicated (%).

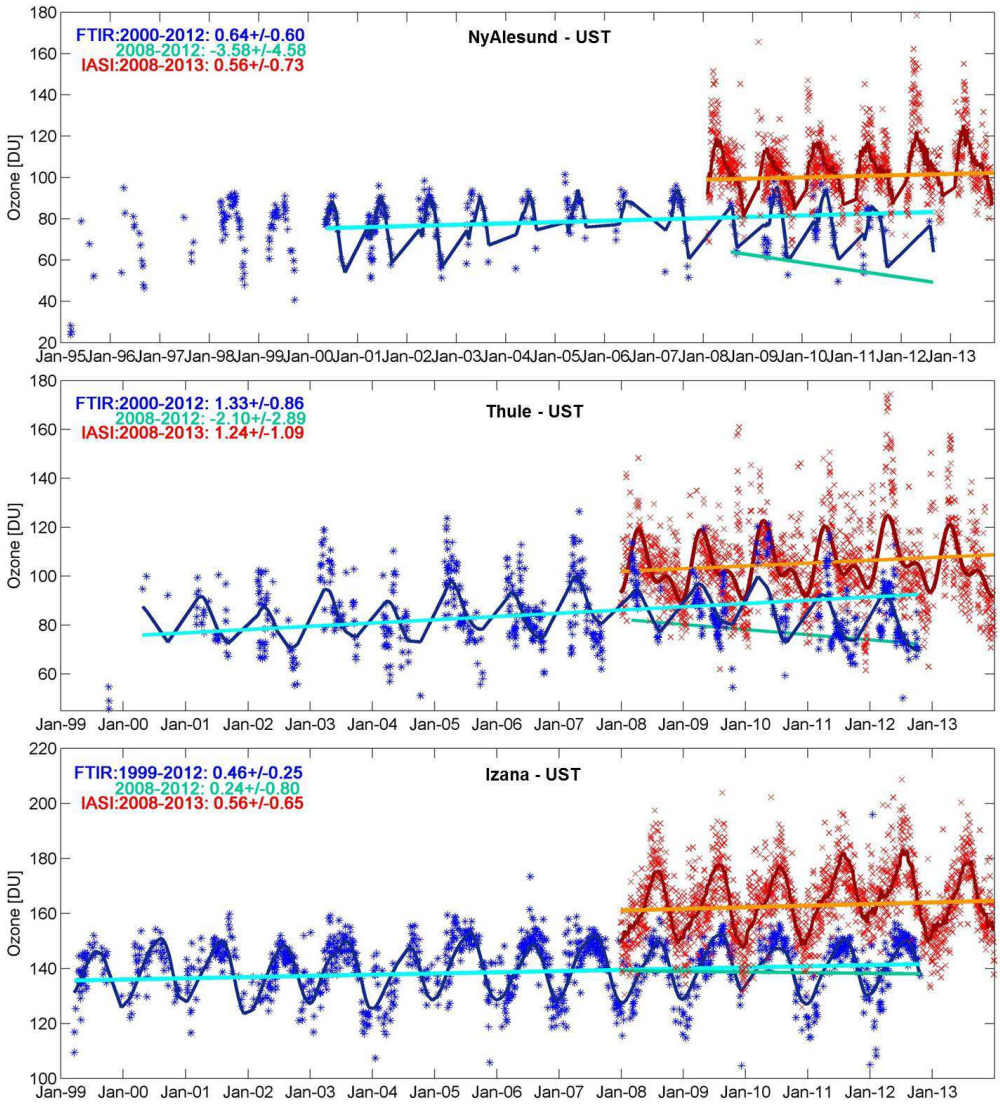

Figure 10. Daily time series of O_3 FTIR (blue symbols) and IASI (red symbols) measurements in the UST at Ny-Alesund (top), Thule (middle) and Izana (bottom), covering the 1995-2012 and the 1999-2012 periods, respectively (given in DU). The fitted regression models (dark blue and dark red lines, for FTIR and IASI, respectively) and the linear trends calculated for periods starting after the turnaround over 1999/2000-2012 and over 2008-2012 for FTIR (light blue and green lines), and the 2008-2013 period for IASI (orange line) are also represented (DU/yr). The trend values given in DU/year are indicated.

Contents of this file

Sections 1 to 4 ~~—~~ Table S1 – Figures S1 to ~~S3~~S6

Introduction

This supporting information provides, in Table S1, a tabulated summary of the variables that are kept in the statistical model at the 95% level at the end of the iterative backward selection for each 20° latitude bands and for each partial column analyzed in the manuscript.

This supplement also gives details on model-measurement comparisons~~.~~ in subsections below. First, we evaluate the variations in O_3 simulated with MOZART-4 (Emmons et al., 2010a) against IASI by using the regression model described in the manuscript (Section 3). This statistical model is used as a tool for understanding possible biases between MOZART-4 and IASI. Then, the stratospheric influence as seen by IASI in the O_3 tropospheric column (Section 4 of the manuscript) is estimated.

S.1 MOZART-4 simulation set up

The simulations are performed over the IASI period after a 6-month spin-up and they are driven by offline meteorological fields from the NASA Global Modeling and Assimilation Office (GMAO) Goddard Earth Observing System (GEOS-5) assimilation products (http://gmao.gsfc.nasa.gov/products/). MOZART-4 was run with a horizontal resolution of 2.5°×1.9°, with 56 levels in the vertical and with its standard chemical mechanism. In the stratosphere, MOZART-4 does not have a detailed chemistry and O_3 is constrained to observations from satellite and ozonesondes (Horowitz et al., 2003). ~~The emissions are the same as used in Wespes et al. (2012), with the constant in time anthropogenic emissions from D. Streets' ARCTAS inventory (see http://www.cgrer.uiowa.edu/arctas/emission.html) and the fire emissions from the daily Fire Inventory from NCAR (FINN, Wiedinmyer et al., 2011).~~The emissions inventory used here is the same as in Wespes et al. (2012) and in Duflot et al. (2015). The anthropogenic emissions are from the inventory provided by D. Streets (Argonne National Lab) and University of Iowa for ARCTAS (http://bio.cgrer.uiowa.edu/arctas/emission.html; http://bio.cgrer.uiowa.edu/arctas/arctas/07222009/). It is a composite dataset of regional

emissions representative of emissions for 2008: it is built upon the INTEX-B Asia inventory (Zhang et al.,2009) with the US NEI (National Emission Inventory) 2002 and CAC 2005 for North America and the EMEP (European Monitoring and Evaluation Programme) 2006 for Europe inventory to make up NH emissions (see http://bio.cgrer.uiowa.edu/arctas/emission.html and Emmons et al. 2015 for an evaluation of the inventory with several models in the frame of the POLARCAT Model Intercomparison Program (POLMIP)). Emissions from EDGAR (Emissions Database for Global Atmospheric Research) were used for missing regions and species. The anthropogenic emissions are constant over years with no monthly variations. Daily biomass burning emissions are taken from the global Fire INventory from NCAR (FINN, Wiedinmyer et al., 2011). They vary with year. The oceanic emissions are taken from the POET emissions dataset (Granier et al., 2005) and the biogenic emissions from MEGANv2 (Model of Emissions of Gases and Aerosols from Nature) inventory (Guenther et al., 2006). Details on chemical mechanisms, parameterizations and emission sources can be found in Emmons et al. (2010a; 2012; 2015). MOZART-4 simulations of numerous species (including O_3 and related tracers) have been previously compared to ~~in situ~~ozonesondes, aircrafts and satellite observations and used to track the intercontinental transport of pollution (e.g., Emmons et al., 2010b; ~~2013~~2015; Pfister et al., 2006; 2008; Wespes et al., 2012). Results have shown that MOZART-4 is slightly biased low over the troposphere (around 5-15%), but that it reproduces generally well the variability of observations in space and time.

S.2 O_3 time series from MOZART-4 *vs* IASI

In Fig. S~~1~~2, the seasonal cycles of ozone columns from MOZART-4 fitted regression model are compared against the IASI fitted columns by taking into account its associated averaging kernels (see Section 2 of the manuscript) following the formalism of Rodgers (2000):

$$X_{Model\_Smoothed} = X_a + \mathbf{A}(X_{Model} - X_a) \quad \text{(S1)}$$

where X_{Model} represents the O_3 profile modeled by MOZART-4 which is first vertically interpolated to the pressure levels of the a priori profiles (Xa) used in the FORLI-O_3 retrieval algorithm. In the stratosphere (UST and MLST), despite the non-explicit representation of the chemistry and the coarse vertical resolution in this layer, MOZART-4 reproduces the observations in terms of ozone concentrations, amplitude of the seasonal cycle and timing of the

maximum. Differences between the fitted cycles associated with the simulations and the observations are lower than 10%, except over the Southern polar region where they reach 30%. In the UTLS region, while the amplitudes of the seasonal cycles and the timing of the maxima are well captured in the model, we observe a systematic bias with an underestimation of O_3 concentrations in the model of around 30% over the high latitudes (north of 50°N and south of 50°S), possibly resulting from a misrepresentation of the STE processes.

In the troposphere, on the contrary to the upper layers, the model shows for each 20-degree latitude band an overestimation of the ozone concentrations, particularly in tropical and extra-tropical regions (reaching 25% in the equatorial belt), as well as a mismatch in the timing of the maximum which occurs one to two months before the observed spring peak, especially in the N.H. The shift of the maximum from high to mid-latitudes observed by IASI in the N.H. (see Section 4.1 and Fig. 7 of the manuscript) is not reproduced by MOZART-4 which shows a latitudinal independent maximum in April. This is likely explained by the constant in time anthropogenic emissions used in MOZART-4. This finding gives further confidence to the ability of IASI to detect anthropogenic production of O_3. The mismatch in the timing of the maximum in the troposphere is characterized by different regression coefficients for the annual term from MOZART-4 and IASI. The annual component (Constant scaled a_1+b_1) decreases from Northern latitudes (from 5% to 10%) to high Southern latitudes (from -30% to 0%) with negative amplitudes south of 10°N and a maximum positive amplitude at 20°N (10%) for MOZART-4, while IASI shows negative values both south of the equator (-20-0%) and north of 30°N (-10-0%) and a similar maximum at 20°N (see Fig.8b of the manuscript). Note that this mis-representation of MOZART-4 in the UTLS and in the troposphere is unlikely due to errors in climatology values used in the stratosphere since the concentrations and the timing of the maximum are well reproduced in that layer.

To better evaluate the sources of the discrepancies between model and measurement, we compare the constant terms from MOZART-4 time series with IASI (Fig.S~~2~~3, also Fig.8a of the manuscript) using the regression procedure (Section 3 of the manuscript). The comparison indicates that MOZART-4 has a good climatology in the US and MLS (differences < 10%). The

biases of MOZART-4 in the UTLS and in the troposphere reported above are highlighted in the fitted constant with, in UTLS, underestimations of ~35% and ~15% over the high Southern and Northern latitudes, respectively, and, in the troposphere, an overestimation of ~25% in the tropics. The latter could possibly point out issues with horizontal transport in the model or overestimated ozone production efficiency at these latitudes.

S.3 Stratospheric influences as seen by IASI

After verifying above the agreement between the O_3 time series from IASI and from MOZART-4, we can investigate to what extent the stratosphere could influence the O_3 variations seen by IASI in the troposphere. To this end, we focus hereafter on variations in the MLT, using a "tagging" method to track all tropospheric odd nitrogen sources (the "tagged" nitrogen species) producing ozone ($O_3^{tagged\_NOx}$) through the tropospheric photochemical reactions ~~(~~in MOZART-4 (see Emmons et al~~,~~ . (2012~~).~~) for detailed information on the "tagging" approach and on the photolysis and kinetic reactions for the tagged species). This method allows ~~isolating~~the quantification of the portion of the stratosphere to the tropospheric O_3. Since the method is fully linear, this contribution is simply calculated as the difference between the total simulated O_3 and the $O_3^{tagged\_NOx}$ (Emmons et al., 2012; Wespes et al., 2012). Fig.S~~3~~4 (a) presents, for each 20-degree latitude band, the averaged seasonal cycles in the MLT for total O_3 (solid line) and $O_3^{tagged\_NOx}$ (dashed lines) from fitted MOZART-4 time series~~ accounting for the IASI averaging kernels.~~. The difference between total O_3 and $O_3^{tagged\_NOx}$ ~~represents the stratospheric part as seen by IASI in the troposphere. It~~ is expressed in Fig.S~~3~~4 (b) as a percentage of the total O_3. ~~The stratospheric~~It represents the natural stratospheric influence into the MLT columns as modeled by MOZART-4 and it ranges between ~20% to 45% with, as expected, the largest contribution above the winter southern latitudes. Fig. S5 is the same as Fig. S4 but the model time series account for the IASI vertical sensitivity by applying the averaging kernels of each specific IASI observations to the corresponding gridded MOZART-4 profile (see Eq. S1), similarly to Wespes et al. (2012). Eq. S1 can be expressed as :

$$X_{Model\_Smoothed} = [\mathbf{A}X_{O3\_tagged\_NOx}] + [\mathbf{A}(X_{Model} - X_{O3\_tagged\_NOx})] + [X_a - \mathbf{A}(X_a)] \quad \text{(S2)}$$

where the first two terms represent the contributions from all the tropospheric odd nitrogen sources and from the stratosphere smoothed by the averaging kernels, respectively. The third component represents the contribution from the a priori to the ozone columns due to the limited vertical sensitivity of the IASI instrument. These terms are represented in Fig. S5 (a) and (b) for the MLT. The second term which is illustrated as a percentage of the total O_3 in Fig. S5 (b) (solid lines), simulates the stratospheric part as seen by IASI in the troposphere. This IASI stratospheric contribution, which is amplified by the limited vertical sensitivity of the instrument in the MLT when compared with the MOZART-4 stratospheric influence (Fig. S4 (b)), ~~The difference between total O_3 and $O_3^{tagged\_NOx}$ represents the stratospheric part as seen by IASI in the troposphere. It is expressed in Fig.S3 (b) as a percentage of the total O_3. The stratospheric contribution~~ ranges between 30 and 65% depending on latitude and season. The largest contributions are calculated for the highest latitudes in winter-spring and they are attributed to both descent of stratospheric air mass into the polar vortex and to less IASI sensitivity~~. Exception is found~~ over the poles. The low contribution above the South polar region ~~which shows a minimum~~ (~25%) is explained by a loss of IASI sensitivity which translates to a large a priori contribution (40%). The smallest stratospheric contributions are calculated in the ~~lower latitudes. As expected from the IASI vertical sensitivity (see Section 2 of the manuscript), the *a priori* contribution is anti correlated with~~ low latitude bands. The difference between the stratospheric ~~contribution to some extent and it~~ contributions simulated by MOZART-4 (Fig. S4 (b)) and those as seen by IASI (Fig. S5 (b)) is the stratospheric portion due to the IASI limited sensitivity and it reflects the smoothing error from the IASI measurements. It ranges between 10%-20% (except for the polar bands). This suggests that the ~~variability~~ limited vertical sensitivity of ~~ozone in the troposphere observed by IASI (Section 4.3.2 of the manuscript) may partly be masked by the *a priori* information~~IASI, which artificially mixes stratospheric and ~~significantly be driven by~~tropospheric air masses, contributes to a lesser extent to the ~~variability in~~IASI MLT than the stratosphere~~.~~ troposphere exchanges. The smoothing error translates also to an *a priori* contribution (dashed lines, Fig. S5 (b)) which, as expected from the analysis of the IASI vertical sensitivity (see Section 2 of the manuscript), is anti-correlated with the stratospheric contribution to some extent. It ranges between ~5% and ~20%. These results suggest that the variability of

tropospheric ozone measured by IASI (Section 4.3.2 of the manuscript) is partly masked by the *a priori* and the stratospheric contributions.

The total portion of the natural variability (from both the troposphere and the stratosphere) into the MLT O_3 measured by IASI can be estimated by subtracting from the IASI O_3 time series the *a priori* contribution and the stratospheric one due to the IASI limited sensitivity. This is illustrated in Fig.S6 (a). This natural contribution is larger than 50% of the IASI MLT O_3 column everywhere. Interestingly, the 30°N-50°N band shows the highest detectable natural portion (~80-85%) in the MLT columns, from which ~25-35% originates from the stratosphere (Fig. S4 (b)), and~50-60% from the troposphere (Fig.S6 (b)). It is also worth to note that the positive bias of MOZART-4 *vs.* IASI in the MLT (see Section S2) should not affect the calculated tropospheric contribution in the IASI MLT columns and that the stratospheric contribution for the 30°N-50°N band should be well estimated from MOZART-4 since the model matches very well the IASI observations in the upper layers for this band (Fig. S2 and S3).

To further characterize the stratospheric influence, the constant factors associated with the $O_3^{tagged\_NOx}$ fitting time series in the troposphere are superimposed in Fig.S~~2~~3 (dashed grey line). They represent between 40 and 60% of the constant factors derived from the total O_3 fitting. The north-south gradient for the $O_3^{tagged\_NOx}$ is smaller than for the total O_3, with maximum over the low latitudes of the N.H. while, for the total O_3, maximum is found over the high latitudes. From Fig.S~~3~~4 (a), we see in the N.H. that the differences between the variability of total O_3 and that of $O_3^{tagged\_NOx}$ mainly result from the timing of the maximum with a shift of 2-3 months (maximum in spring for the total O_3 *vs* maximum in summer for the $O_3^{tagged\_NOx}$). That shift is characterized by a positive annual component (constant scaled *a1+b1*) for the total O_3 (~10%) and a negative one for the $O_3^{tagged\_NOx}$ (~ -20%). In the S.H., we observe a same timing of the maximum between the two runs.

4 Conclusions

Two important results can be derived from MOZART-4 *vs* IASI time series:

1- By comparing the fitted O_3 variations and regression coefficients using the same regression model, systematic biases are found in the troposphere and can be attributed to specific model limitations (no-interannual variability in the anthropogenic emissions, errors in the transport, coarse spatial and vertical resolution of the model and overestimation of ozone production efficiency). In particular, the fact that the MOZART-4 model settings used constant anthropogenic emissions tends to strengthen the ability of IASI to detect anthropogenic production of O_3 and to highlight the need for developing long term continuous anthropogenic emissions inventories (including seasonal and inter-annual variations) for better estimating the impact of anthropogenic pollution changes on tropospheric ozone levels.

2- Our results suggest that even if a large part of the IASI O_3 MLT measurements in the N.H. originates from the troposphere (40-60%), the apparent negative trend in the troposphere observed by IASI in the N.H. summer (see Tables 2 and 3 in Section 4.3.2 of the manuscript) is ~~largely attenuated~~partly masked by the influence of the stratosphere ~~(through STE processes~~ and of the medium vertical sensitivity of IASI ~~in the troposphere).~~. In other words, the decrease of tropospheric O_3, which could be attributed to decline of O_3 precursor emissions, is ~~probably much more important than what we estimate from IASI.~~likely attenuated by the positive changes in O_3 variations detected in upper layers. This would mean that the negative trend deduced from IASI could in reality be more important. This opens perspectives to further comprehensive studies for investigating the influence of stratospheric O_3 recovery on the apparent decrease of O_3 in the troposphere.

References

Duflot, V., C. Wespes, L. Clarisse, D. Hurtmans, Y. Ngadi, N. Jones, C. Paton-Walsh, J. Hadji-Lazaro, C. Vigouroux, M. De Mazière, J.-M. Metzger, E. Mahieu, C. Servais, F. Hase, M. Schneider, C. Clerbaux and P.-F. Coheur: Acetylene (C2H2) and hydrogen cyanide (HCN) from IASI satellite observations: global distributions, validation, and comparison with model, Atmos. Chem. Phys., 15, 10509–10527, doi:10.5194/acp-15-10509-2015, 2015.

Emmons, L. K., Walters, S., Hess, P. G., Lamarque, J.-F., Pfister, G. G., Fillmore, D., Granier, C., Guenther, A., Kinnison, D., Laepple, T., Orlando, J., Tie, X., Tyndall, G., Wiedinmyer, C., Baughcum, S. L., and Kloster, S., Description and evaluation of the Model for Ozone and Related Chemical Tracers, version 4 (MOZART-4), Geosci. Model Dev., 3, 43-67, 2010a.

Emmons, L.K., Apel, E.C., Lamarque, J.-F., Hess, P. G., Avery, M., Blake, D., Brune, W., Campos, T., Crawford, J., DeCarlo, P. F., Hall, S., Heikes, B., Holloway, J., Jimenez, J. L., Knapp, D. J., Kok, G., Mena-Carrasco, M., Olson, J., O'Sullivan, D., Sachse, G., Walega, J., Weibring, P., Weinheimer, A., and Wiedinmyer, C.: Impact of Mexico City emissions on regional air quality from MOZART-4 simulations, Atmos. Chem. Phys., 10, 6195–6212, doi:10.5194/acp-10-6195-2010, 2010b.

Emmons, L. K., P.G. Hess, J.-F. Lamarque, and G. G. Pfister: Tagged ozone mechanism for MOZART-4, CAM-chem and other chemical transport models, Geosci. Model Dev., 5, 1531-1542, doi:10.5194/gmd-5-1531-2012, 2012.

Emmons, L. K., S. R. Arnold, S. A. Monks, V. Huijnen, S. Tilmes, K. S. Law, J. L. Thomas, J.-C. Raut, I. Bouarar, S. Turquety, Y. Long, B. Duncan, S. Steenrod, S. Strode, J. Flemming, J. Mao, J. Langner, A. M. Thompson, D. Tarasick, E. C. Apel, D. R. Blake, R. C. Cohen, J. Dibb, G. S. Diskin, A. Fried, S. R. Hall, L. G. Huey, A. J. Weinheimer, A. Wisthaler, T. Mikoviny, J. Nowak, J. Peischl, J. M. Roberts, T. Ryerson, C. Warneke, and D. Helmig: The POLARCAT Model Intercomparison Project (POLMIP):overview and evaluation with observations, Atmos. Chem. Phys., 15, 6721–6744, 2015.

Granier, C., Lamarque, J., Mieville, A., Müller, J., Olivier, J., Orlando, J., Peters, J., Petron, G., Tyndall, G., and Wallens, S.: POET, a database of surface emissions of ozone precursors, available at: http://www.pole-ether.fr/eccad (last access: 22 September 2015), 2005.

Guenther, A., Karl, T., Harley, P., Wiedinmyer, C., Palmer, P. I., and Geron, C.: Estimates of global terrestrial isoprene emissions using MEGAN (Model of Emissions of Gases and Aerosols from Nature), Atmos. Chem. Phys., 6, 3181–3210, doi: 10.5194/acp-6-3181-2006, 2006.

Horowitz, L., Walters, S., and Mauzerall, D.S.: A global simulation of tropospheric ozone and related tracers: Description and evaluation of MOZART, version 2, J. Geophys. Res., 108, 4784, doi:10.1029/2002JD002853, 2003.

Pfister, G. G., Emmons, L. K., Hess, P. G., Honrath, R., Lamarque, J.-F., Val Martin, M., Owen, R. C., Avery, M. A., Browell, E. V., Holloway, J. S., Nedelec, P., Purvis, R., Ryerson, T. B., Sachse, G. W., and Schlager, H.: Ozone production from the 2004 North American boreal fires, J. Geophys. Res., 111, D24S07, doi:10.1029/2006JD007695, 2006.

Pfister, G. G., Emmons, L. K., Hess, P. G., Lamarque, J.-F., Thompson, A. M., and Yorks, J. E.: Analysis of the summer 2004 ozone budget over the United States using Intercontinental Transport Experiment Ozonesonde Network Study (IONS) observations and Model of Ozone and Related Tracers (MOZART-4) simulations, J. Geophys. Res., 113, D23306, doi:10.1029/2008JD010190, 2008.

Wespes, C., L. Emmons, D. P. Edwards, J. Hannigan, D. Hurtmans, M. Saunois, P.-F. Coheur, C. Clerbaux, M. T. Coffey, R. L. Batchelor, R. Lindenmaier, K. Strong, A. J. Weinheimer, J. B. Nowak, T. B. Ryerson, J. D. Crounse, and P. O. Wennberg: Analysis of ozone and nitric acid in spring and summer arctic pollution using aircraft, ground-based, satellite observations and mozart-4 model: source attribution and partitioning, Atmos. Chem. Phys., 12, 237-259, 2012.

Wiedinmyer, C., Akagi, S. K., Yokelson, R. J., Emmons, L. K., Al-Saadi, J. A., Orlando, J. J., and Soja, A. J.: The Fire INventory from NCAR (FINN) – a high resolution global model to estimate the emissions from open burning, Geosci. Model Dev., 3, 2439-2476, doi:10.5194/gmd-3-2439-2010, 2011.

Table S1 List of the proxies retained in the stepwise backward elimination approach which are significant at the 95% level (see text for details) for each 20-degree latitude bands and for each partial column. Proxies are indicated for Solar flux (blue), QBO10 (green), QBO30 (orange), ENSO (red) and NAO (pink)/AAO (purple). Symbols indicated between parentheses refer to proxies which are not significant statistically when accounting for the autocorrelation in the noise residuals.

Proxies	Ground-300hPa (Troposphere)	300-150hPa (UTLS)	150-25hPa (MLST)	25-3hPa (UST)	Total columns
70°N-90°N	(O) (O) O O	O(O) O (O)	O (O) (O)O O	(O)O (O) O	O (O) O O O
50°N-70°N	O (O) (O) O (O)	O O (O) O	O (O) (O)O O	(O)(O)	O (O) (O)O O
30°N-50°N	(O) (O) (O)O	O(O)(O)O	O (O) O O(O)	O (O) (O)(O)	O (O) (O)O O
10°N-30°N	(O) (O) (O)	(O)O(O) O (O)	(O)(O)(O)O O	O (O) (O)	O (O) O O
10°S-10°N	(O) O (O) (O)(O)	O O O O O	(O) OO(O)(O)	O O O	(O) O O O(O)(O)
30°S-10°S	(O) (O)(O) (O)	(O)O(O) O (O)	O (O) O O (O)	(O)O O O (O)	(O) (O) O O O
50°S-30°S	(O) (O)(O) O (O)	(O)O(O) O O	O O O (O)	(O)O O O (O)	(O) (O) O O (O)
70°S-50°S	O (O) (O)	(O)O (O) O	(O)(O) O (O) O	(O)O O (O)	(O) (O) O O O
90°S-70°S	(O) O O	(O) O(O) O	(O)(O)(O)(O)(O)	O(O) O	(O)(O)(O)(O)(O)

Figure captions

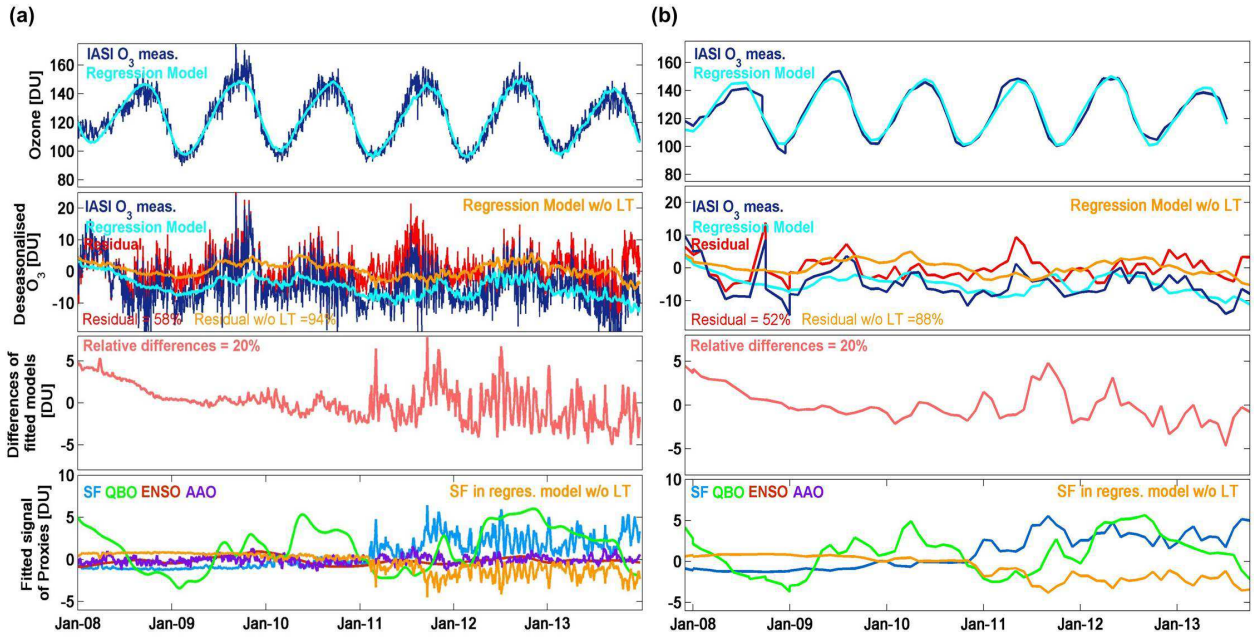

Figure S1: Same as Figure 9 of the manuscript, but in the UST for the 30°S-50°S latitude band.

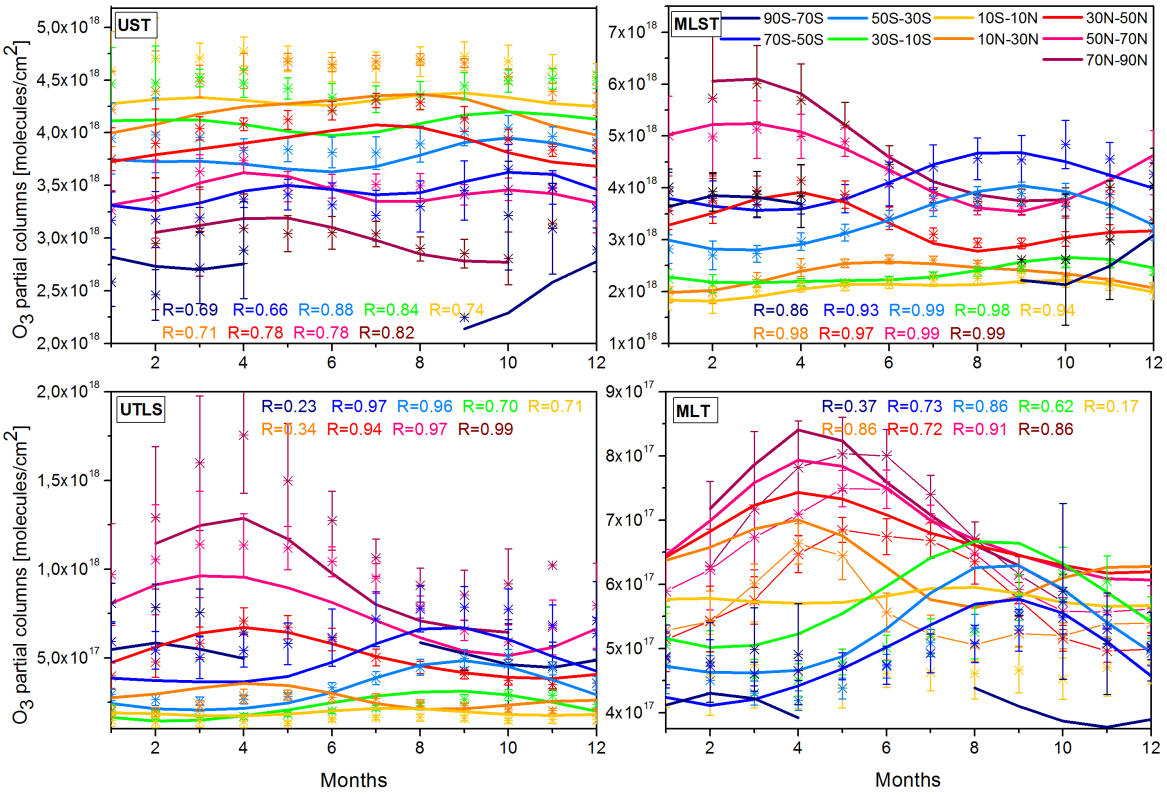

295

296 **Figure S~~1~~2:** Same as Figure 7 of the manuscript, but for the fit of MOZART-4 simulations (line)
297 smoothed according to the averaging kernels of the IASI observations. The IASI O_3 columns
298 observations (stars) are indicated for the sake of comparison. In the N.H. for the MLT, they are
299 plotted with lines and symbols for clarity. Correlation coefficients (R) between the daily median
300 fitting of IASI and of the smoothed MOZART-4 are also indicated. Note that the scales are
301 different.

302

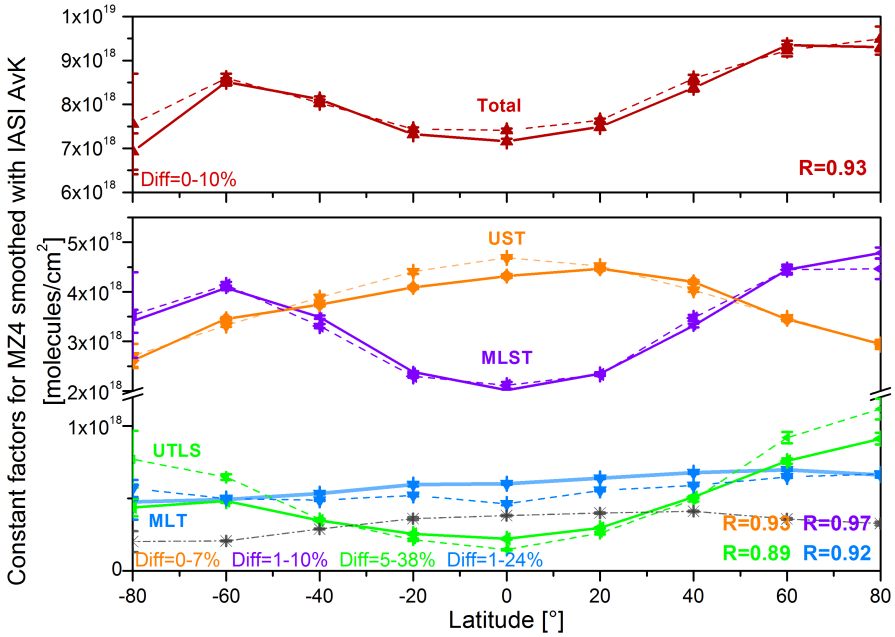

Figure S~~2~~3. Same as Fig.8 (a) of the manuscript but for the MOZART-4 O_3 time series, smoothed according to the averaging kernels of IASI. Correlation coefficient (R) and relative differences between the Constant factors in the IASI fitting time series (dashed line) and in the MOZART-4 fitting time series (full line) are also indicated. For the troposphere, the Constant factors in the MOZART-4 $O_3^{tagged\_NOx}$ fitting time series are also represented (dashed grey).

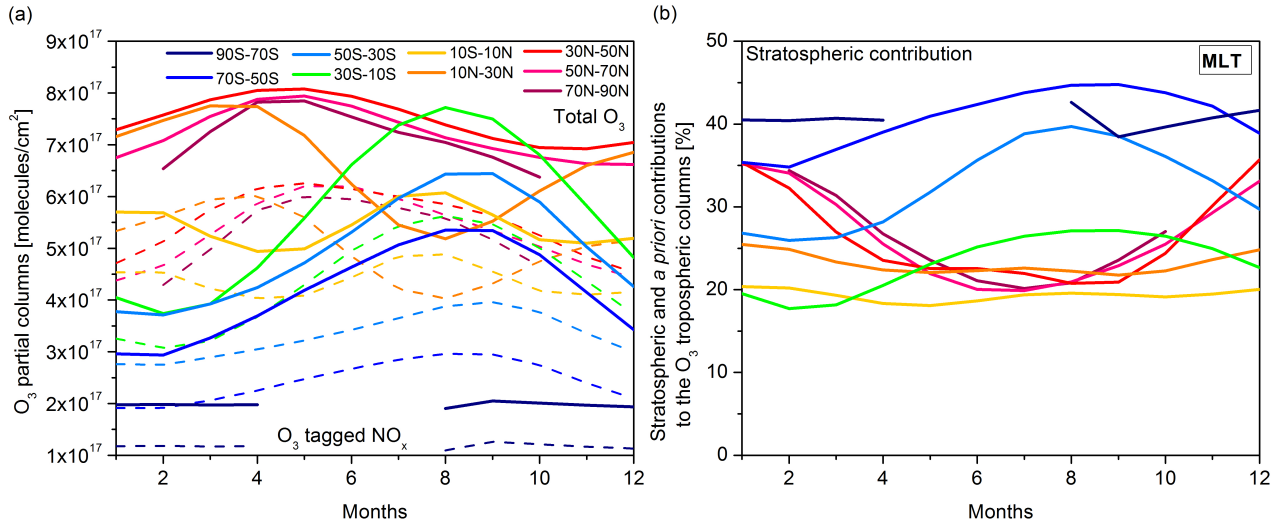

317

318 **Figure S34:** (a) Same as Figure 7 of the manuscript in the MLT layer, but for the fit of
319 MOZART-4 O_3 (full line) and of $O_3^{tagged\_NOx}$ time series (dashed line). (b) Stratospheric
320 influence into the MLT columns as simulated by MOZART-4 (%).

321

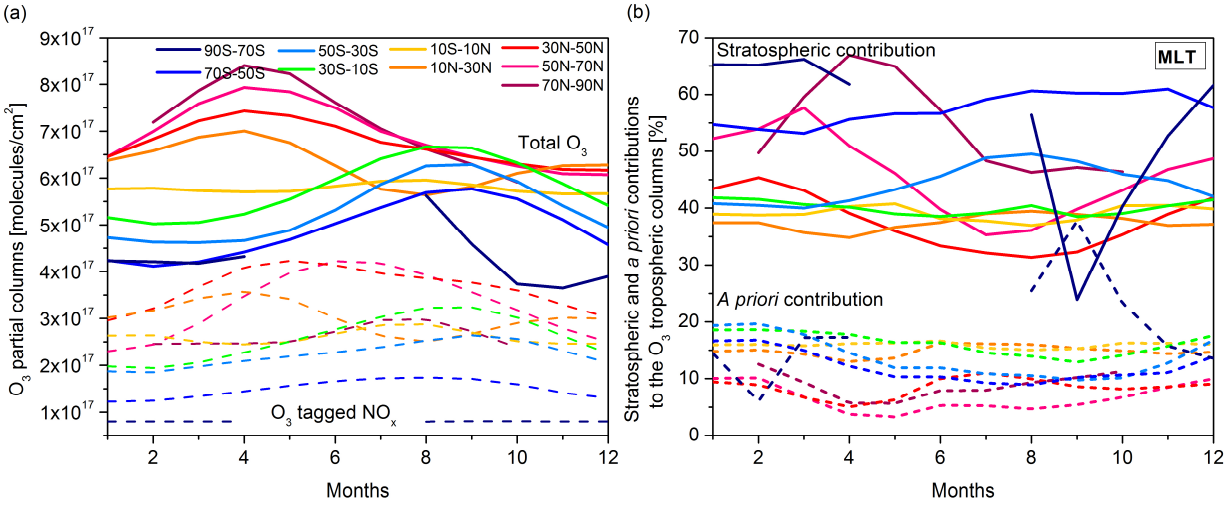

322

323 **Figure S5:** (a) Same as Figure S4 but accounting for the IASI sensitivity. (b) Contribution to the
324 MLT columns (%) from the stratosphere simulated by MOZART-4 accounting for the IASI
325 sensitivity (full line) and from the *a priori* information (dashed line).

326

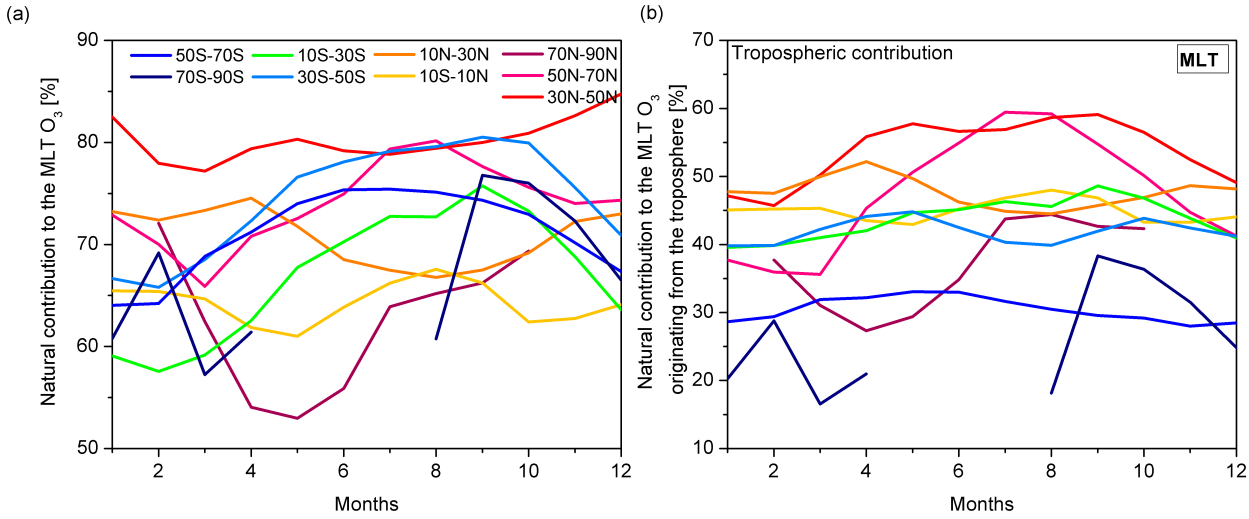

Figure S6: Contribution to the IASI MLT O_3 columns (%) (a) of the natural variability (troposphere and stratosphere) and (b) from the troposphere.